Supplementary Material

A Neutral Pyridine-Pyrazole-Based N^N*N^N Ligand as a Tetradentate Chromophore for Diverse Transition Metal Cations

Tobias Theiss,[a,b] María Victoria Cappellari,[a,b] Jutta Kösters,[a] Alexander Hepp,[a] and Cristian A. Strassert[a,b]

[a] Institut für Anorganische und Analytische Chemie, Universität Münster, Corrensstraße 28/30, 48149 Münster, Germany

[b] CiMIC, SoN, CeNTech, Universität Münster, Heisenbergstraße 11, 48149 Münster, Germany

Corresponding author: ca.s@wwu.de

Table of Contents

Section S1: Synthesis and characterization

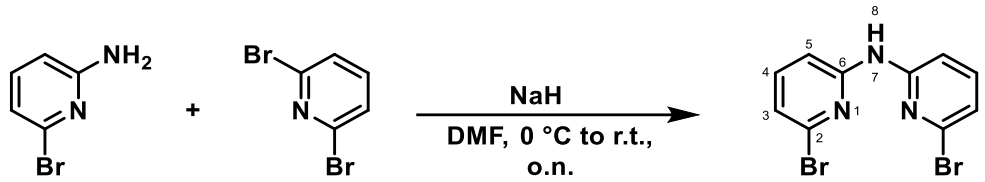

54 %

1

Bis(6-bromopyridin-2-yl)-amine (1). 2-amino-6-bromopyridine (10.03 g, 57.97 mmol, 1.0 eq.) was dissolved in anhydrous DMF (100 mL) and the solution was cooled down to 0 °C. Sodium hydride (4.31 g, 179.17 mmol, 3.1 eq.) was added and the mixture was stirred for 15 minutes. 2,6-dibromopyridine (13.71 g, 57.87 mmol, 1.0 eq.) was added and the solution was allowed to reach room temperature overnight. Distilled water was added to the reaction mixture to precipitate a white solid that was filtered off and washed with cold water. The crude product was purified by column chromatographic separation on silica (toluene) to yield **1** as a white solid. Yield: 10.37 g, 31.52 mmol, 54 %. Colorless crystals were obtained from slow evaporation of a saturated acetone solution of **1**.

EM-MS-ESI (MeOH, $C_{10}H_7Br_2N_3$): calcd. $[M+H]^+$ = 327.9079, found $[M+H]^+$ = 327.9085; calcd. $[M+Na]^+$ = 349.8899, found $[M+Na]^+$ = 349.8905.

^{1}H-NMR (500 MHz, acetone-d_6): δ (ppm) = 9.14 (s, 1 H, H_8), 7.77 (d, $^3J_{HH}$ = 8.5 Hz, 2 H, H_5), 7.63 (t, $^3J_{HH}$ = 7.8 Hz, 2 H, H_4), 7.11 (d, $^3J_{HH}$ = 7.5 Hz, 2 H, H_3).

^{13}C{^{1}H}-NMR (126 MHz, acetone-d_6): δ (ppm) = 154.1 (C_6), 140.7 (C_4), 139.1 (C_2), 120.2 (C_3), 110.7 (C_5).

^{15}N-NMR (41 MHz, acetone-d_6): δ (ppm) = 116 (N_7).

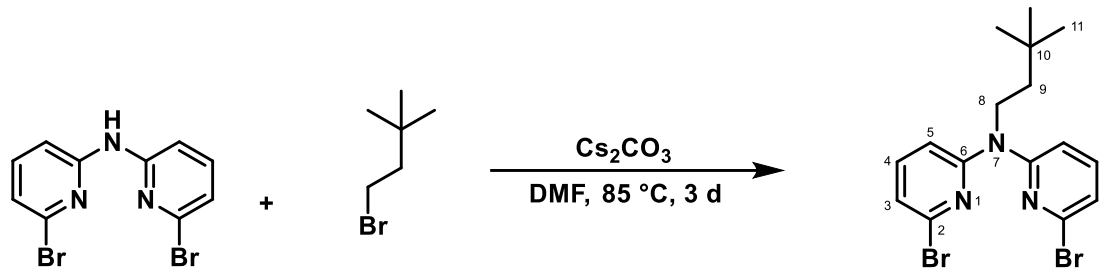

Bis(6-bromopyridin-2-yl)-3,3-dimethylbutylamine (2a). **1** (3.3586 g, 10.21 mmol, 1.0 eq.) and 1-bromo-3,3-dimethylbutane (3.000 g, 18.17 mmol, 1.8 eq.) were dissolved in DMF (40 mL) and Cs_2CO_3 (16.0151 g, 48.15 mmol, 4.7 eq.) was added to this solution. The reaction mixture was heated up to 85 °C and stirred for three days. After cooling the mixture to room temperature, the Cs_2CO_3 was filtered off and the solvent was removed under reduced pressure. The crude product was purified by column chromatographic separation on silica (toluene) to yield **2a** as a white solid. Yield: 3.8585 g, 9.34 mmol, 91 %.

EM-MS-ESI (MeOH, $C_{10}H_7Br_2N_3$): calcd. $[M+H]^+$ = 412.0018, found $[M+H]^+$ = 412.0028; calcd. $[M+Na]^+$ = 433.9838, found $[M+Na]^+$ = 433.9844.

^{1}H-NMR (500 MHz, acetone-d_6): δ (ppm) = 7.41 (t, $^3J_{HH}$ = 7.9 Hz, 2 H, H_4), 7.12 (d, $^3J_{HH}$ = 8.2 Hz, 2 H, H_5), 7.05 (d, $^3J_{HH}$ = 7.6 Hz, 2 H, H_3), 4.15 (m, 2 H, H_8), 1.57 (m, 2 H, H_9), 1.00 (s, 2 H, H_{11}).

^{13}C{^{1}H}-NMR (126 MHz, acetone-d_6): δ (ppm) = 156.7 (C_6), 140.0 (C_2), 139.8 (C_4), 121.1 (C_3), 113.1 (C_5), 45.8 (C_8), 41.0 (C_9), 30.2 (C_{10}), 29.4 (C_{11}).

^{15}N-NMR (41 MHz, acetone-d_6): δ (ppm) = 286 (N_1), 115 (N_7).

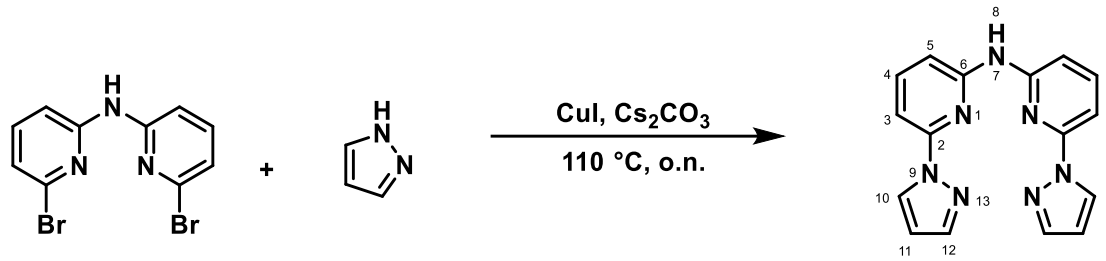

Bis(6-(1*H*-pyrazol-1-yl)-pyridin-2-yl)-amine (2b). A reaction tube was loaded with **1** (3.002 g, 9.10 mmol, 1.0 eq.), CuI (0.5707 g, 3.00 mmol, 0.3 eq.), Cs_2CO_3 (7.0060 g, 21.50 mmol, 2.4 eq.) and pyrazole (10.0000 g, 146.91 mmol, 16.1 eq.). After flushing the tube with argon, the mixture was heated up to 110 °C and stirred overnight. After cooling down to room temperature, the crude compound was washed with water to remove the pyrazole and the Cs_2CO_3. The organic residue was purified by column chromatographic separation on silica (toluene to DCM) to yield **2b** as a white solid. Yield: 1.3179 g, 4.34 mmol, 48 %.

EM-MS-ESI (MeOH, $C_{16}H_{13}N_7$): calcd. $[M+H]^+$ = 304.1305, found $[M+H]^+$ = 304.1310; calcd. $[M+Na]^+$ = 326.1125, found $[M+Na]^+$ = 326.1130.

^{1}H-NMR (400 MHz, DMSO-d_6): δ (ppm) = 10.04 (H_8), 8.57 (d, $^3J_{HH}$ = 2.6 Hz, 2 H, H_{10}), 7.90 (t, $^3J_{HH}$ = 8.1 Hz, 2 H, H_4), 7.81 (d, $^3J_{HH}$ = 1.6 Hz, 2 H, H_{12}), 7.66 (d, $^3J_{HH}$ = 8.3 Hz, 2 H, H_5), 7.44 (d, $^3J_{HH}$ = 8.0 Hz, 2 H, H_3), 6.58 (dd, $^3J_{HH}$ = 2.6 Hz, $^3J_{HH}$ = 2.6 Hz, 2 H, H_{11}).

^{13}C{^{1}H}-NMR (101 MHz, DMSO-d_6): δ (ppm) = 152.6 (C_6), 149.1 (C_2), 141.8 (C_{12}), 140.6 (C_4), 126.7 (C_{10}), 109.3 (C_5), 107.8 (C_{11}), 103.3 (C_3).

^{15}N-NMR (41 MHz, DMSO-d_6): δ (ppm) = 118 (N_7).

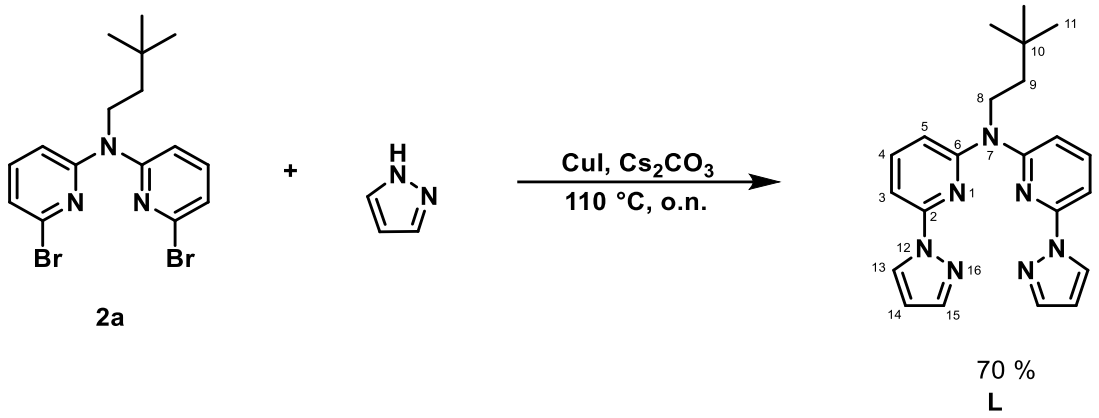

2a

L

Bis(6-(1*H*-pyrazol-1-yl)-pyridin-2-yl)-3,3-dimethylbutylamine (L). A reaction tube was loaded with **2a** (2.5836 g, 6.25 mmol, 1.0 eq.), CuI (0.3978 g, 2.09 mmol, 0.33 eq.), Cs_2CO_3 (4.8164 g, 14.78 mmol, 2.4 eq.) and pyrazole (6.4303 g, 94.47 mmol, 15.1 eq.). After flushing the tube with argon, the mixture was heated up to 110 °C and stirred overnight. After cooling down to room temperature, the crude product was washed with water to remove the excess of pyrazole and the Cs_2CO_3. The organic residue was purified by column chromatographic separation on silica (toluene) to yield **L** as a white solid. Yield: 1.1816 g, 3.05 mmol, 70 %. Colorless crystals were obtained from slow evaporation of a saturated acetone solution of **L**.

EM-MS-ESI (MeOH, $C_{10}H_7Br_2N_3$): calcd. $[M+H]^+$ = 388.2244, found $[M+H]^+$ = 388.2250; calcd. $[M+Na]^+$ = 410.2064, found $[M+Na]^+$ = 410.2071.

^{1}H-NMR (500 MHz, acetone-d_6): δ (ppm) = 8.48 (d, $^3J_{HH}$ = 2.6 Hz, 2 H, H_{13}), 7.71 (2 H, H_{15}), 7.69 (t, $^3J_{HH}$ = 8.0 Hz, 2 H, H_4), 7.53 (d, $^3J_{HH}$ = 7.9 Hz, 2 H, H_3), 7.10 (d, $^3J_{HH}$ = 8.3 Hz, 2 H, H_5), 6.45 (dd, $^3J_{HH}$ = 2.6 Hz, $^3J_{HH}$ = 1.6 Hz, 2 H, H_{14}), 4.34 (m, 2 H, H_8), 1.72 (m, 2 H, H_9), 1.05 (s, 2 H, H_{11}).

^{13}C{^{1}H}-NMR (101 MHz, acetone-d_6): δ (ppm) = 155.9 (C_6), 150.7 (C_2), 142.1 (C_{15}), 140.1 (C_4), 127.1 (C_{13}), 112.0 (C_5), 107.8 (C_{14}), 104.8 (C_3), 45.4 (C_8), 41.4 (C_9), 30.2 (C_{10}), 29.6 (C_{11}).

^{15}N-NMR (41 MHz, acetone-d_6): δ (ppm) = 298 (N_{16}), 254 (N_1), 226 (N_{12}), 254 (N_7).

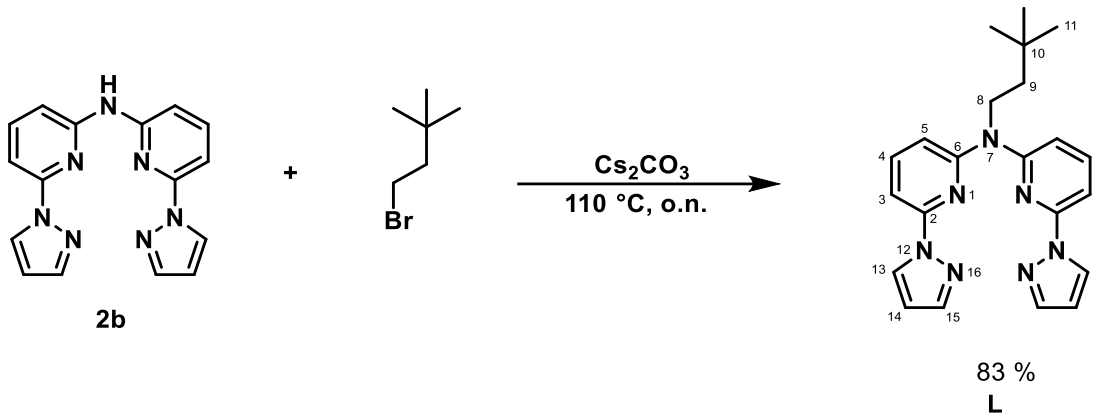

83 %

L

Bis(6-(1*H*-pyrazol-1-yl)-pyridin-2-yl)-3,3-dimethylbutylamine (L). **2b** (0.4072 g, 1.34 mmol, 1.0 eq.) and 1-bromo-3,3-dimethylbutane (0.46 g, 2.79 mmol, 2.1 eq.) were dissolved in DMF (20 mL) and Cs_2CO_3 (2.2444 g, 6.89 mmol, 5.1 eq.) was added to this solution. The reaction mixture was heated up to 85 °C and stirred for three days. After cooling the mixture to room temperature, the Cs_2CO_3 was filtered off and the solvent was removed under reduced pressure. The crude product was purified by column chromatographic separation on silica (toluene) to yield **L** as a white solid. Yield: 0.4319 g, 1.11 mmol, 83 %.

For the analytical data, see previous experimental description.

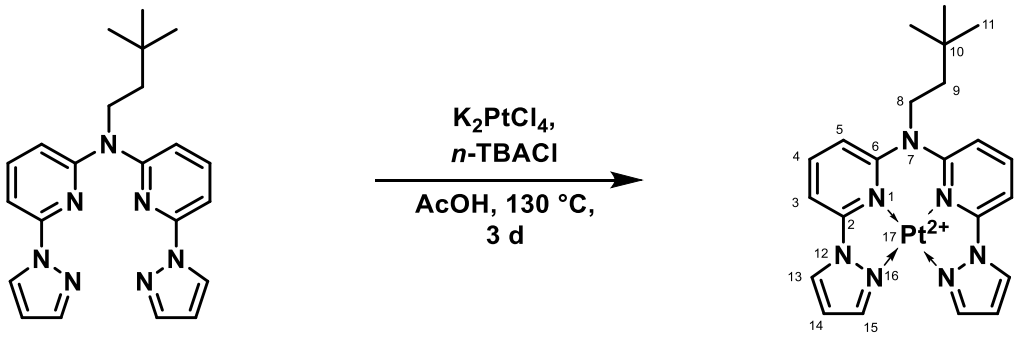

Pt(II) complex (C1). L (0.1581 g, 0.41 mmol, 1.0 eq.), K_2PtCl_4 (0.1677 g, 0.40 mmol, 1.0 eq.) and *n*-TBACl (catalytic amount) were dissolved in glacial acetic acid (25 mL). The reaction mixture was purged with Argon at room temperature for 10 minutes and then stirred for three days at 130 °C. After cooling to room temperature, the solvent was removed under reduced pressure. The crude product was washed with acetone (3 x 20 mL) to yield **C1** as a yellow solid.

EM-MS-ESI (MeOH, $C_{22}H_{25}ClN_7Pt^+$): calcd. $[M]^+$ = 617.1502, found $[M]^+$ = 617.1514.

EM-MS-ESI (MeOH, $C_{22}H_{25}N_7Pt^{2+}$): calcd. $[M]^+$ = 291.0907, found $[M]^+$ = 291.0916.

^{1}H-NMR (400 MHz, methanol-d_4): δ (ppm) = 9.28 (d, $^3J_{HH}$ = 3.2 Hz, 2 H, H_{13}), 8.91 (d, $^3J_{HH}$ = 2.3 Hz, 2 H, H_{15}), 8.62 (t, $^3J_{HH}$ = 8.5 Hz, 2 H, H_4), 8.18 (d, $^3J_{HH}$ = 8.1 Hz, 2 H, H_3), 7.85 (d, $^3J_{HH}$ = 8.8 Hz, 2 H, H_5), 7.21 (t, $^3J_{HH}$ = 2.8 Hz, 2 H, H_{14}), 4.60 (m, 2 H, H_8), 1.97 (m, 2 H, H_9), 1.14 (s, 2 H, H_{11}).

^{13}C{^{1}H}-NMR (126 MHz, methanol-d_4): δ (ppm) = 149.4 (C_6), 148.2 (C_2), 146.3 (C_{15}), 145.2 (C_4), 134.5 (C_{13}), 116.8 (C_5), 112.5 (C_{14}), 107.7 (C_3), 55.4 (C_8), 41.2 (C_9), 31.4 (C_{10}), 29.6 (C_{11}).

^{15}N-NMR (51 MHz, methanol-d_4): δ (ppm) = 222 (N_{12}), 199 (N_{16}), 155 (N_1), 119 (N_7).

^{195}Pt-NMR (86 MHz, methanol-d_4): δ (ppm) = -2867 (Pt_{17}).

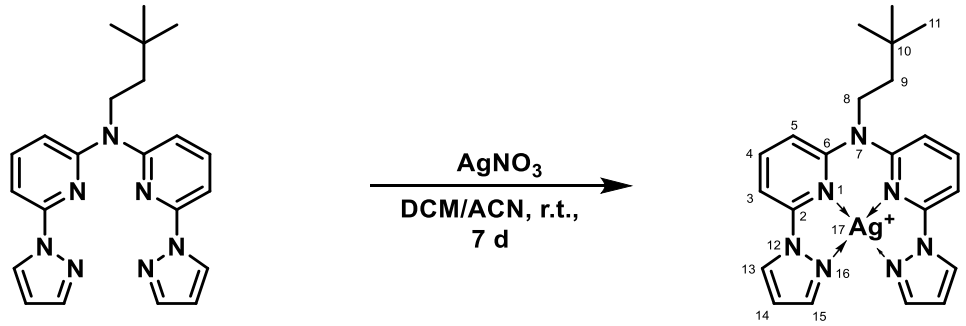

L C2

Ag(I) complex (C2). L (0.1110 g, 0.29 mmol, 1.0 eq.) and $AgNO_3$ (0.0515g, 0.30 mmol, 1.0 eq.) were dissolved in a mixture of DCM (20 mL) and ACN (5 mL). The reaction mixture was stirred for seven days at room temperature in a light-protected environment. The solvent was removed under reduced pressure and the crude was washed with acetone (3 x 20 mL). **C2** was obtained as a white solid. Colorless crystals were obtained from slow evaporation of a saturated MeOH solution of **C2** in a light-protected environment.

EM-MS-ESI (MeOH, $C_{22}H_{25}N_7Ag^+$): calcd. $[M]^+$ = 494.1217, found $[M]^+$ = 494.1228.

^{1}H-NMR (400 MHz, DMSO-d_6): δ (ppm) = 8.44 (d, $^3J_{HH}$ = 2.4 Hz, 2 H, H_{13}), 7.85 (t, $^3J_{HH}$ = 8.0 Hz, 2 H, H_4), 7.81 (d, $^3J_{HH}$ = 1.8 Hz, 2 H, H_{15}), 7.47 (d, $^3J_{HH}$ = 7.8 Hz, 2 H, H_3), 7.17 (d, $^3J_{HH}$ = 8.2 Hz, 2 H, H_5), 6.59 (dd, $^3J_{HH}$ = 2.4 Hz, $^3J_{HH}$ = 1.8 Hz, 2 H, H_{14}), 4.24 (m, 2 H, H_8), 1.60 (m, 2 H, H_9), 0.98 (s, 9 H, H_{11}).

^{13}C{^{1}H}-NMR (101 MHz, DMSO-d_6): δ (ppm) = 154.7 (C_6), 149.2 (C_2), 142.1 (C_{15}), 140.7 (C_4), 126.6 (C_{13}), 111.7 (C_5), 108.0 (C_{14}), 104.4 (C_3), 44.6 (C_8), 40.5 (C_9), 29.5 (C_{10}), 29.1 (C_{11}).

^{15}N-NMR (41 MHz, DMSO-d_6): δ (ppm) = 298 (N_{16}), 251 (N_1), 225 (N_{12}), 113 (N_7).

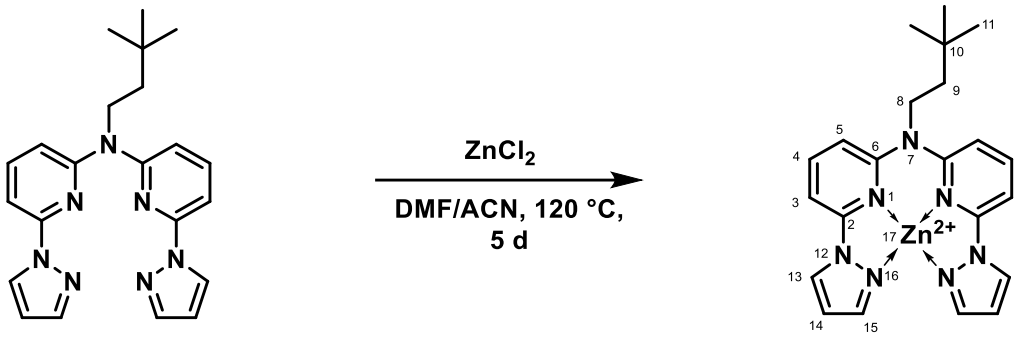

L C3

Zn(II) complex (C3). L (0.1438 g, 0.37 mmol, 1.0 eq.) and $ZnCl_2$ (0.081 g, 0.59 mmol, 1.6 eq.) were dissolved in a mixture of DMF (18 mL) and ACN (2 mL). The reaction mixture was purged with argon at room temperature for 10 minutes and then stirred for five days at 120 °C. After cooling to room temperature, the solvent was removed under reduced pressure. The crude product was washed with DCM (3 x 20 mL) and acetone (3 x 20 mL) to yield **C3** as a white solid. Colorless crystals were obtained from slow evaporation of a saturated MeOH solution of **C3**.

EM-MS-ESI (MeOH, $C_{22}H_{25}ClN_7Zn^+$): calcd. $[M]^+$ = 486.1146, found $[M]^+$ = 486.1147.

^{1}H-NMR (400 MHz, DMSO-d_6): δ (ppm) = 8.44 (d, $^3J_{HH}$ = 2.5 Hz, 2 H, H_{13}), 7.85 (t, $^3J_{HH}$ = 8.0 Hz, 2 H, H_4), 7.81 (d, $^3J_{HH}$ = 1.2 Hz, 2 H, H_{15}), 7.48 (d, $^3J_{HH}$ = 7.8 Hz, 2 H, H_3), 7.18 (d, $^3J_{HH}$ = 8.2 Hz, 2 H, H_5), 6.58 (dd, $^3J_{HH}$ = 2.5 Hz, $^3J_{HH}$ = 1.2 Hz, 2 H, H_{14}), 4.29 (m, 2 H, H_8), 1.62 (m, 2 H, H_9), 0.99 (s, 9 H, H_{11}).

^{13}C{^{1}H}-NMR (101 MHz, DMSO-d_6): δ (ppm) = 155.2 (C_6), 149.4 (C_2), 142.0 (C_{15}), 140.6 (C_4), 126.4 (C_{13}), 111.7 (C_5), 108.0 (C_{14}), 104.2 (C_3), 44.4 (C_8), 40.6 (C_9), 29.5 (C_{10}), 29.1 (C_{11}).

^{15}N-NMR (51 MHz, DMSO-d_6): δ (ppm) = 301 (N_{16}), 252 (N_1), 226 (N_{12}), 113 (N_7).

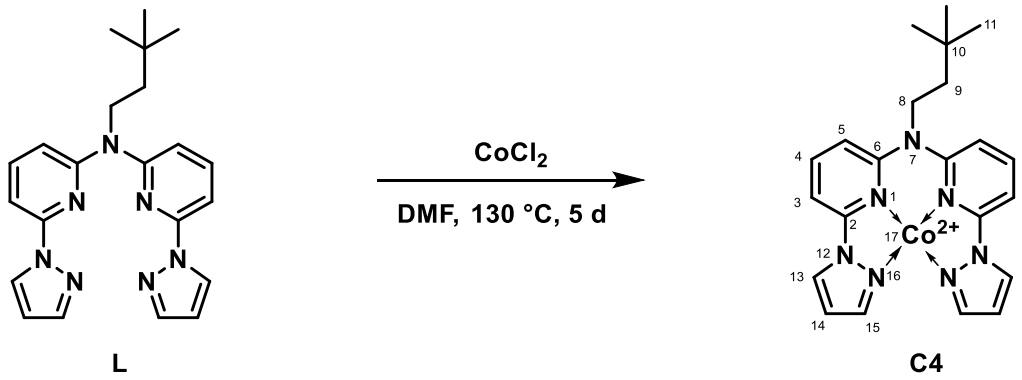

L C4

Co(II) complex (C4). L (0.2003 g, 0.52 mmol, 1.0 eq.) and $CoCl_2$ (0.0702 g, 0.54 mmol, 1.0 eq.) were dissolved in DMF (20 mL). The reaction mixture was purged with argon at room temperature for 10 minutes and then stirred for five days at 130 °C. After cooling to room temperature, the solvent was removed under reduced pressure. The crude product was washed with acetone (3 x 20 mL) to yield **C4** as a green solid.

EM-MS-ESI (MeOH, $C_{22}H_{25}ClCoN_7^+$): calcd. $[M]^+$ = 481.1186, found $[M]^+$ = 481.1207.

^{1}H-NMR (500 MHz, DMSO-d_6): δ (ppm) = 8.38 (br., 2 H, H_{13}), 7.77 (t, br., $^3J_{HH}$ = 7.8 Hz, 2 H, H_4), 7.73 (br., 2 H, H_{15}), 7.41 (d, br., $^3J_{HH}$ = 7.5 Hz, 2 H, H_3), 7.12 (d, br., $^3J_{HH}$ = 7.8 Hz, 2 H, H_5), 6.51 (br., 2 H, H_{14}), 4.22 (br., 2 H, H_8), 1.55 (br., 2 H, H_9), 0.93 (s, 9 H, H_{11}).

^{13}C{^{1}H}-NMR (126 MHz, DMSO-d_6): δ (ppm) = 152.4 (C_6), 147.0 (C_2), 139.8 (C_{15}), 138.3 (C_4), 124.1 (C_{13}), 109.4 (C_5), 105.7 (C_{14}), 101.9 (C_3), 42.0 (C_8), 38.2 (C_9), 27.1 (C_{10}), 26.8 (C_{11}).

^{15}N-NMR (51 MHz, DMSO-d_6): δ (ppm) = 301 (N_{16}), 225 (N_{12}).

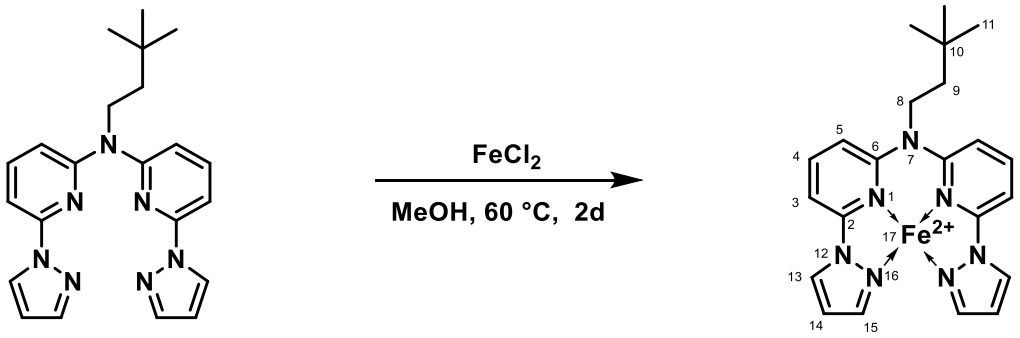

L C5

Fe(II) complex (C5). L (0.1011 g, 0.26 mmol, 1.0 eq.) and $FeCl_2$ x 4 H_2O (0.0622 g, 0.31 mmol, 1.2 eq.) were dissolved in MeOH (20 mL). The reaction mixture was purged with Argon at room temperature for 10 minutes and then stirred for two days at 60 °C. After cooling to room temperature, the solvent was removed under reduced pressure. The crude product was washed with water (3 x 20 mL) and acetone (3 x 10 mL) to yield **C5** as an orange solid. Yellowish crystals were obtained from slow evaporation of a saturated MeOH/acetone (1:1) solution of **C5**.

EM-MS-ESI (MeOH, $C_{22}H_{25}ClFeN_7^+$): calcd. $[M]^+$ = 478.1198, found $[M]^+$ = 478.1215.

^{1}H-NMR (400 MHz, DMSO-d_6): δ (ppm) = 8.41 (br., 2 H, H_{13}), 7.80 (br., 2 H, H_4), 7.79 (br., 2 H, H_{15}), 7.44 (br., 2 H, H_3), 7.15 (br., 2 H, H_5), 6.54 (br., 2 H, H_{14}), 4.25 (br., 2 H, H_8), 1.59 (br. 2H, H_9), 0.96 (s, 9 H, H_{11}).

^{13}C{^{1}H}-NMR (101 MHz, DMSO-d_6): δ (ppm) = 153.0 (C_6), 147.6 (C_2), 140.3 (C_{15}), 138.9 (C_4), 124.6 (C_{13}), 110.0 (C_5), 106.2 (C_{14}), 102.5 (C_3), 42.6 (C_8), 38.8 (C_9), 27.7 (C_{10}), 27.4 (C_{11}).

Section S2: NMR and mass spectra

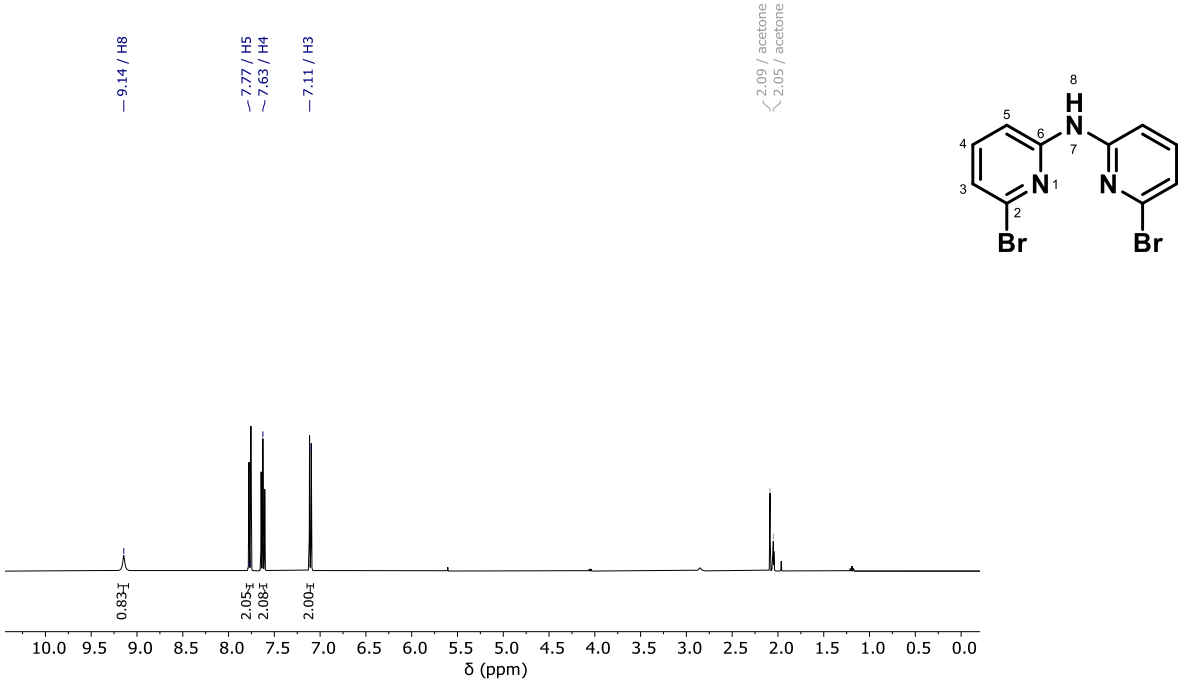

Figure S1. ^{1}H-NMR spectrum (400 MHz, acetone-d_6) of **1**.

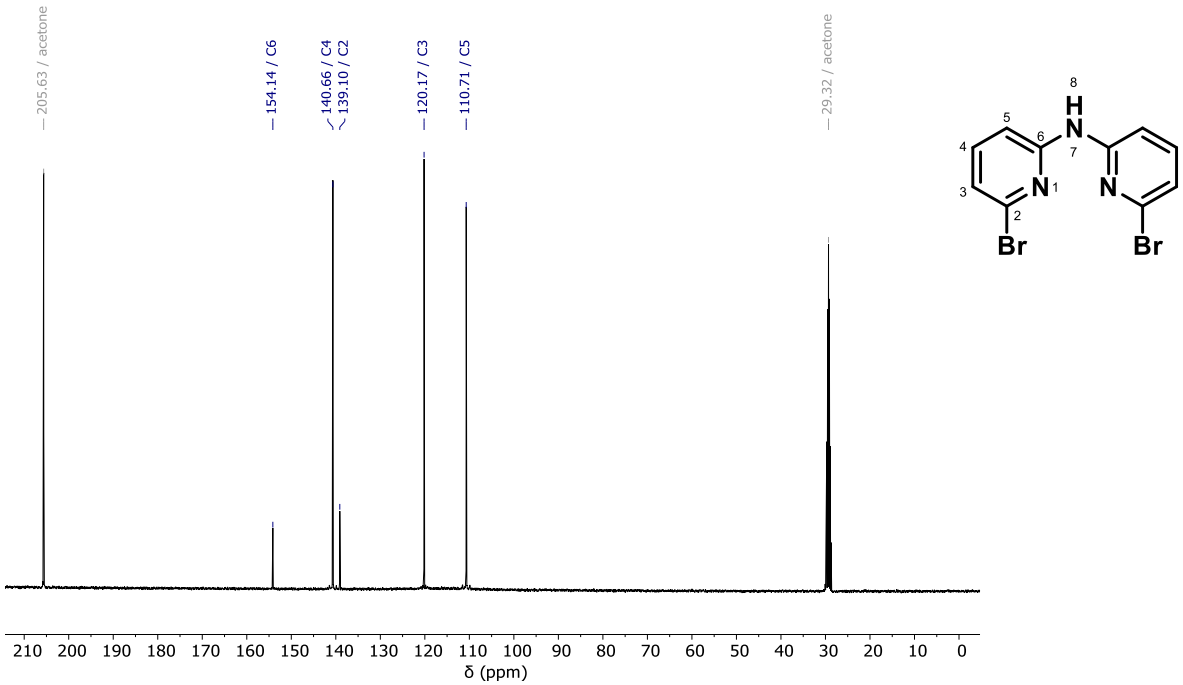

Figure S2. ^{13}C{^{1}H}-NMR spectrum (101 MHz, acetone-d_6) of **1**.

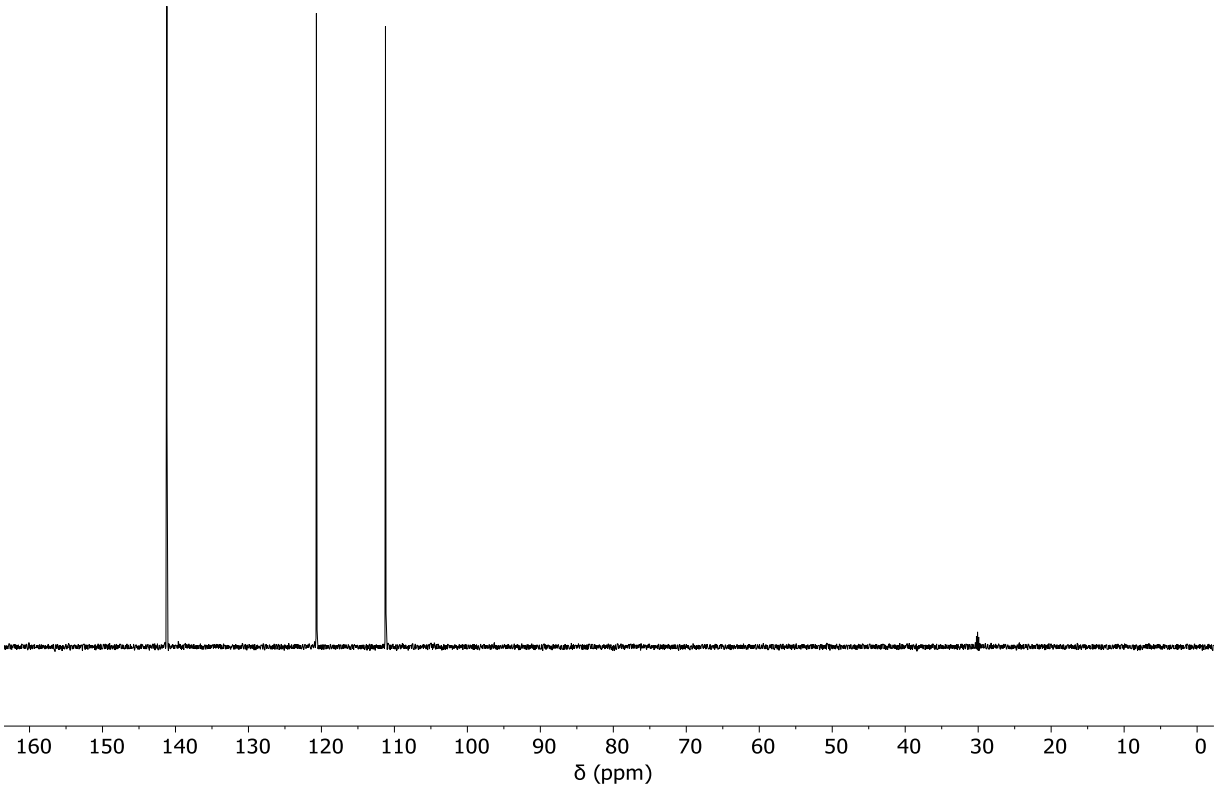

Figure S3. $^{13}C\{^{1}H\}$-NMR DEPT135 spectrum (126 MHz, acetone-d_6) of **1**.

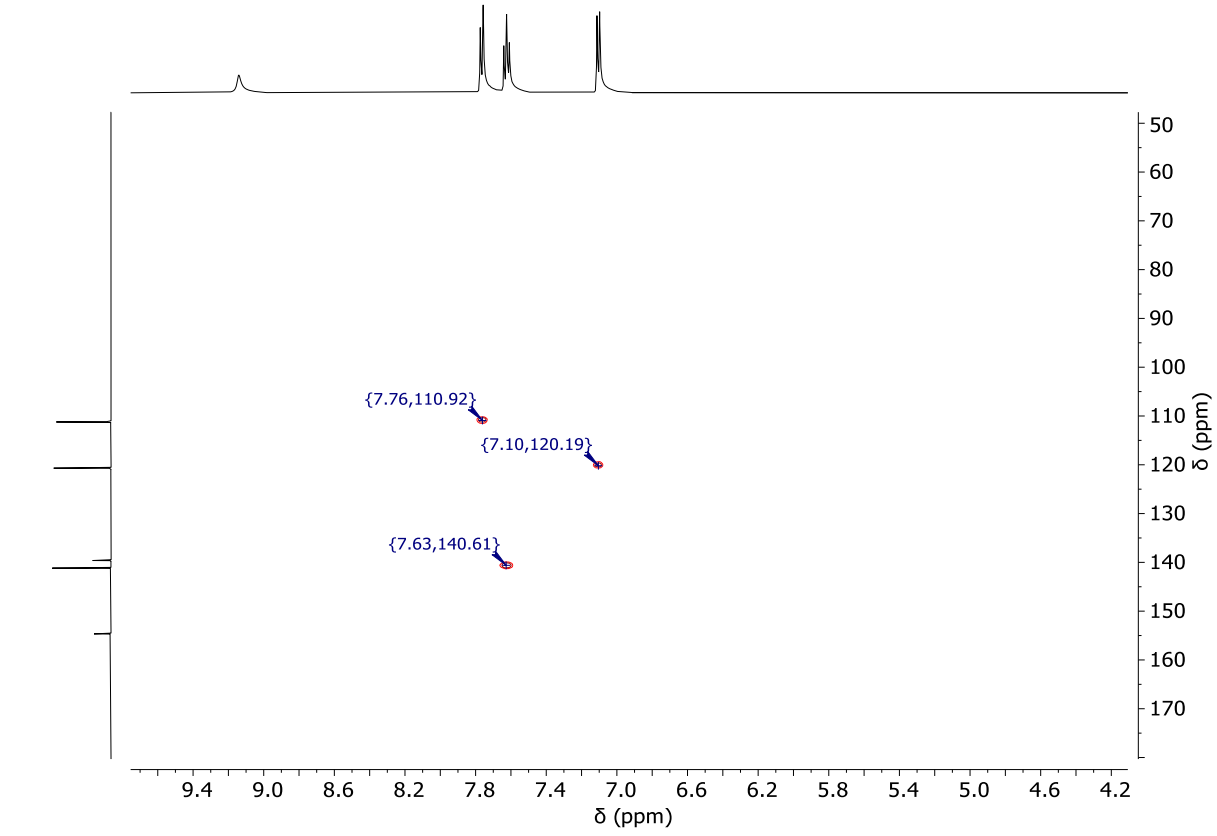

Figure S4. HC-HSQC spectrum (101 MHz (^{13}C), 400 MHz (^{1}H), acetone-d_6) of **1**.

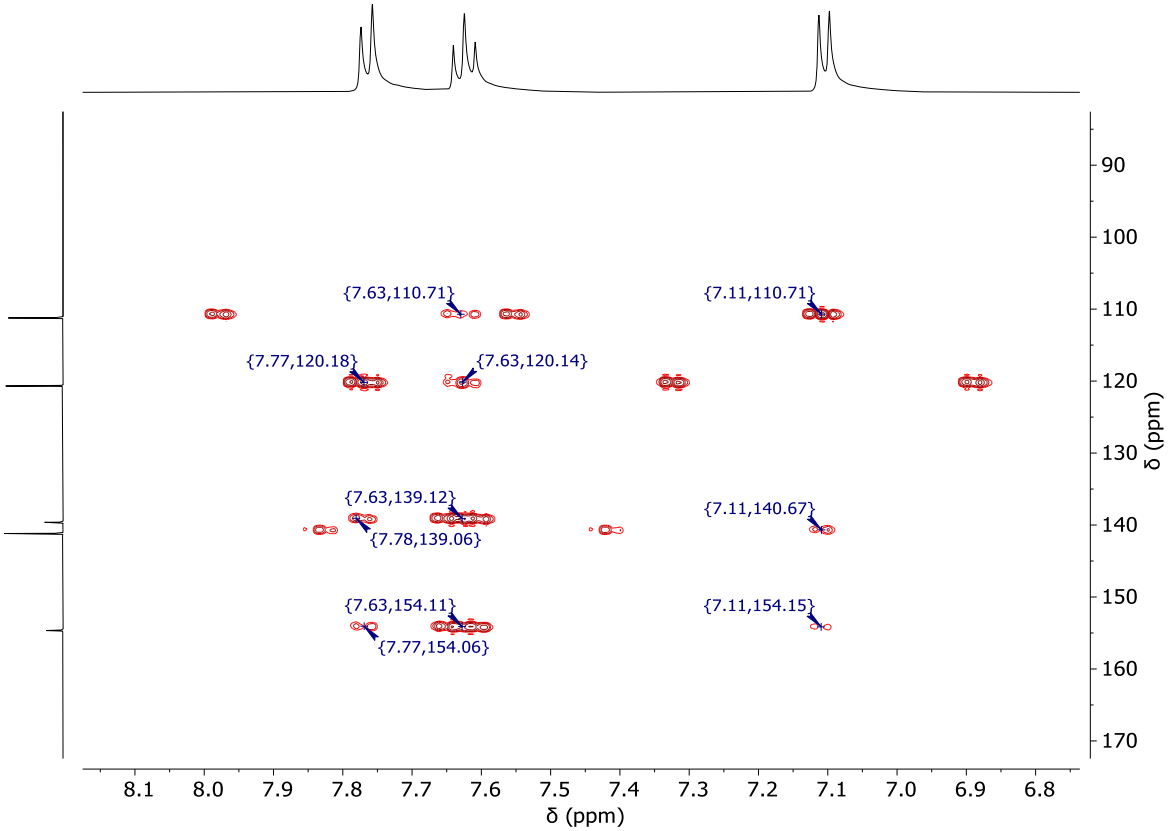

Figure S5. HC-HMBC-NMR spectrum (101 MHz (^{13}C), 400 MHz (^{1}H), acetone-d_6) of **1**.

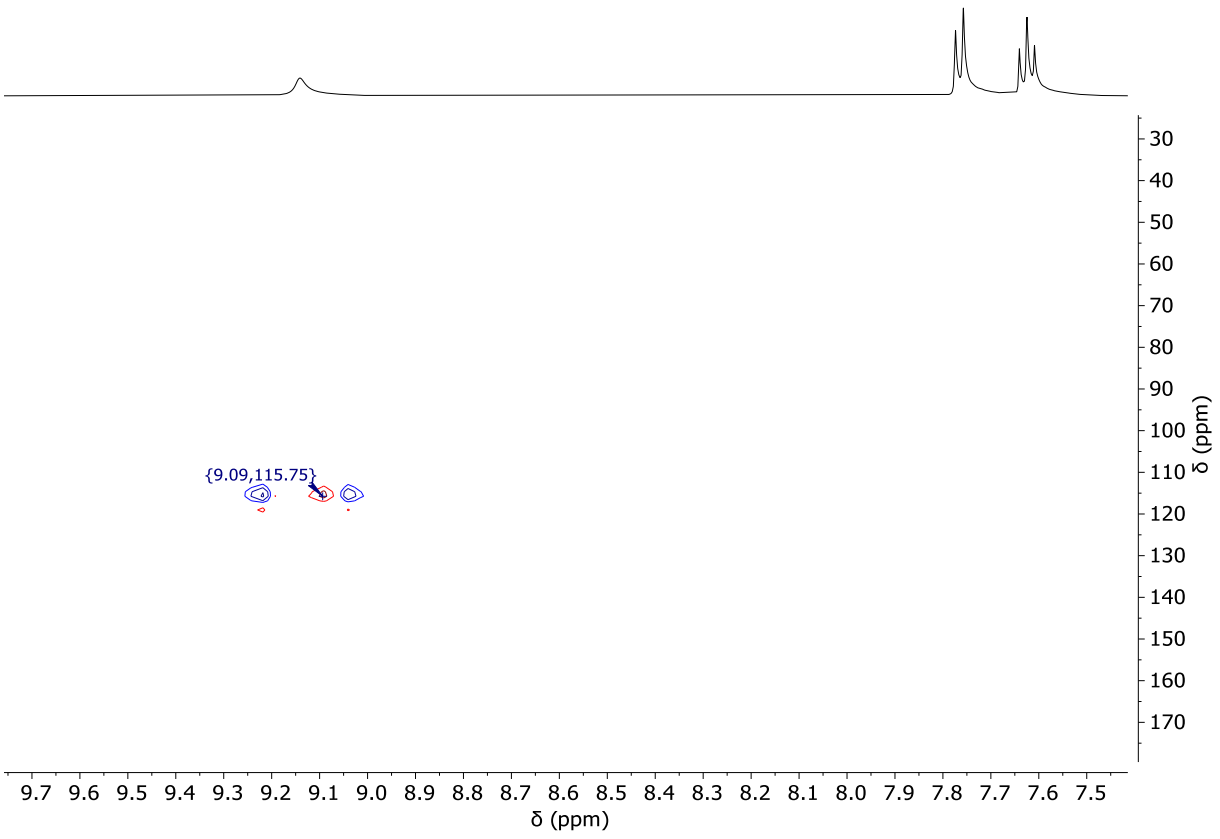

Figure S6. HN-HSQC-NMR spectrum (41 MHz (^{15}N), 400 MHz (^{1}H), acetone-d_6) of **1**.

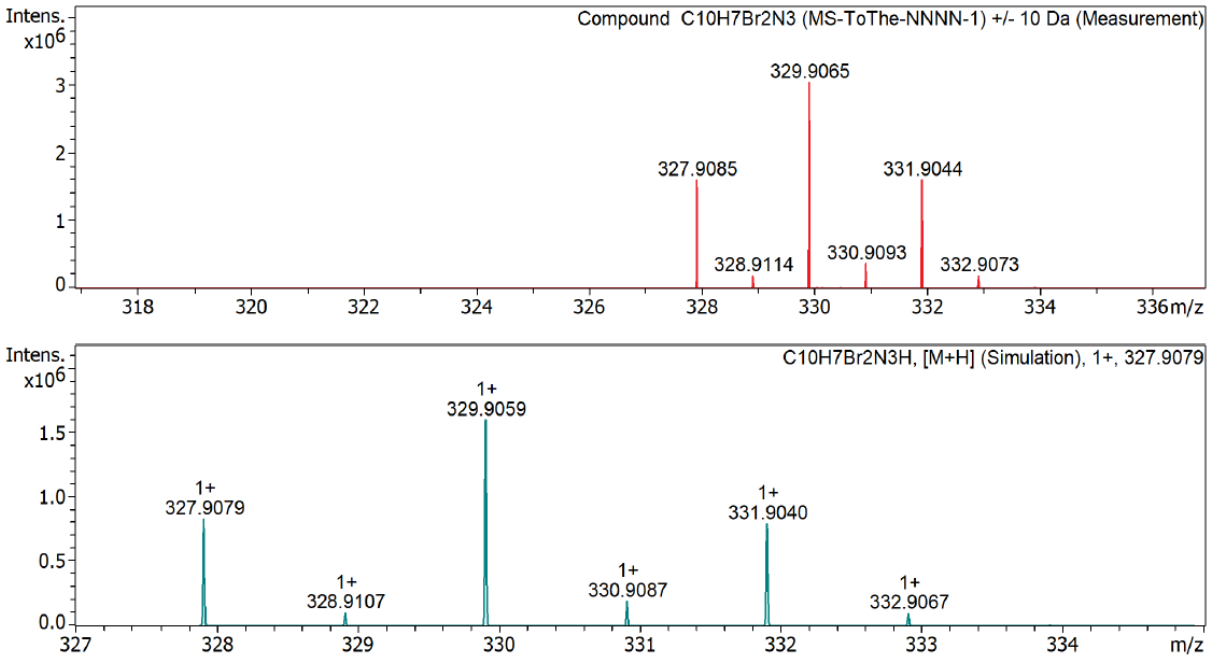

Figure S7. Mass spectrum of **1** (MeOH). Additional simulation for the [**1**+H]$^+$ adduct.

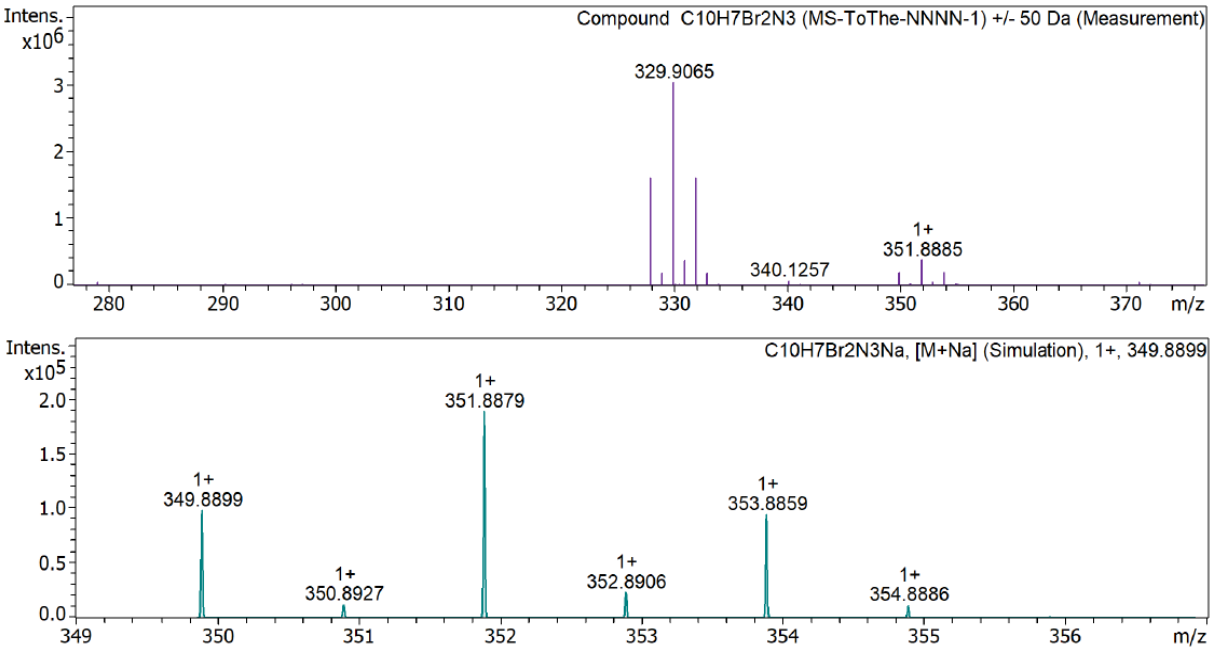

Figure S8. Mass spectrum of **1** (MeOH). Additional simulation for the [**1**+Na]$^+$ adduct.

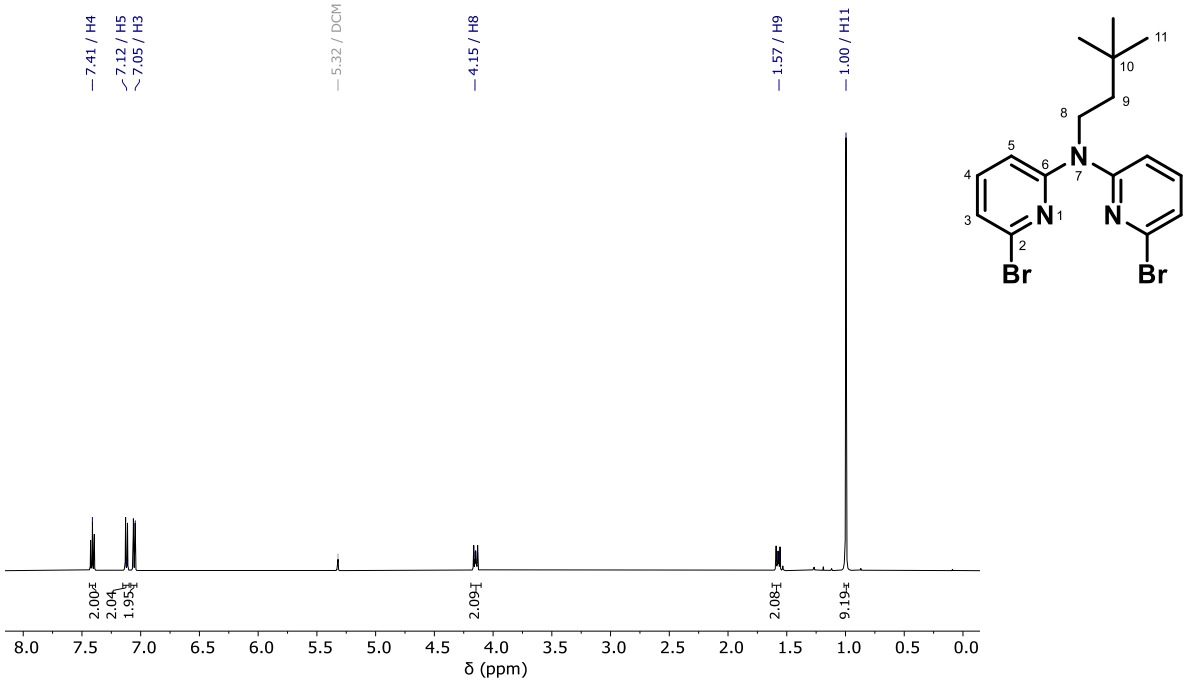

Figure S9. ^{1}H-NMR spectrum (500 MHz, DCM-d_2) of **2a**.

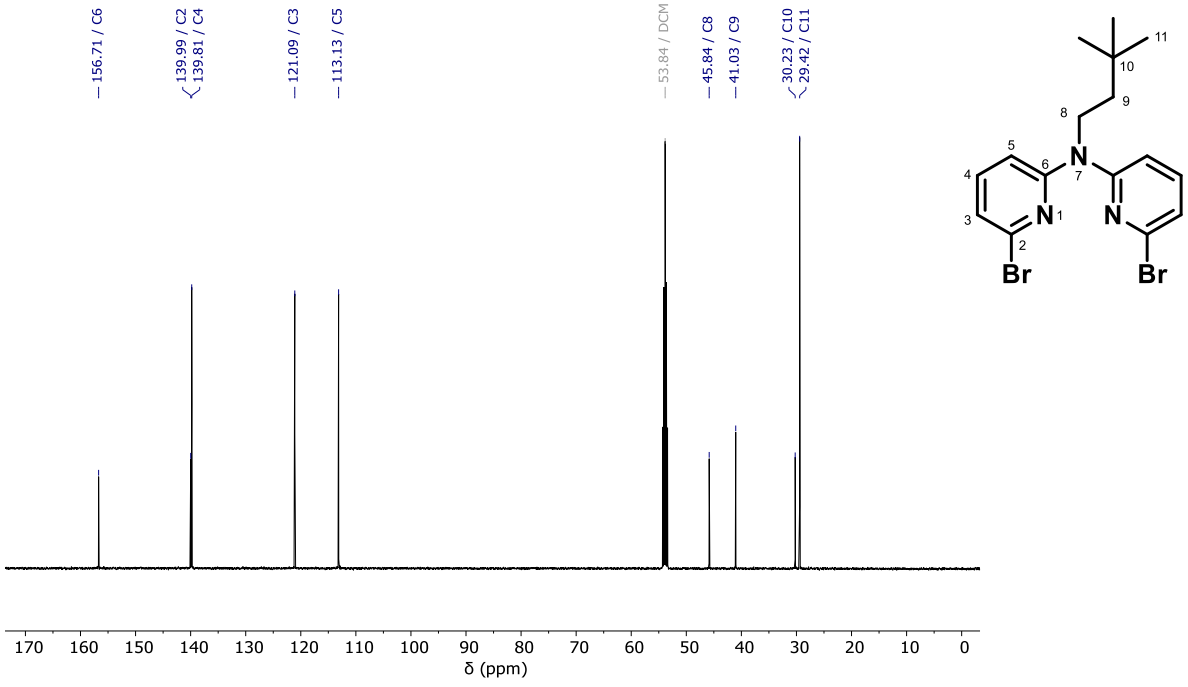

Figure S10. ^{13}C{^{1}H}-NMR spectrum (126 MHz, DCM-d_2) of **2a**.

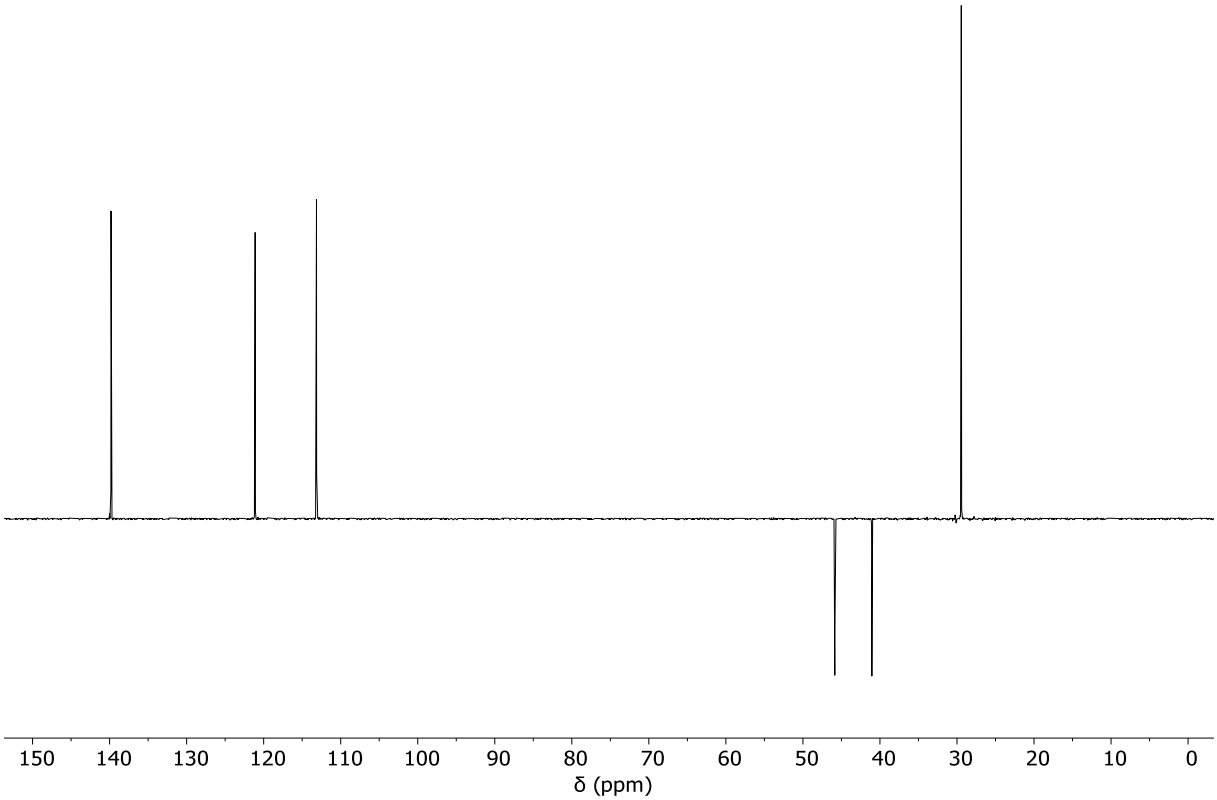

Figure S11. $^{13}C\{^{1}H\}$-NMR DEPT135 spectrum (101 MHz, DCM-d_2) of **2a**.

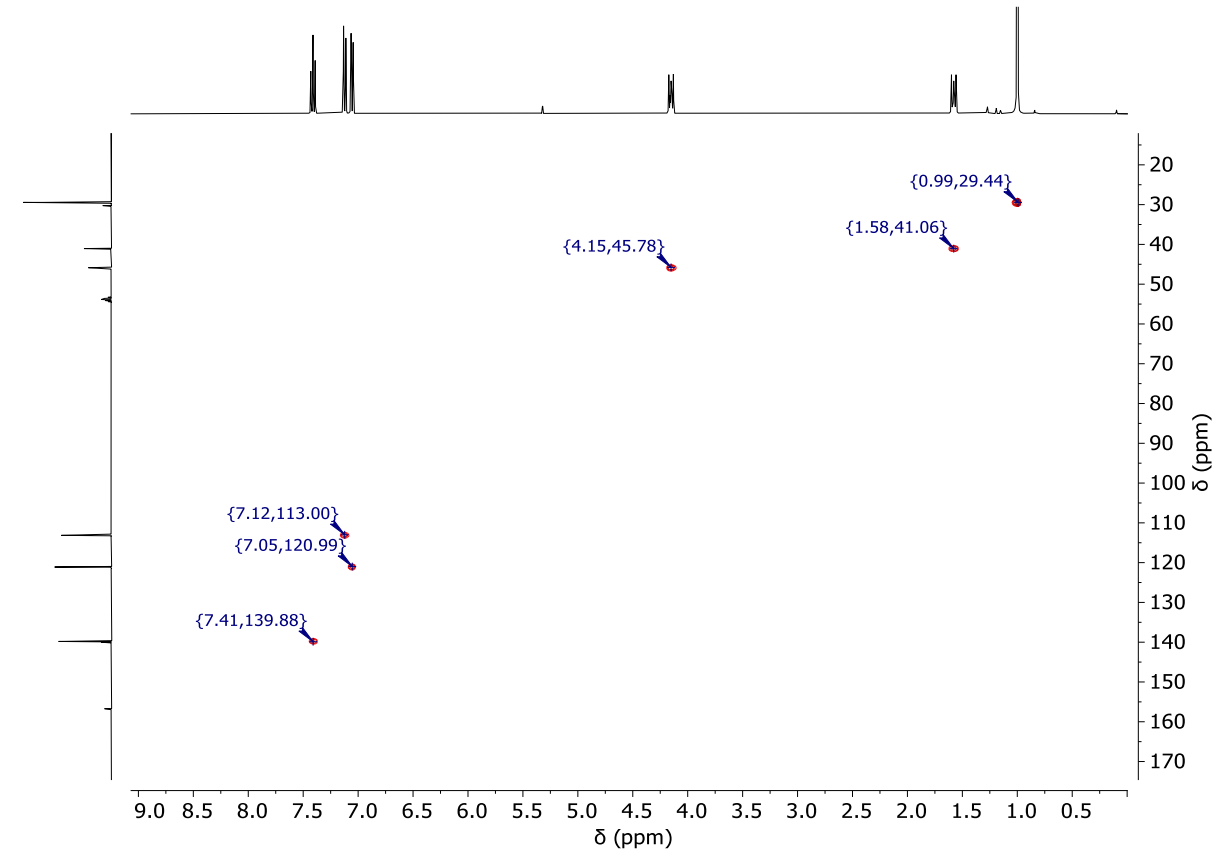

Figure S12. HC-HSQC spectrum (101 MHz (^{13}C), 400 MHz (^{1}H), DCM-d_2) of **2a**.

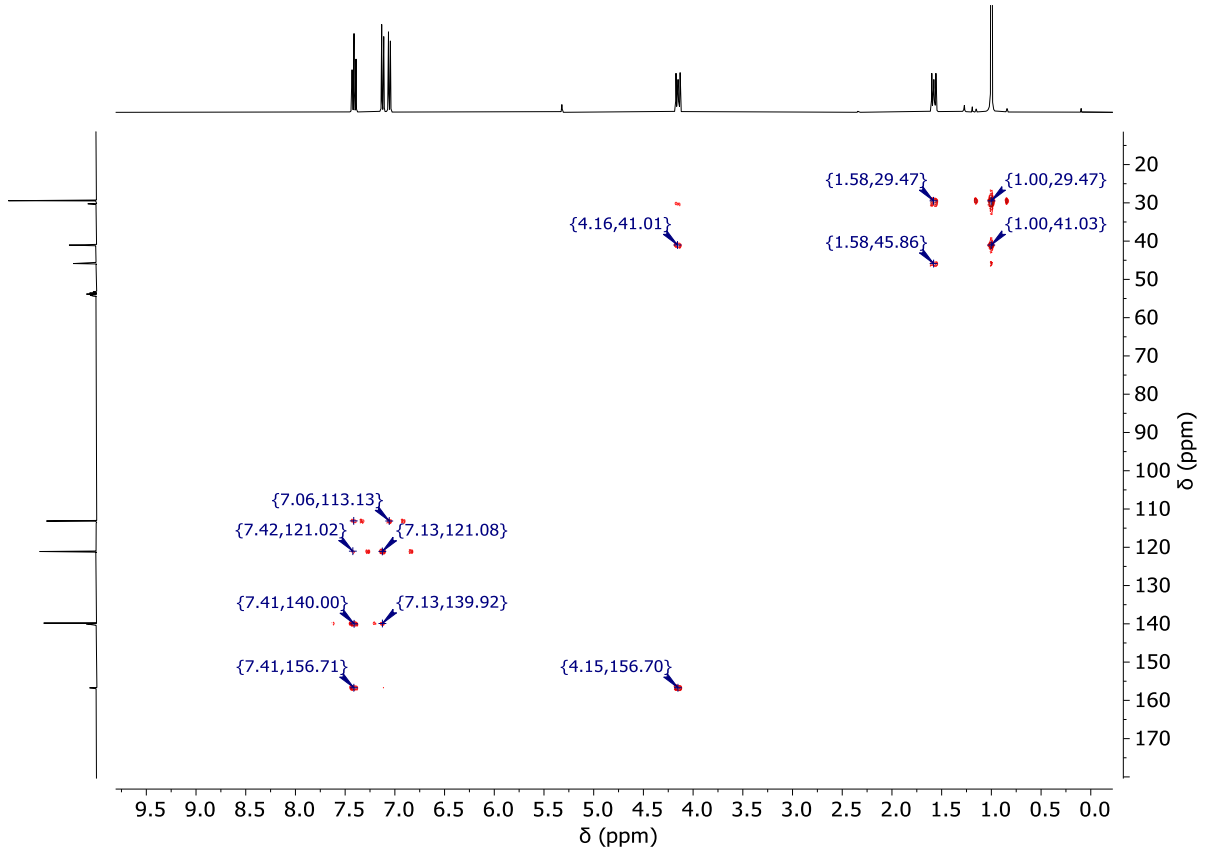

Figure S13. HC-HMBC-NMR spectrum (101 MHz (^{13}C), 400 MHz (^{1}H), DCM-d_2) of **2a**.

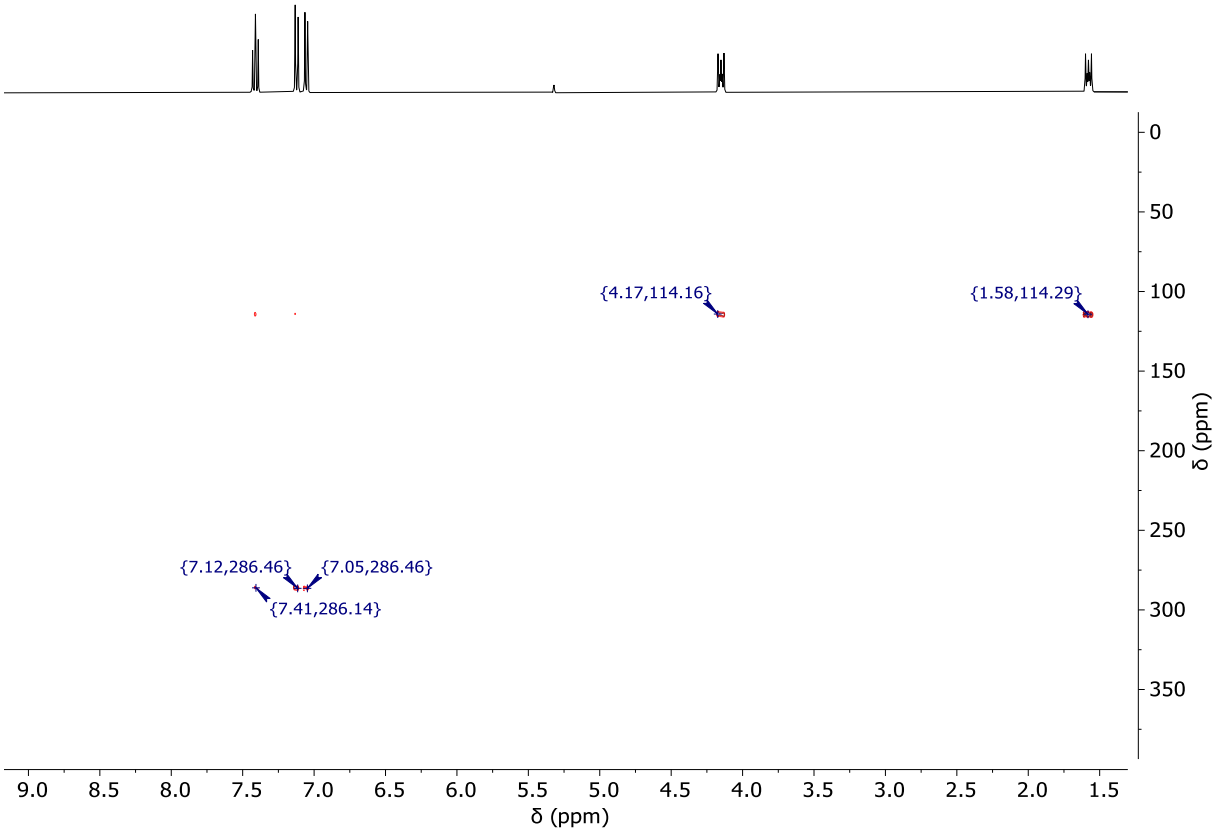

Figure S14. HN-HMBC-NMR spectrum (41 MHz (^{15}N), 400 MHz (^{1}H), DCM-d_2) of **2a**.

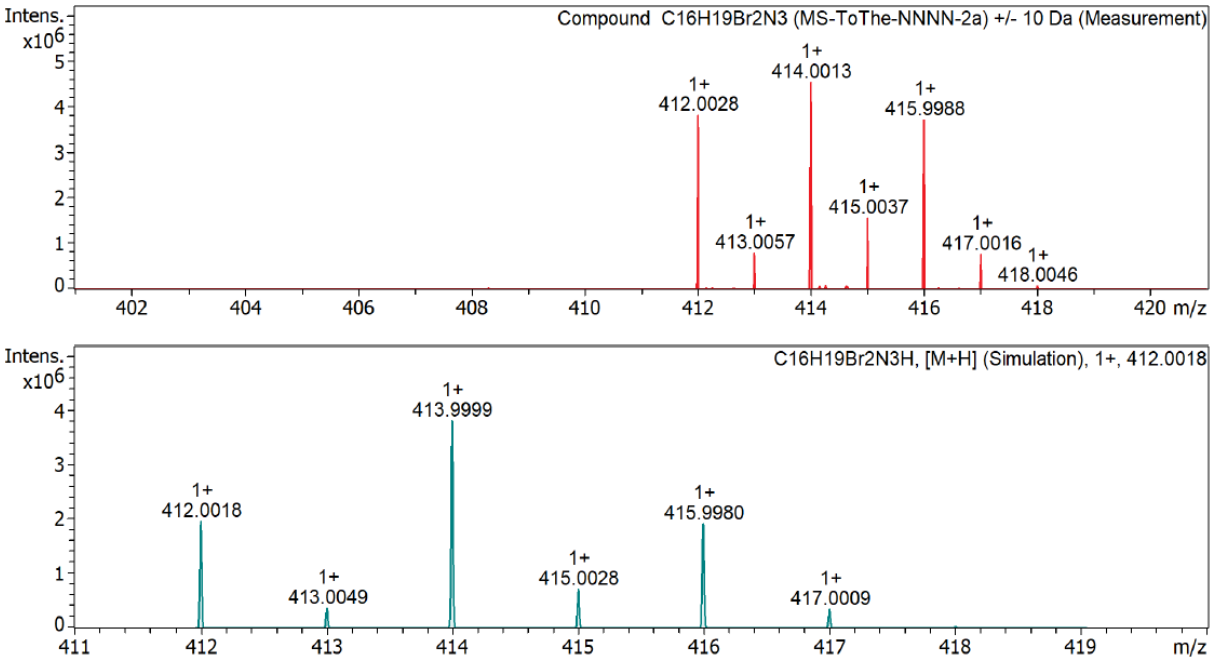

Figure S15. Mass spectrum of **2a** (MeOH). Additional simulation for the [**2a**+H]$^+$ adduct.

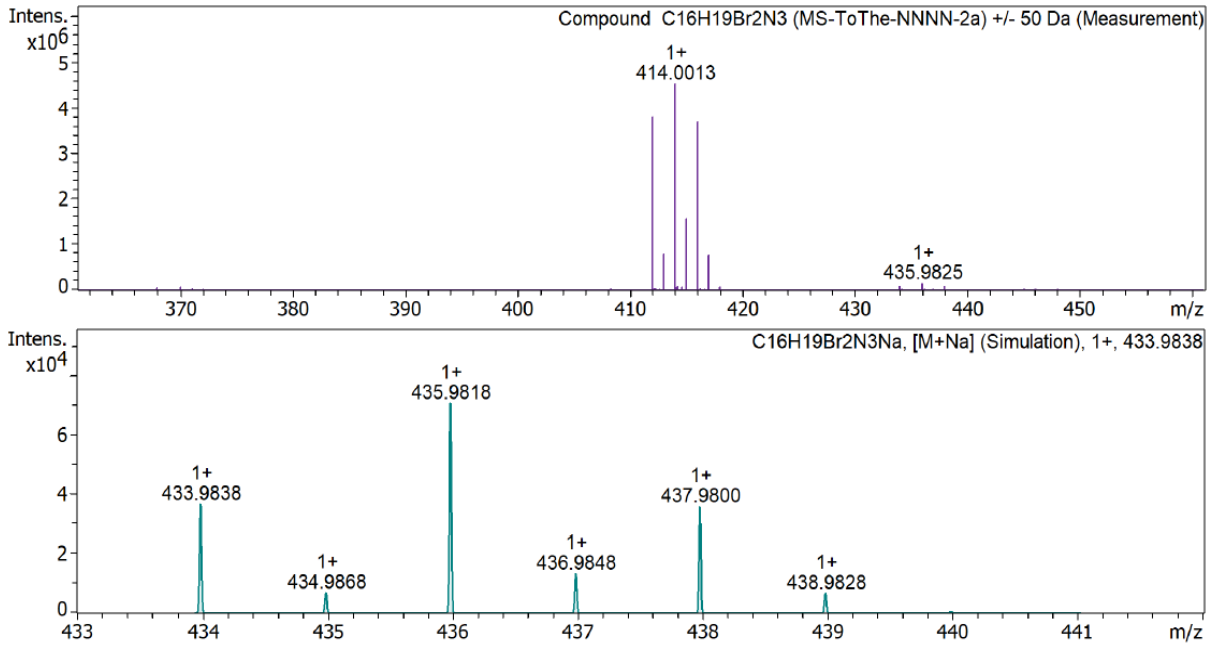

Figure S16. Mass spectrum of **2a** (MeOH). Additional simulation for the [**2a**+Na]$^+$ adduct.

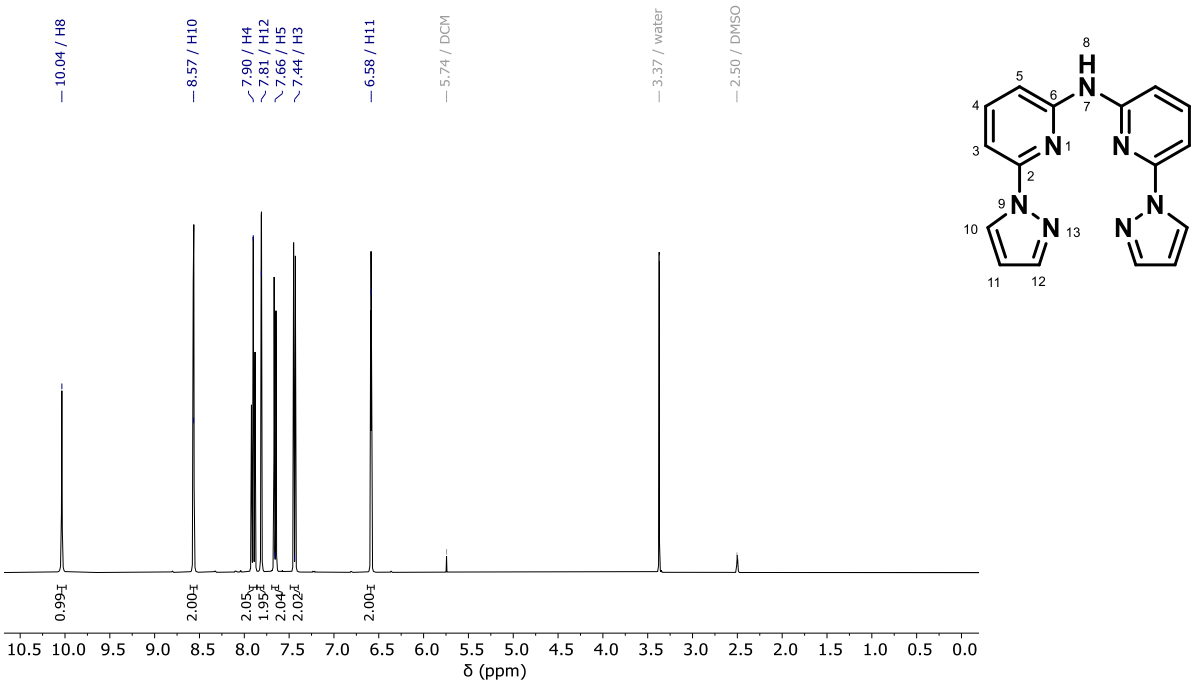

Figure S17. ^{1}H-NMR spectrum (400 MHz, DMSO-d_6) of **2b**.

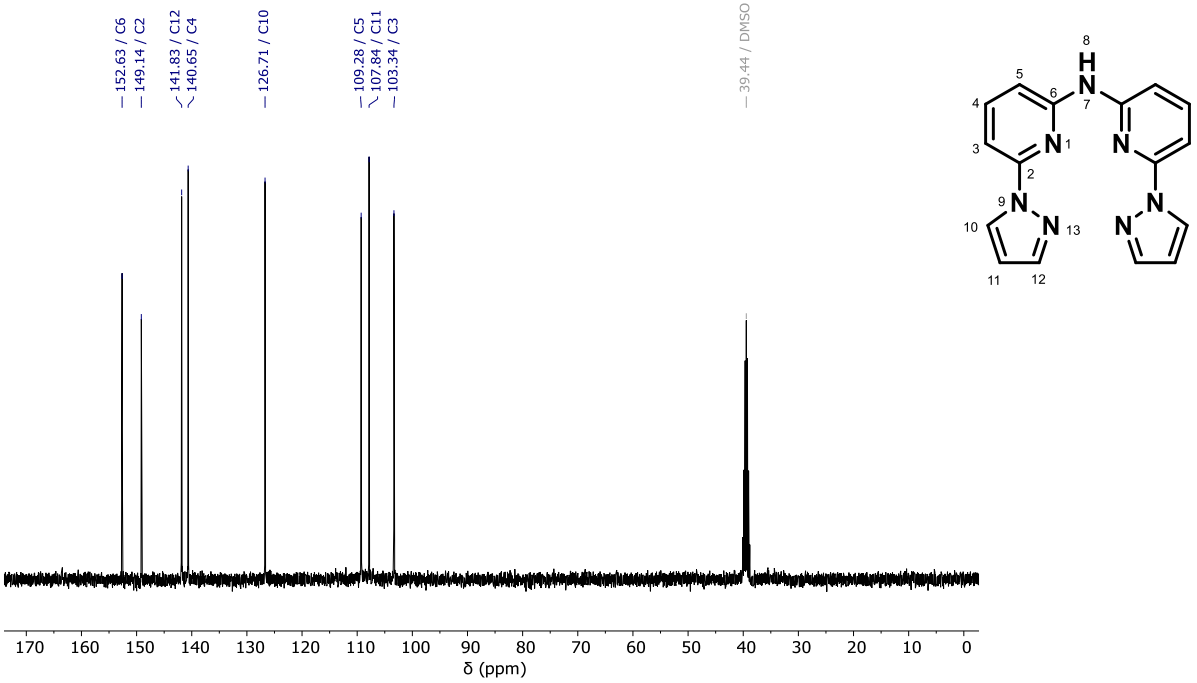

Figure S18. ^{13}C{^{1}H}-NMR spectrum (101 MHz, DMSO-d_6) of **2b**.

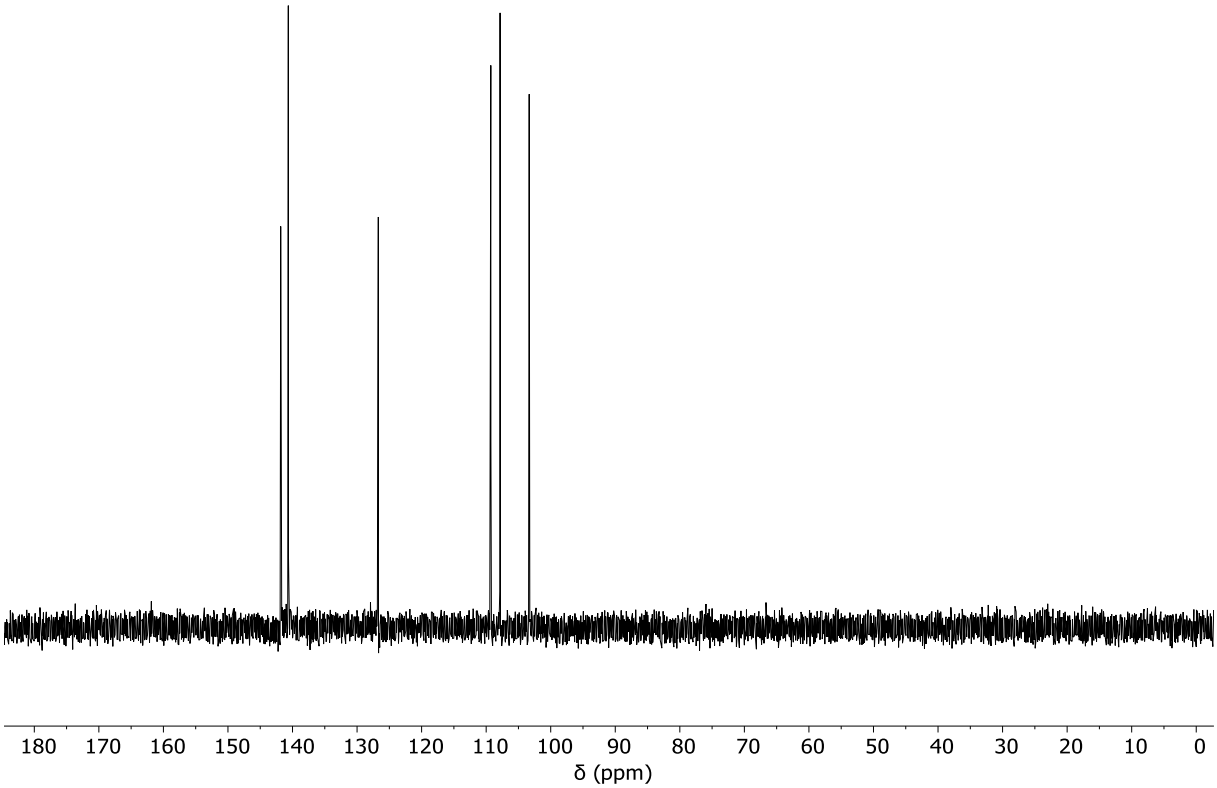

Figure S19. $^{13}C\{^{1}H\}$-NMR DEPT135 spectrum (101 MHz, DMSO-d_6) of **2b**.

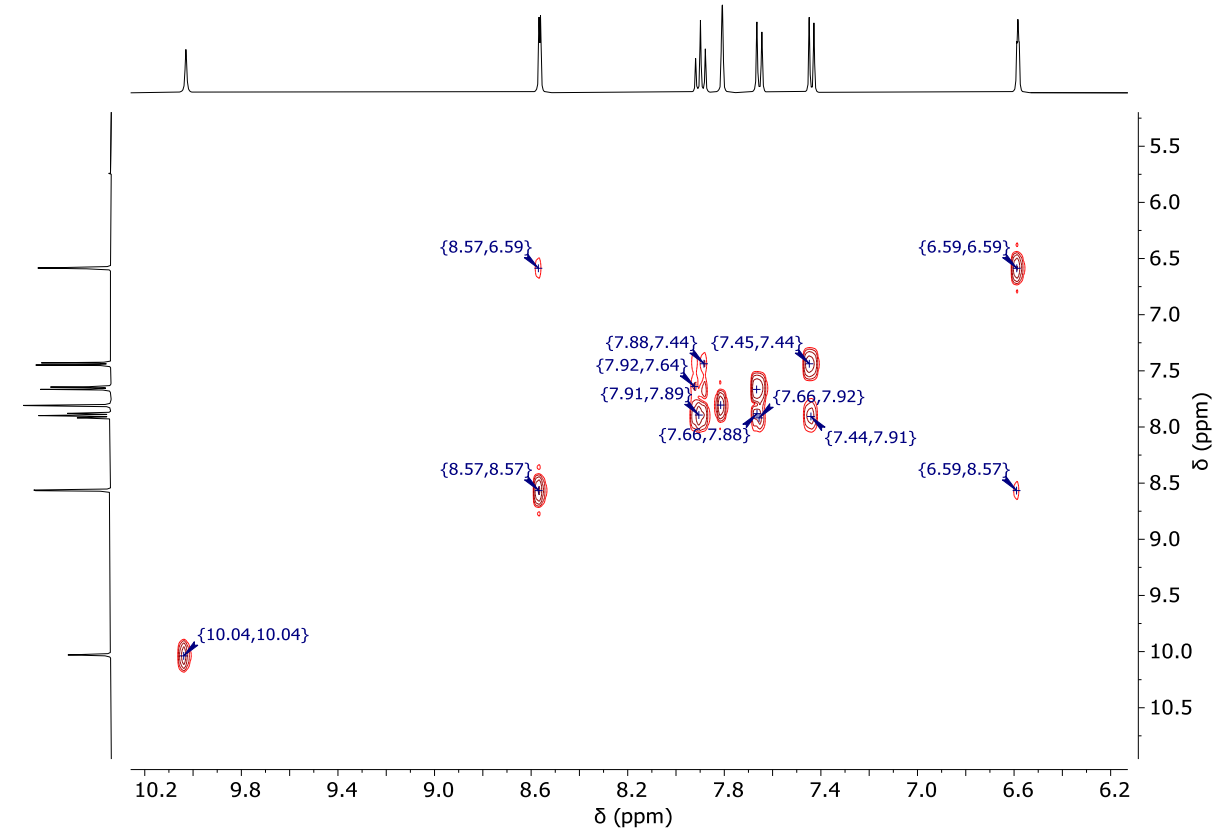

Figure S20. H,H-COSY-NMR spectrum (400 MHz, DMSO-d_6) of **2b**.

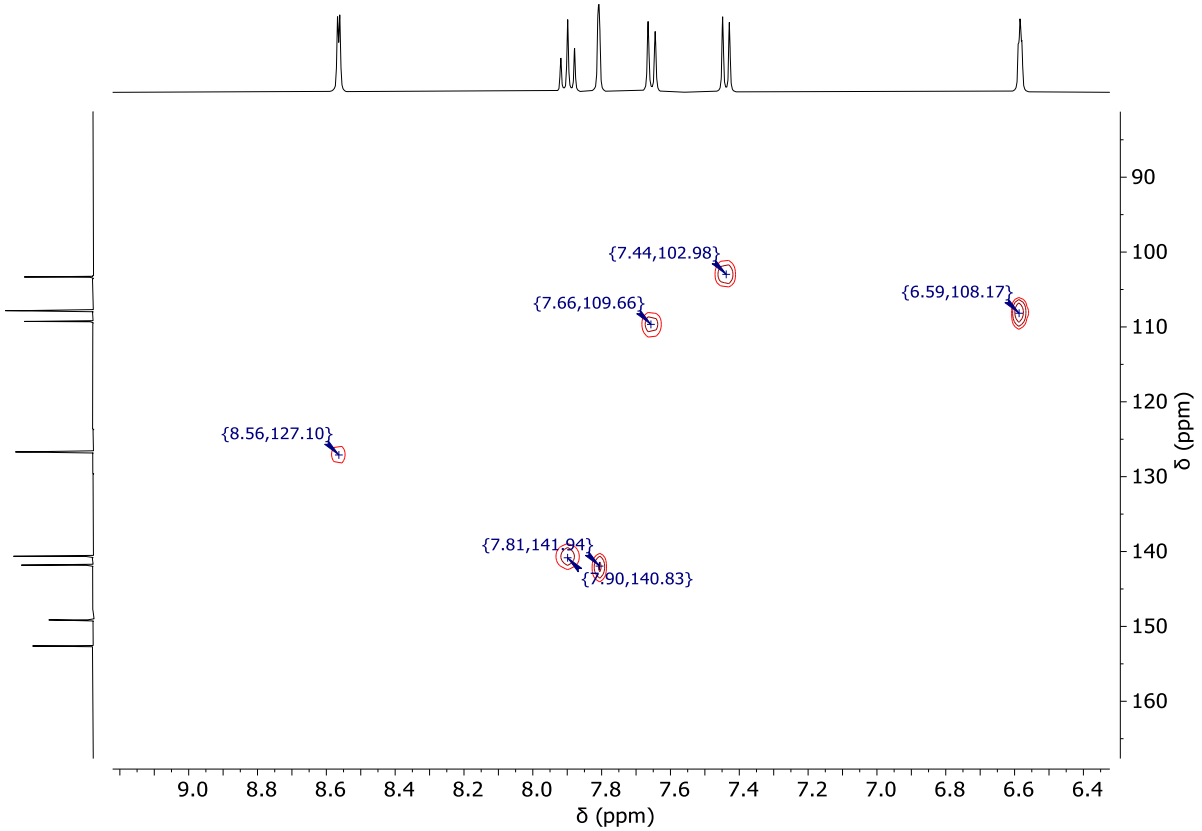

Figure S21. HC-HSQC spectrum (101 MHz (^{13}C), 400 MHz (^{1}H), DMSO-d_6) of **2b**.

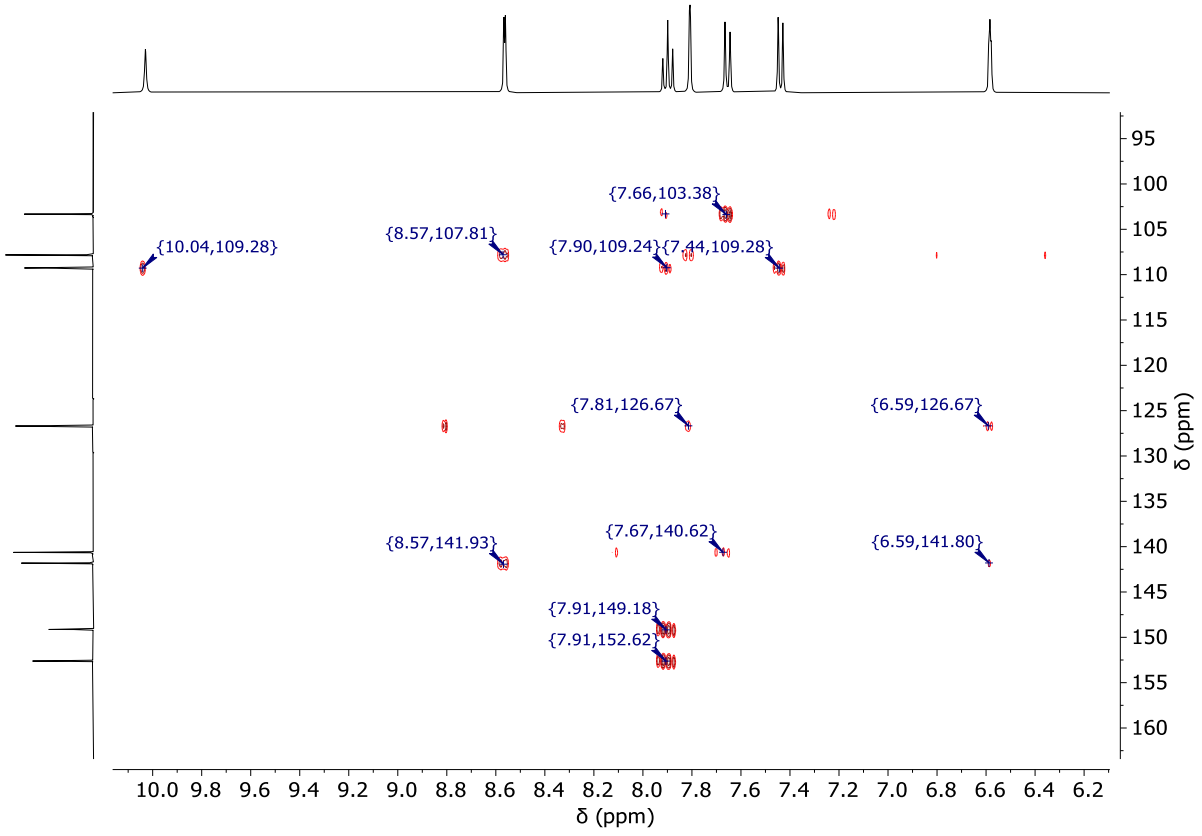

Figure S22. HC-HMBC-NMR spectrum (101 MHz (^{13}C), 400 MHz (^{1}H), DMSO-d_6) of **2b**.

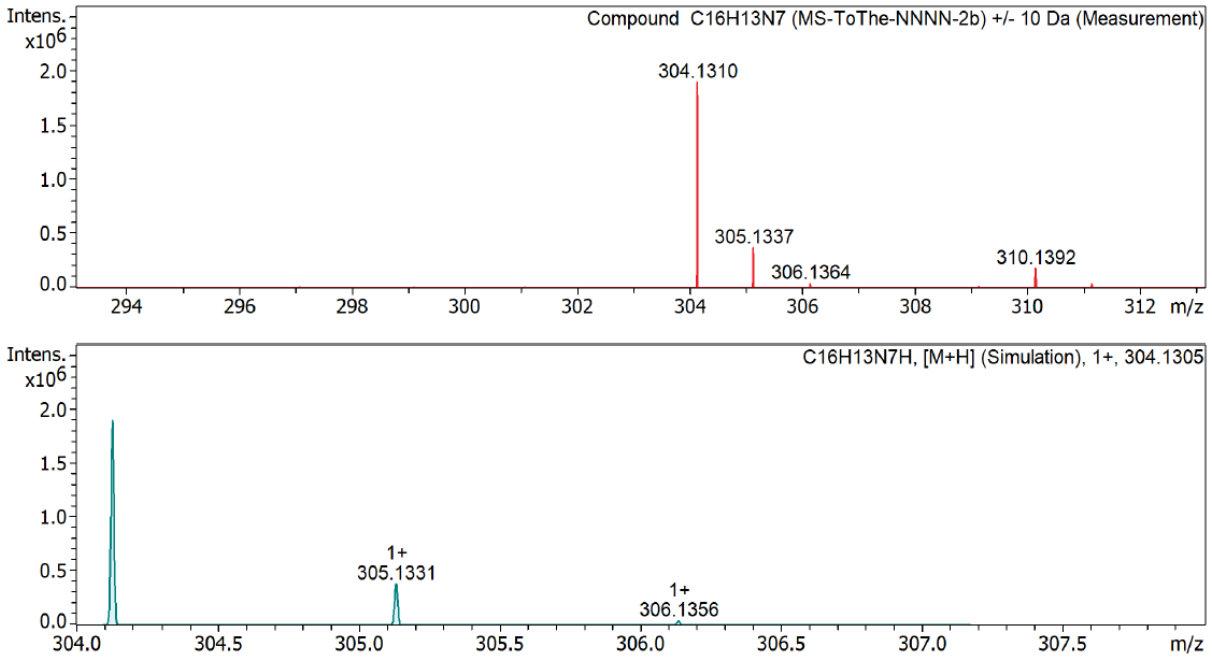

Figure S23. Mass spectrum of **2b** (MeOH). Additional simulation for the [**2b**+H]$^+$ adduct.

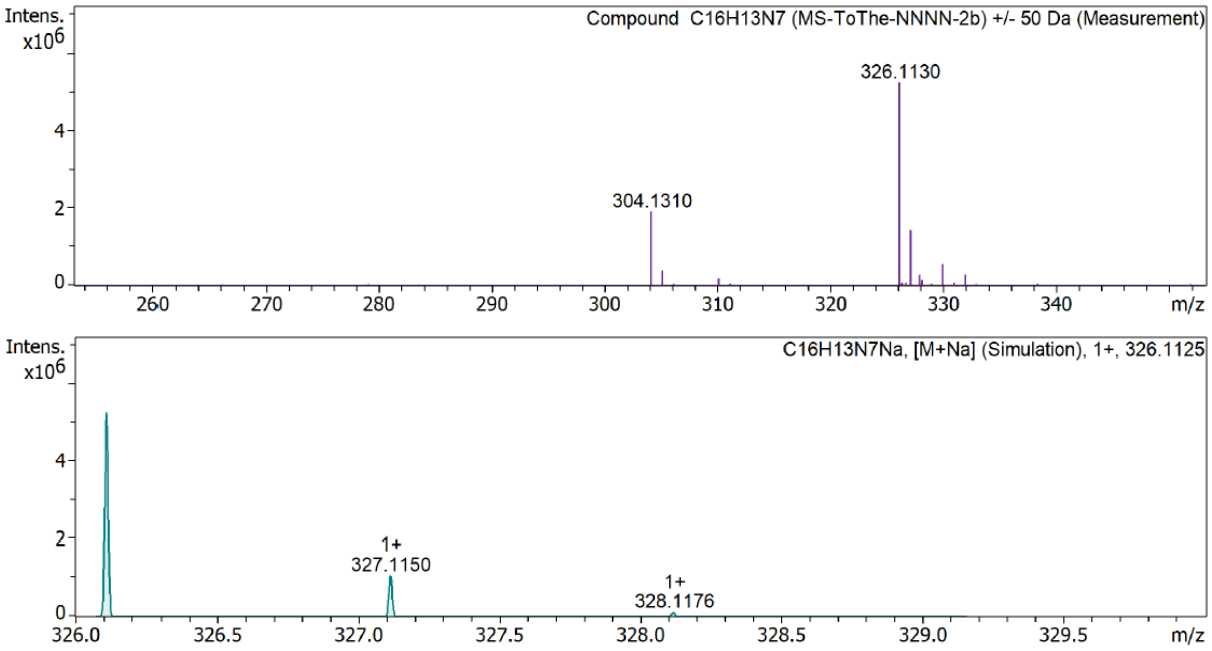

Figure S24. Mass spectrum of **2b** (MeOH). Additional simulation for the [**2b**+Na]$^+$ adduct.

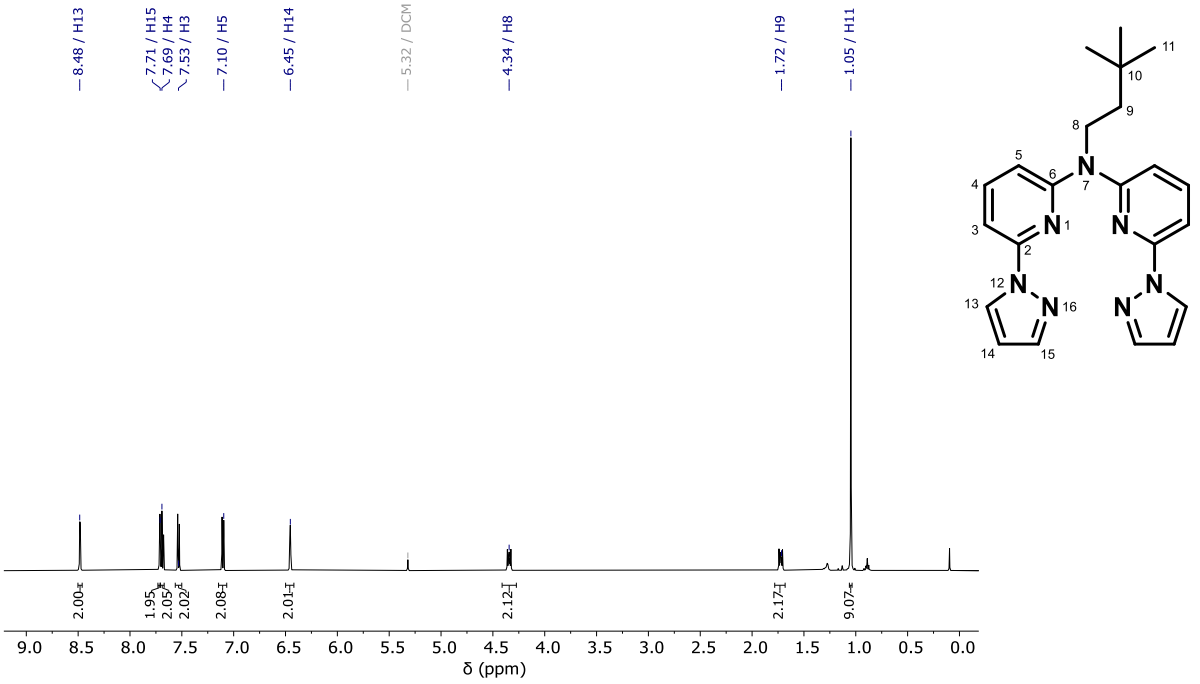

Figure S25. ^{1}H-NMR spectrum (500 MHz, DCM-d_2) of **L**.

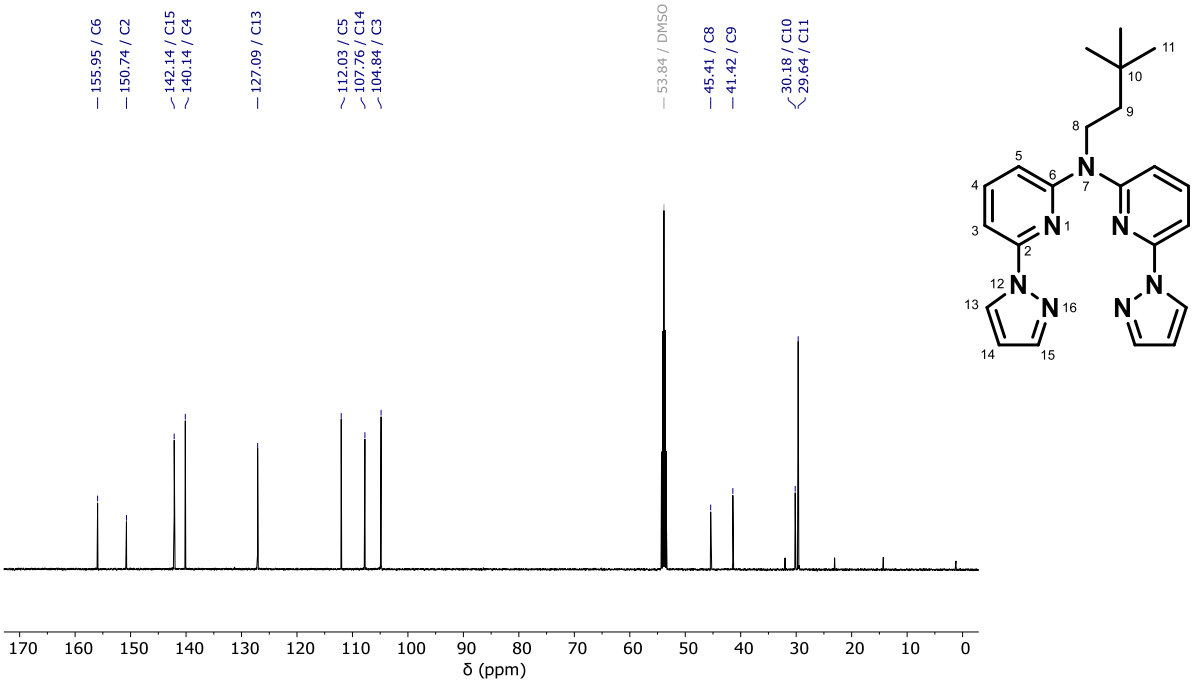

Figure S26. ^{13}C{^{1}H}-NMR spectrum (126 MHz, DCM-d_2) of **L**.

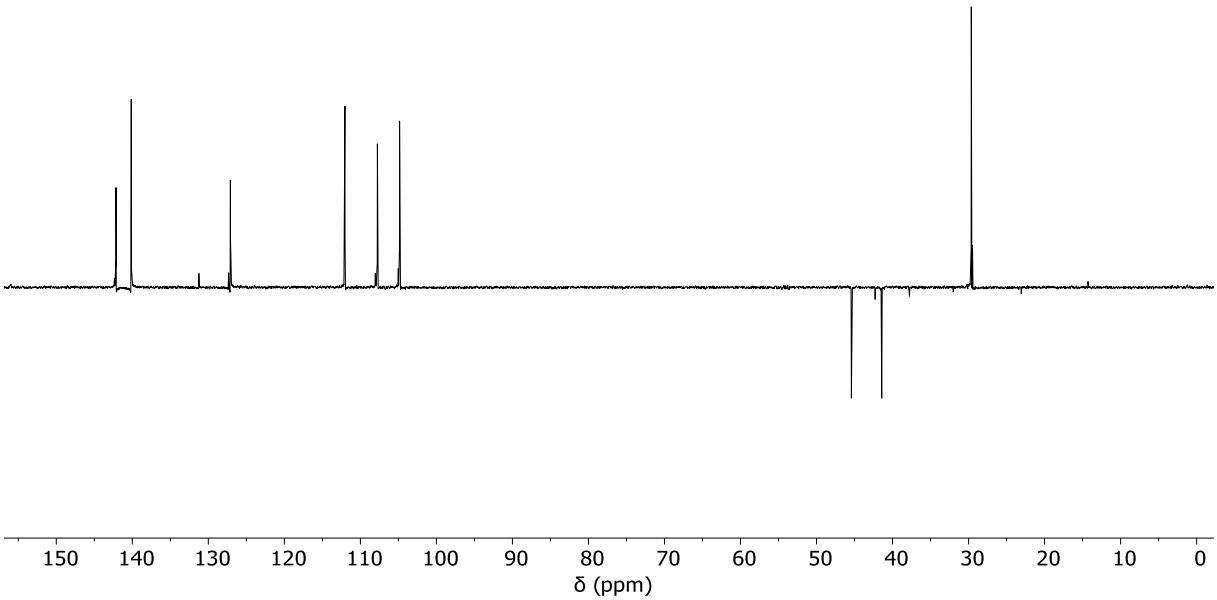

Figure S27. $^{13}C\{^{1}H\}$-NMR DEPT135 spectrum (101 MHz, DCM-d_2) of **L**.

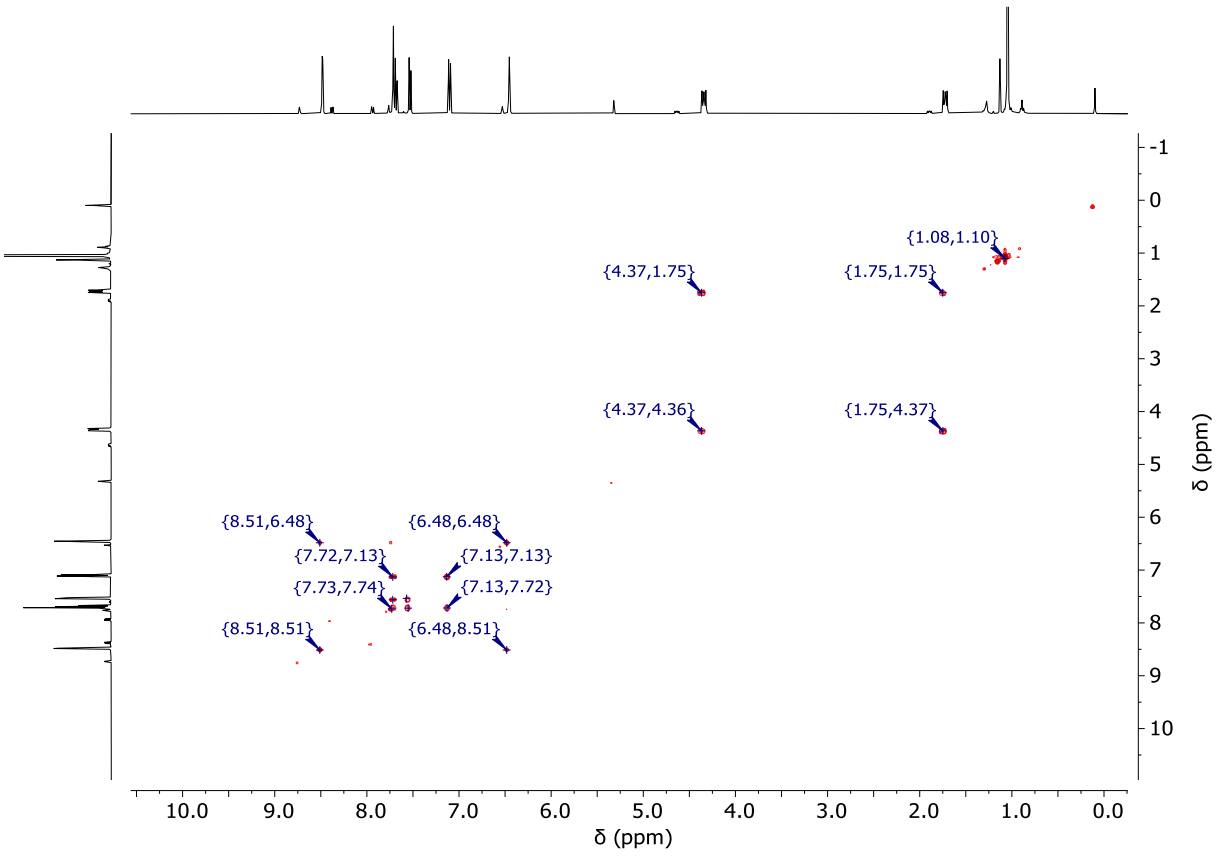

Figure S28. H,H-COSY-NMR spectrum (400 MHz, DCM-d_2) of **L**.

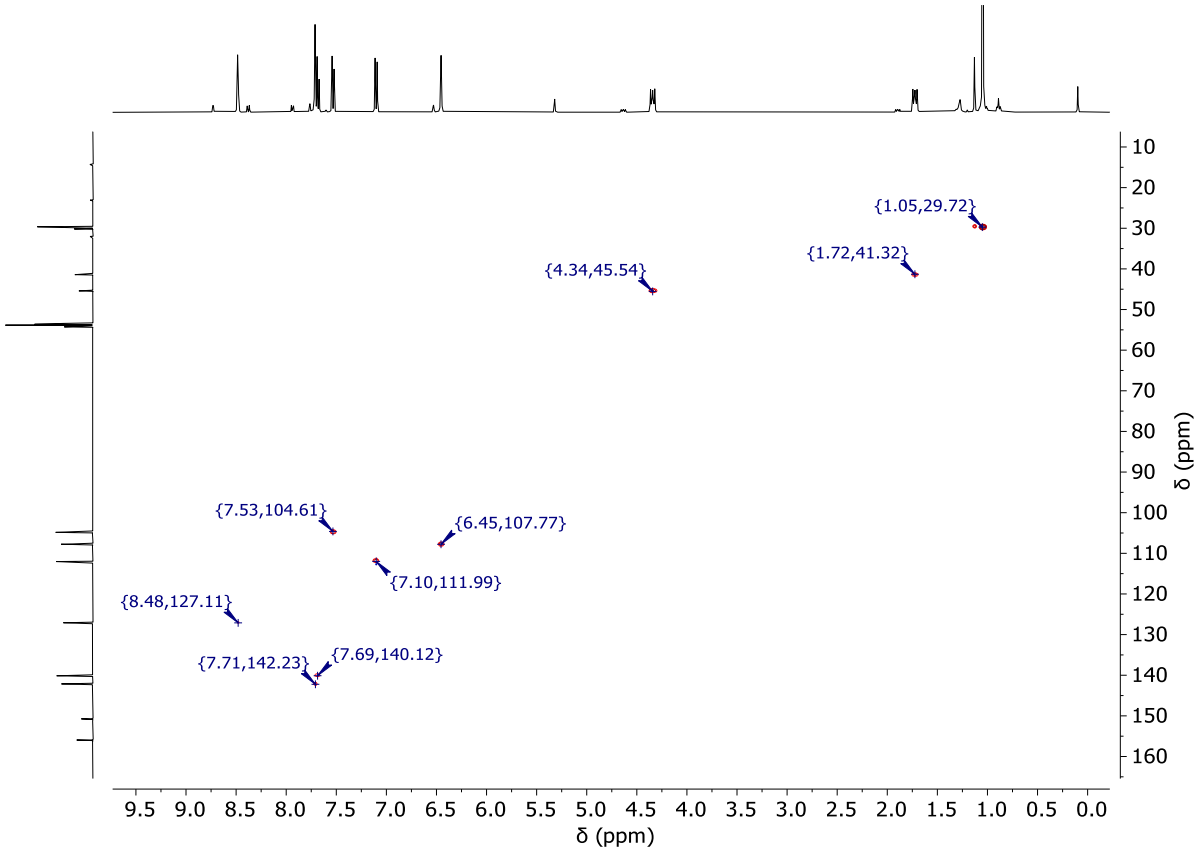

Figure S29. HC-HSQC spectrum (101 MHz (^{13}C), 400 MHz (^{1}H), DCM-d_2) of **L**.

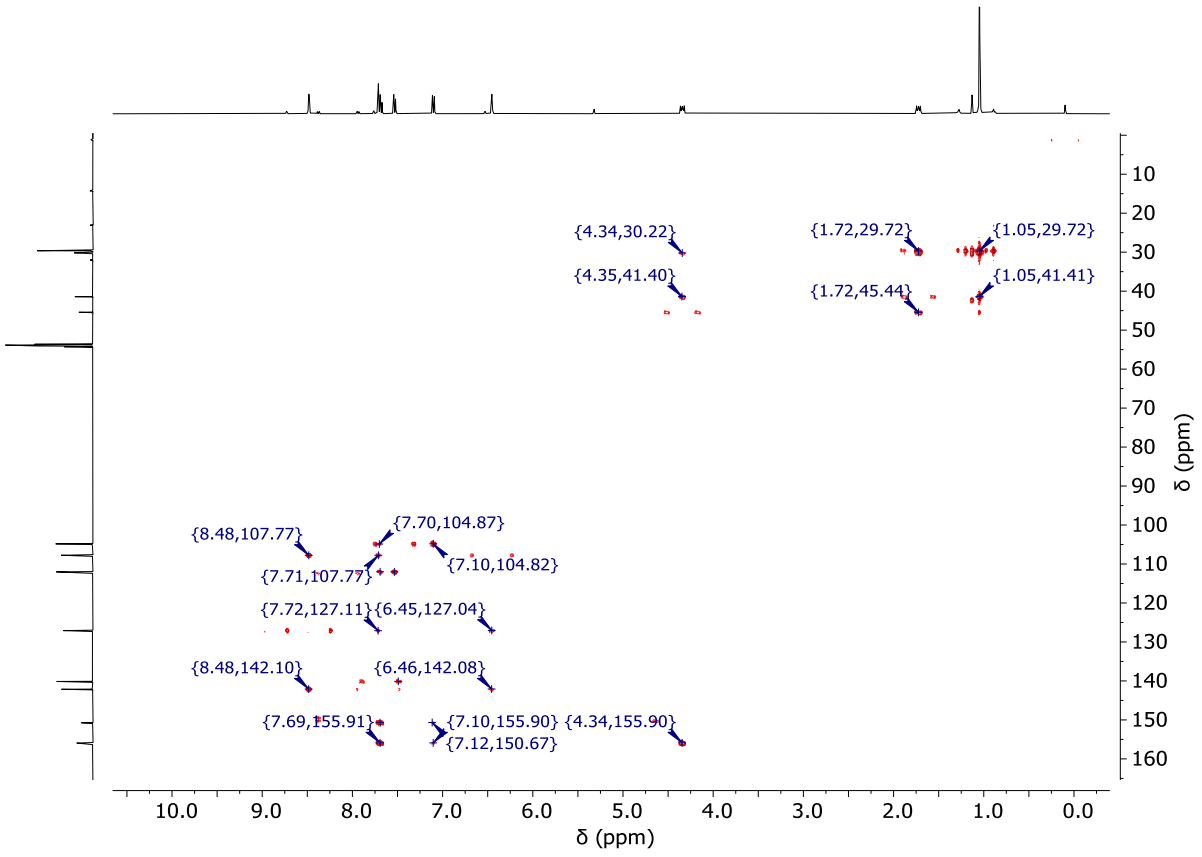

Figure S30. HC-HMBC-NMR spectrum (101 MHz (^{13}C), 400 MHz (^{1}H), DCM-d_2) of **L**.

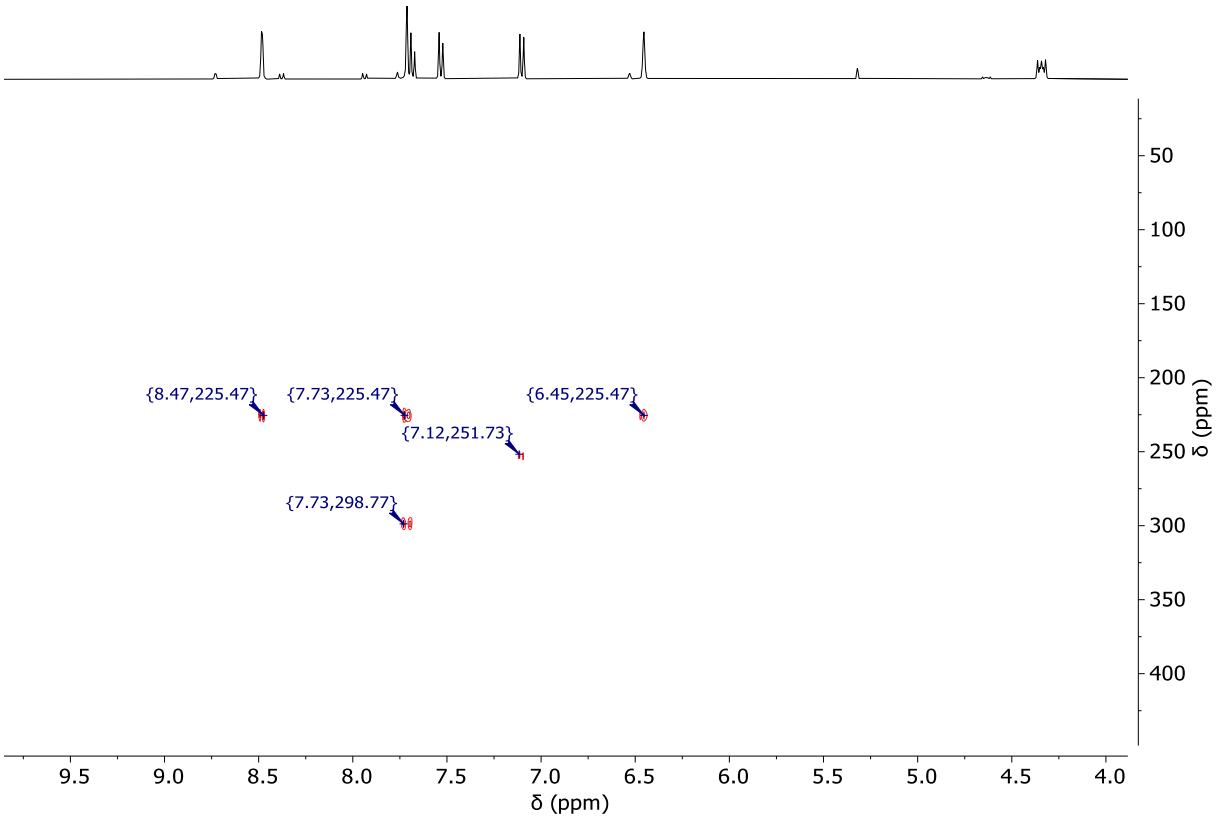

Figure S31. HN-HMBC-NMR spectrum (41 MHz (^{15}N), 400 MHz (^{1}H), DCM-d_2) of **L**.

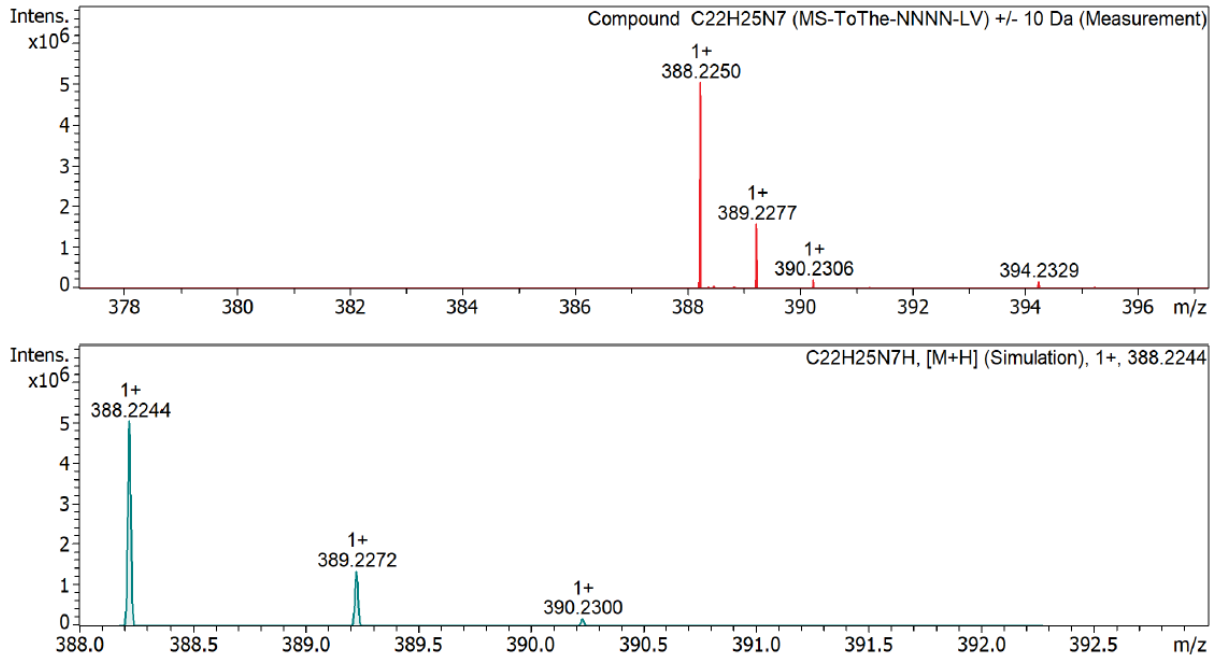

Figure S32. Mass spectrum of **L** (MeOH). Additional simulation for the [**L**+H]$^+$ adduct.

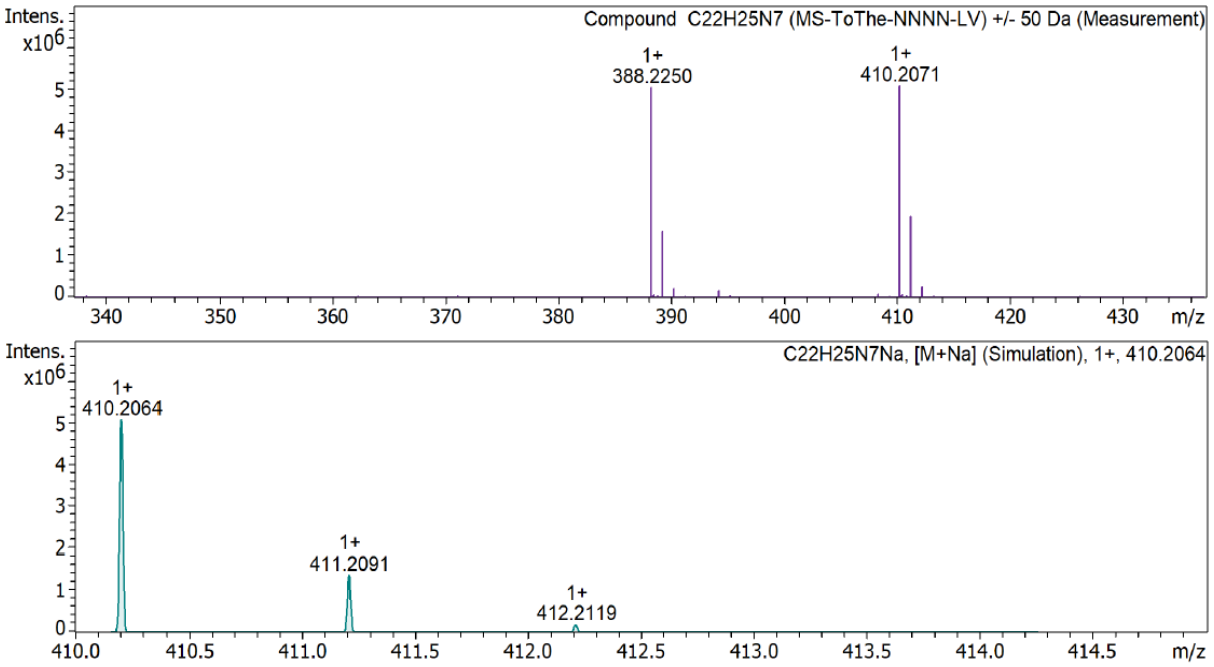

Figure S33. Mass spectrum of **L** (MeOH). Additional simulation for the [**L**+Na]$^+$ adduct.

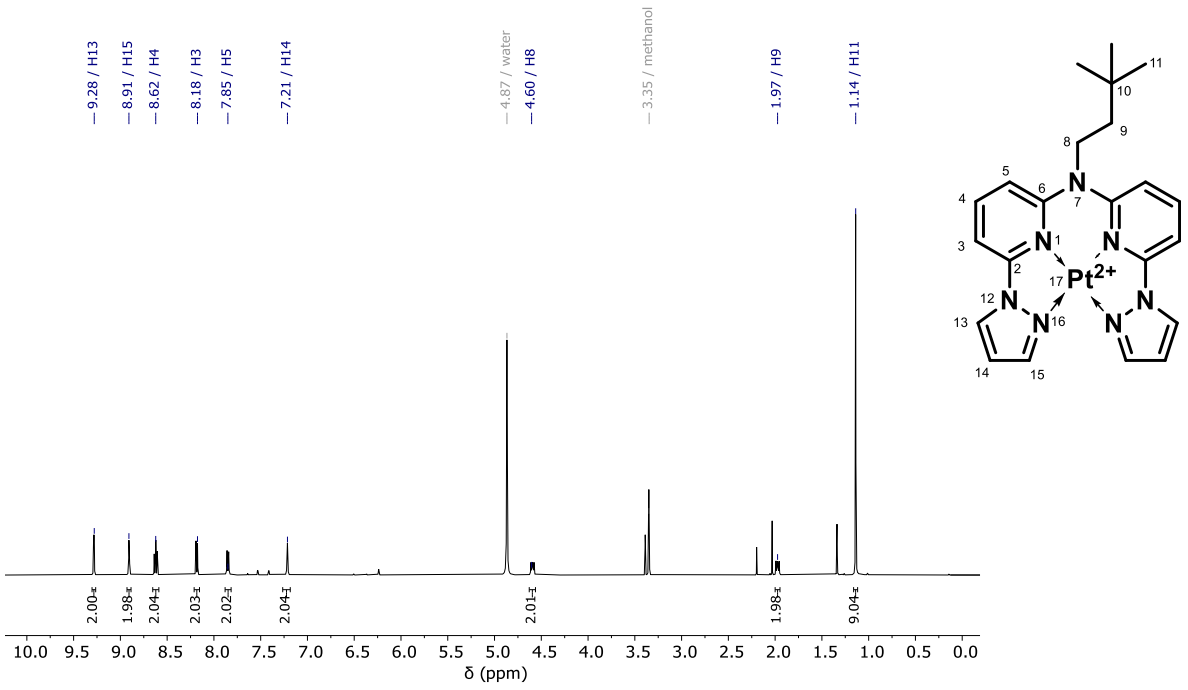

Figure S34. ^{1}H-NMR spectrum (500 MHz, methanol-d_4) of **C1**.

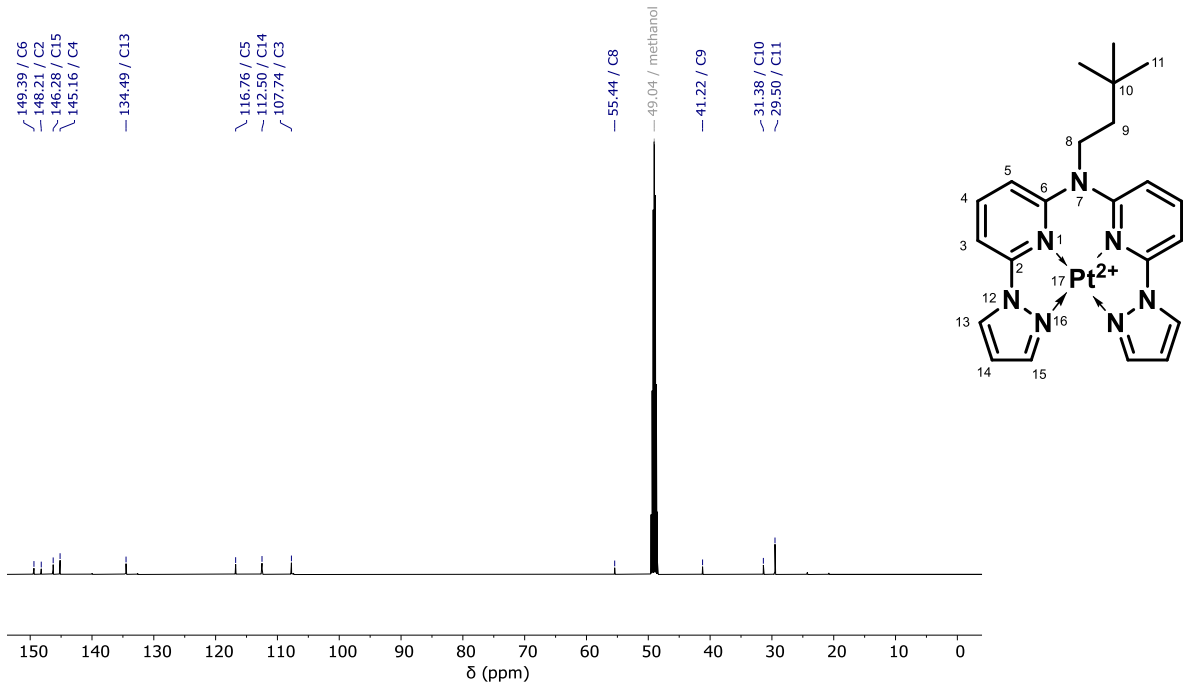

Figure S35. $^{13}C\{^{1}H\}$-NMR spectrum (126 MHz, methanol-d_4) of **C1**.

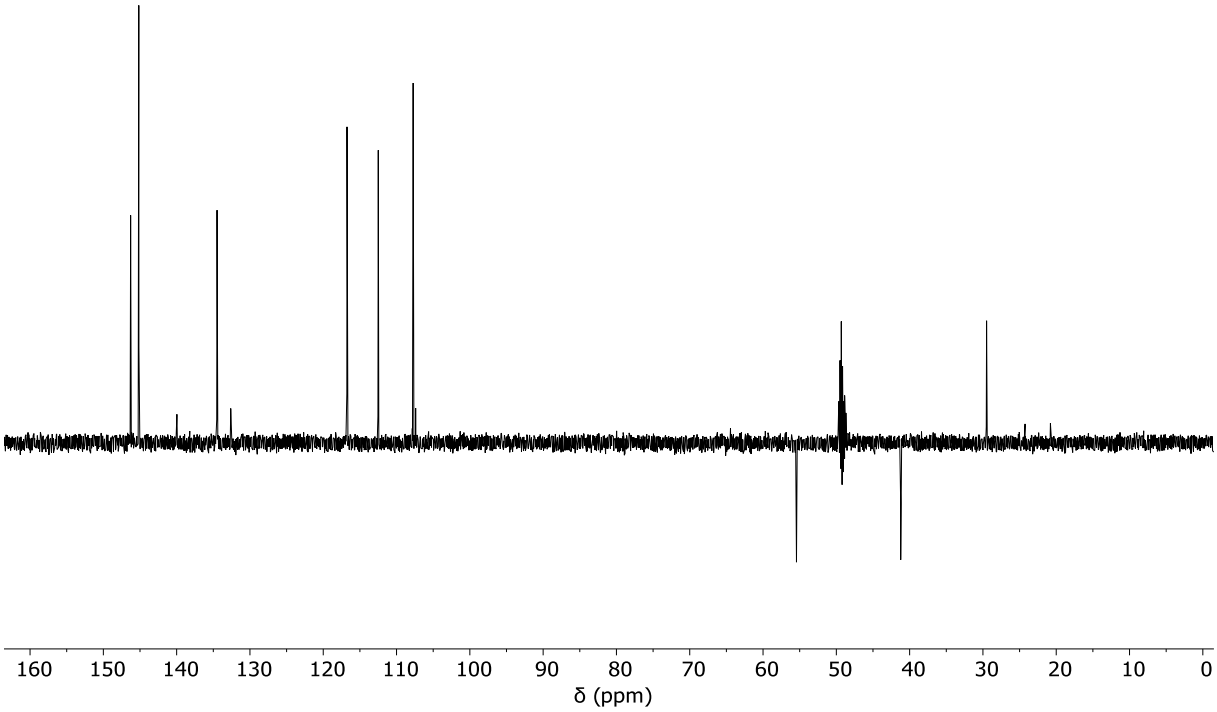

Figure S36. $^{13}C\{^{1}H\}$-NMR DEPT135 spectrum (126 MHz, methanol-d_4) of **C1**.

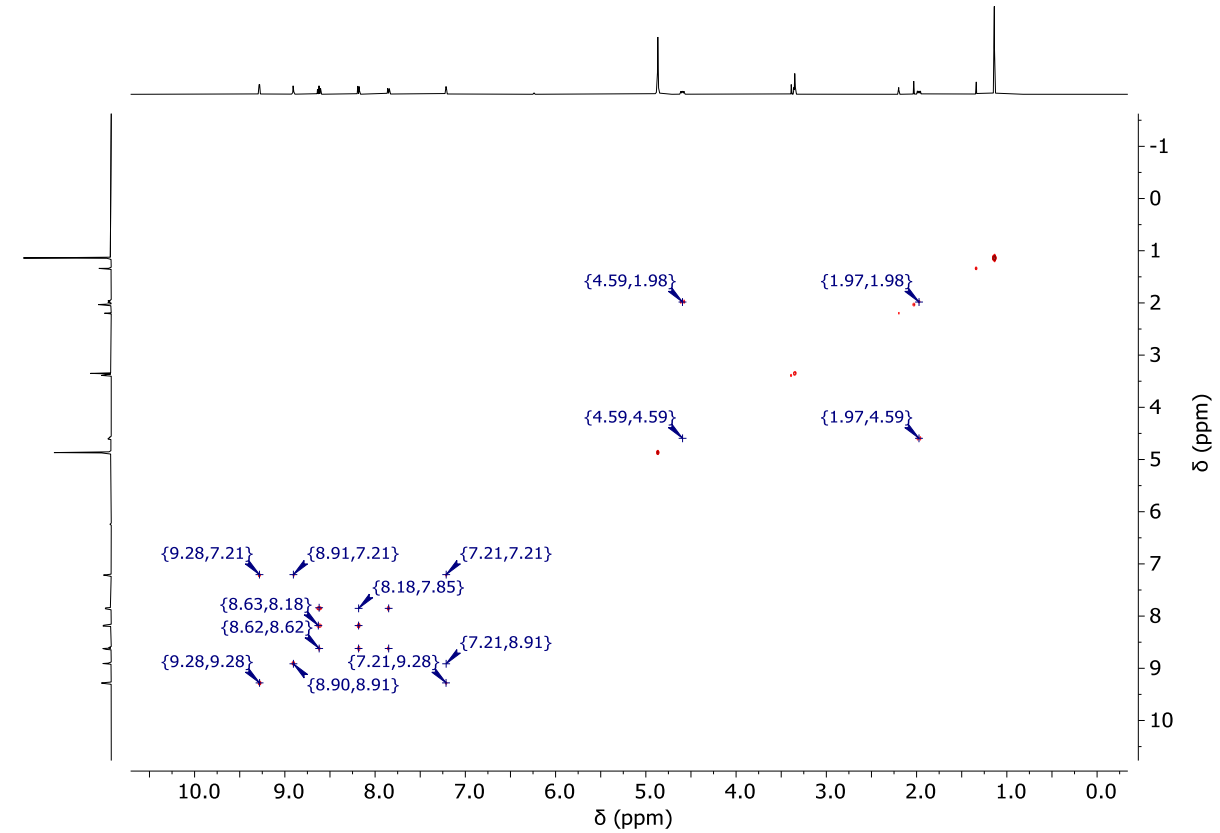

Figure S37. H,H-COSY-NMR spectrum (500 MHz, methanol-d_4) of **C1**.

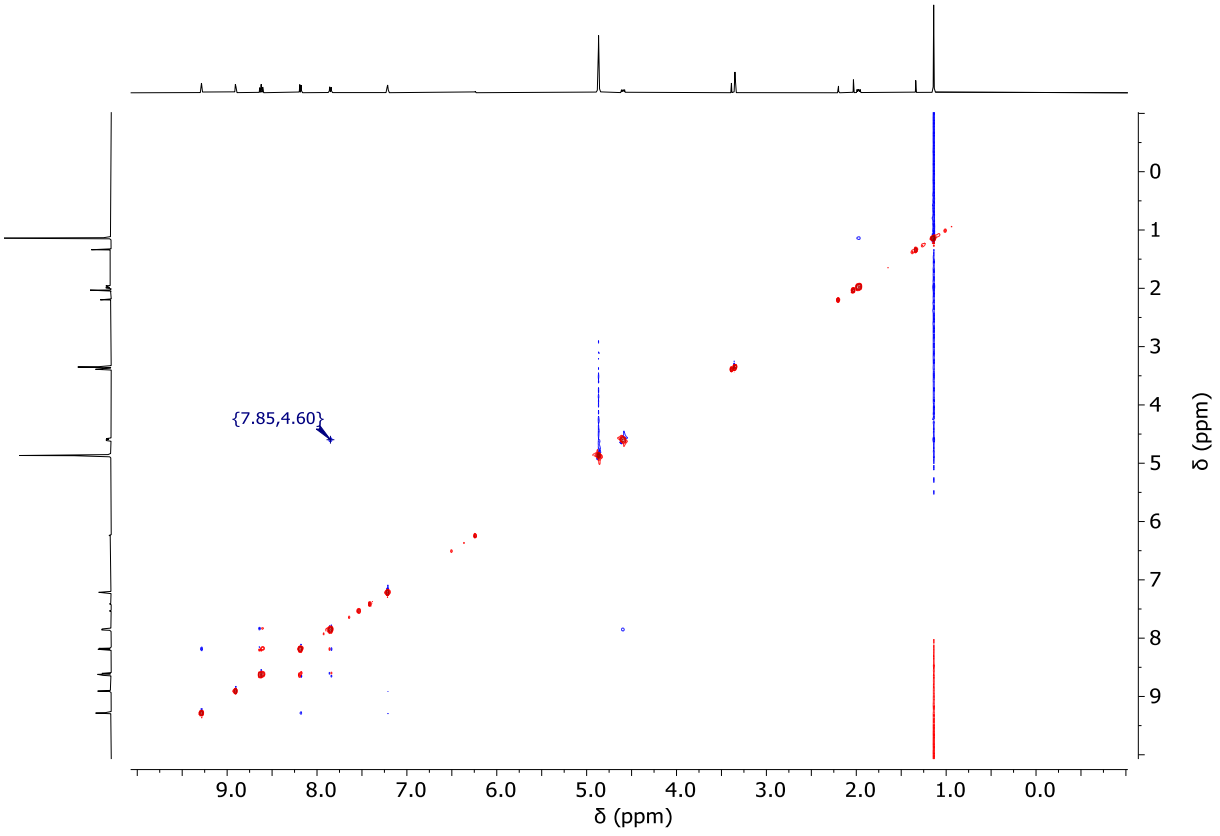

Figure S38. H,H-ROESY-NMR spectrum (500 MHz, methanol-d_4) of **C1**.

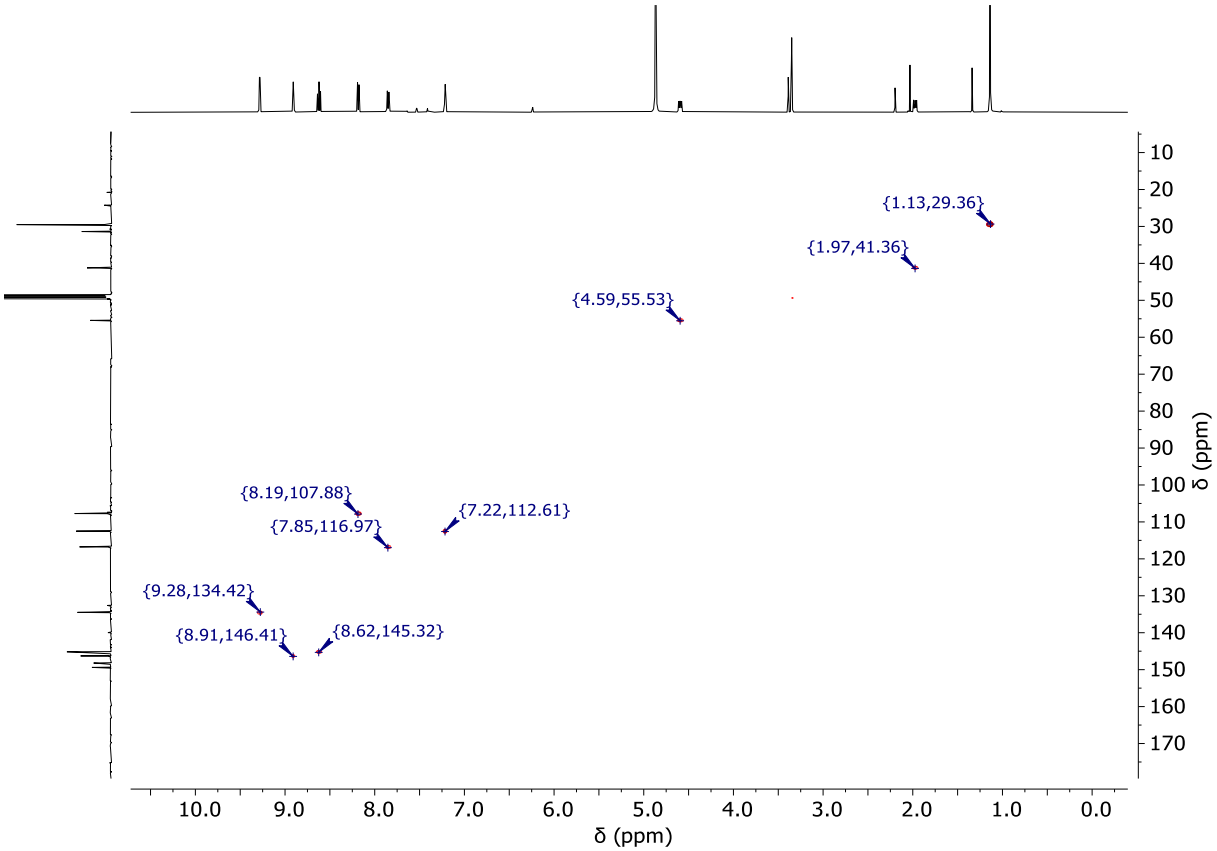

Figure S39. HC-HSQC spectrum (126 MHz (^{13}C), 500 MHz (^{1}H), methanol-d_4) of **C1**.

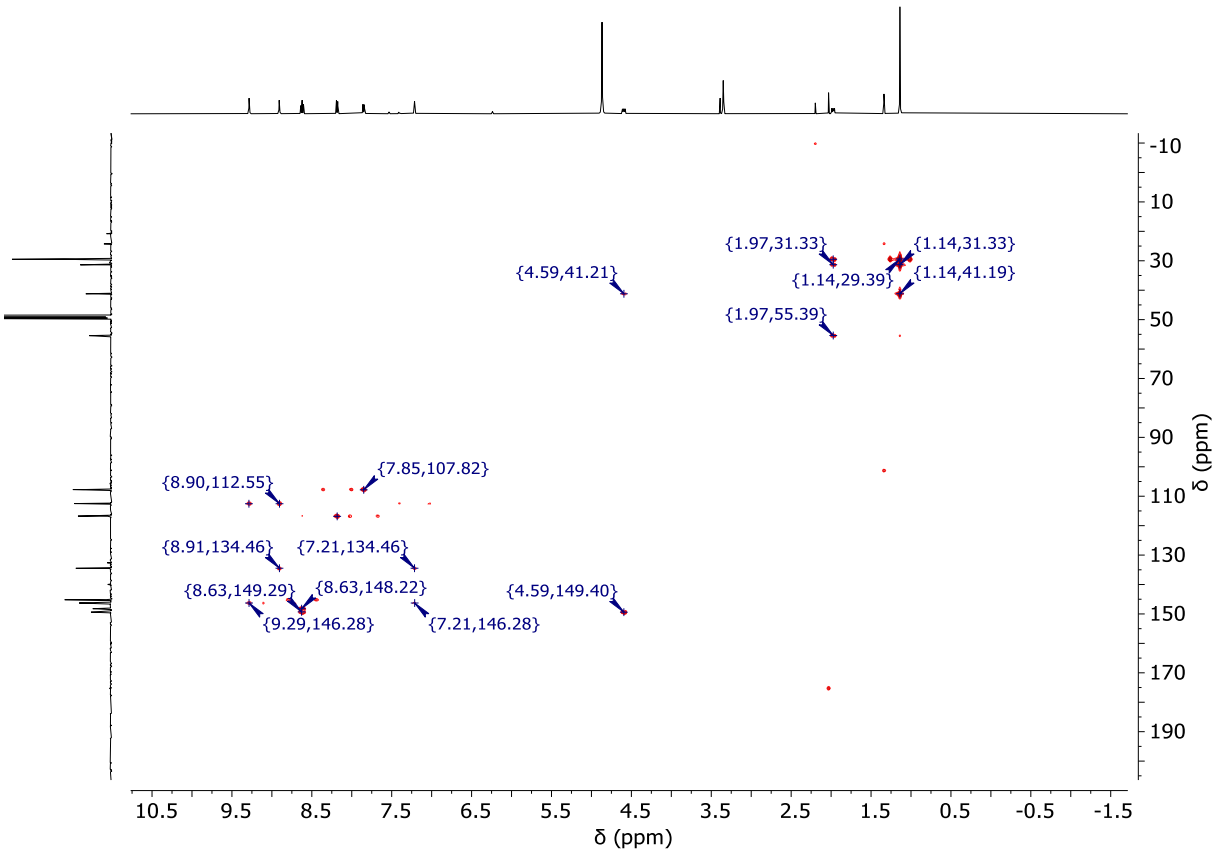

Figure S40. HC-HMBC-NMR spectrum (126 MHz (^{13}C), 500 MHz (^{1}H), methanol-d_4) of **C1**.

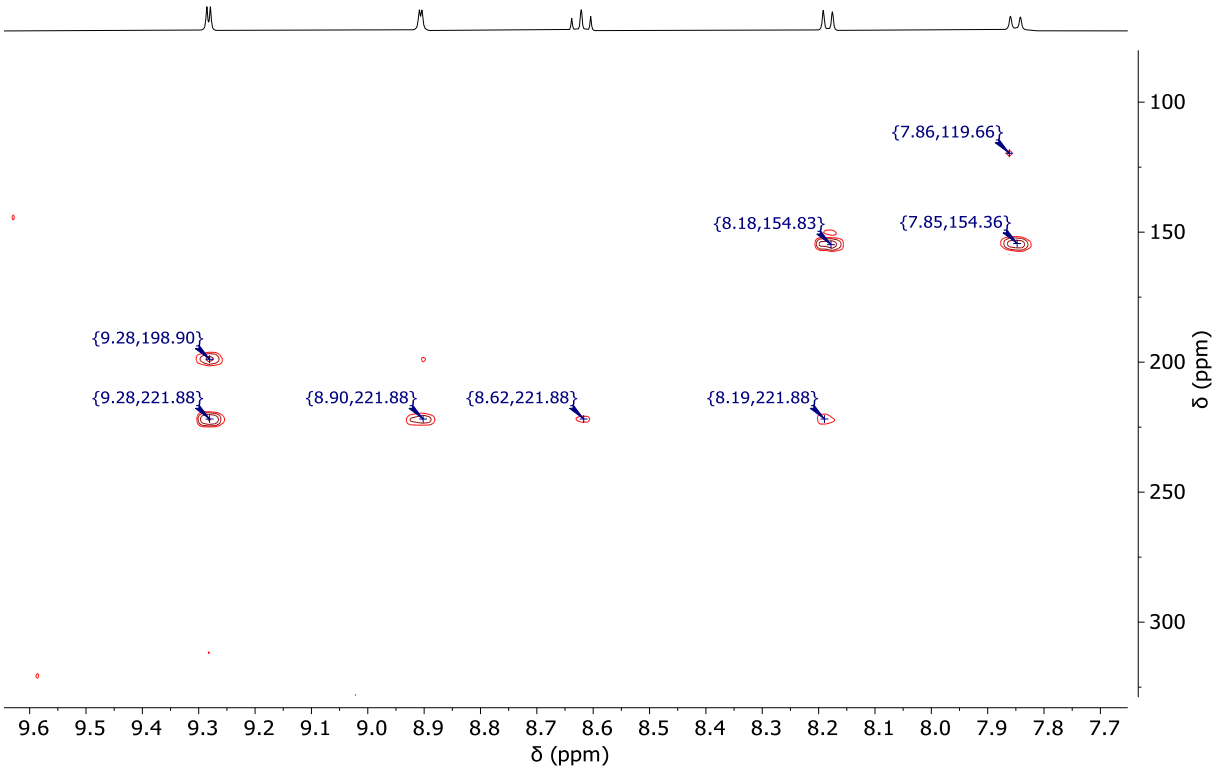

Figure S41. HN-HMBC-NMR spectrum (51 MHz (^{15}N), 500 MHz (^{1}H), acetone-d_6) of **C1**.

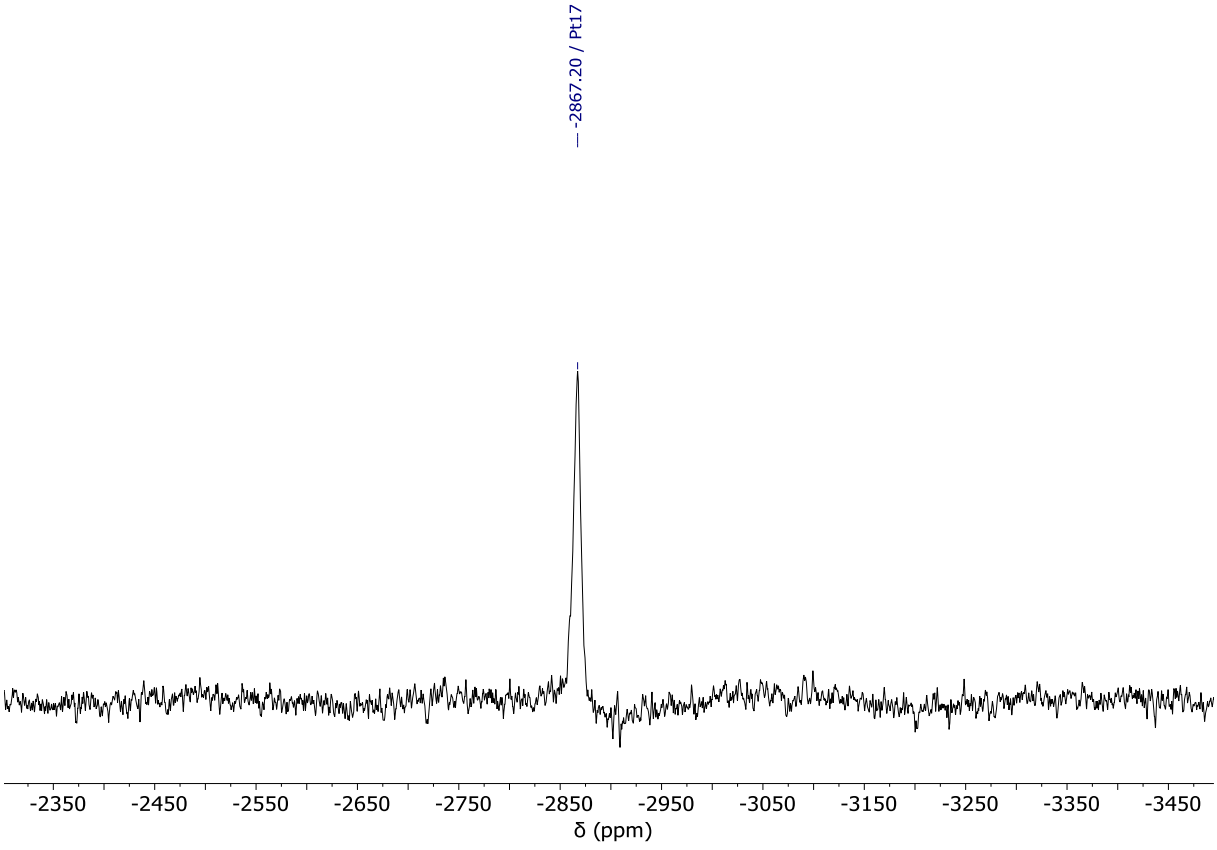

Figure S42. ^{195}Pt-NMR spectrum (86 MHz, methanol-d_4) of **C1**.

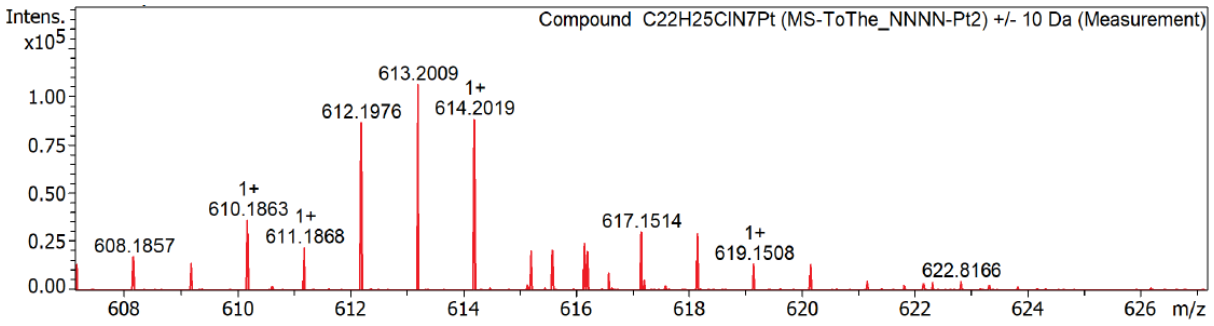

Figure S43. Mass spectrum of **C1** ($C_{22}H_{25}ClN_7Pt^+$).

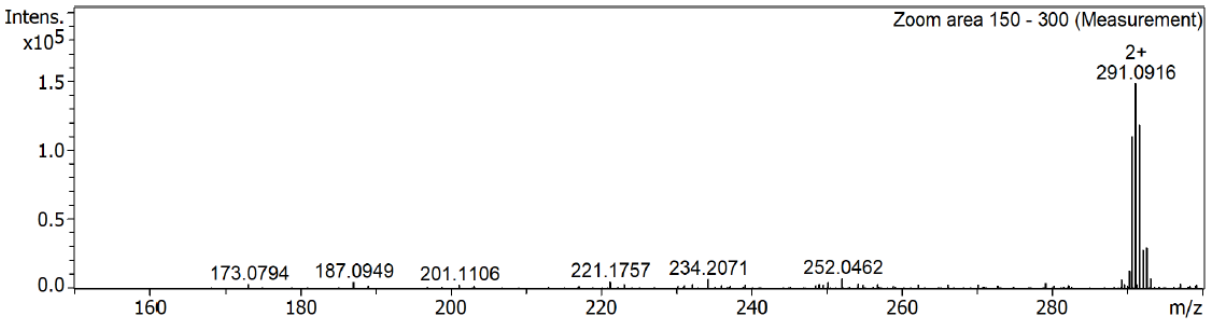

Figure S44. Mass spectrum of **C1** ($C_{22}H_{25}N_7Pt^{2+}$).

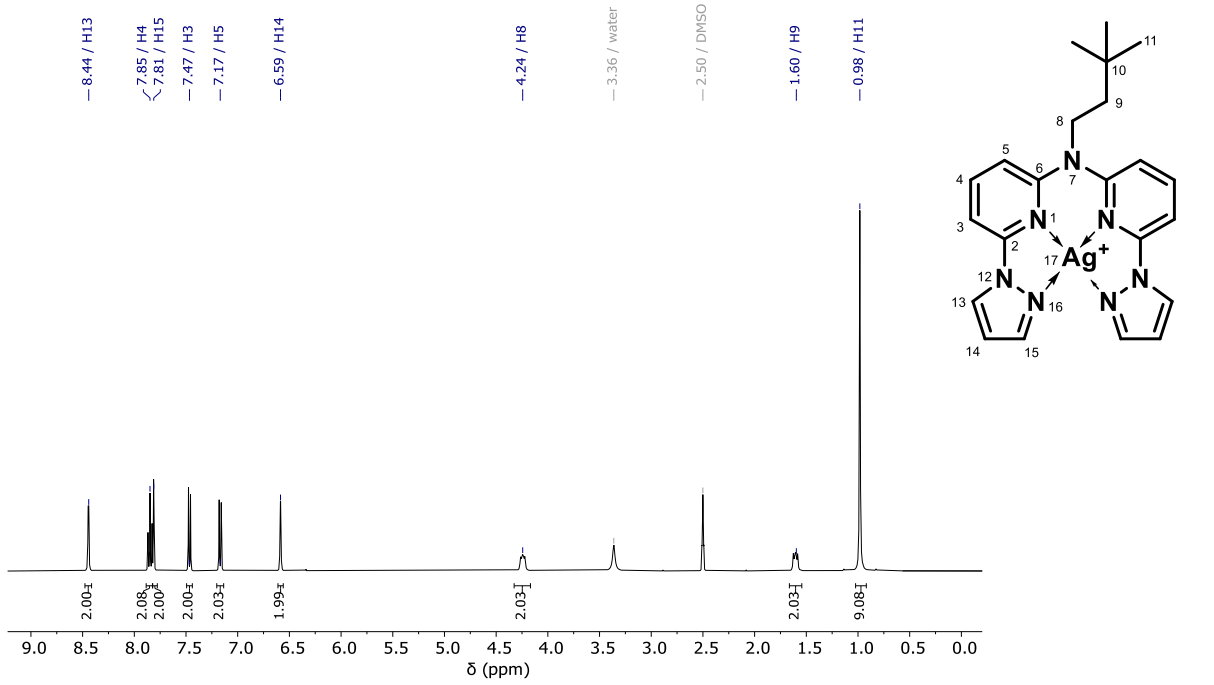

Figure S45. ^{1}H-NMR spectrum (400 MHz, DMSO-d_6) of **C2**.

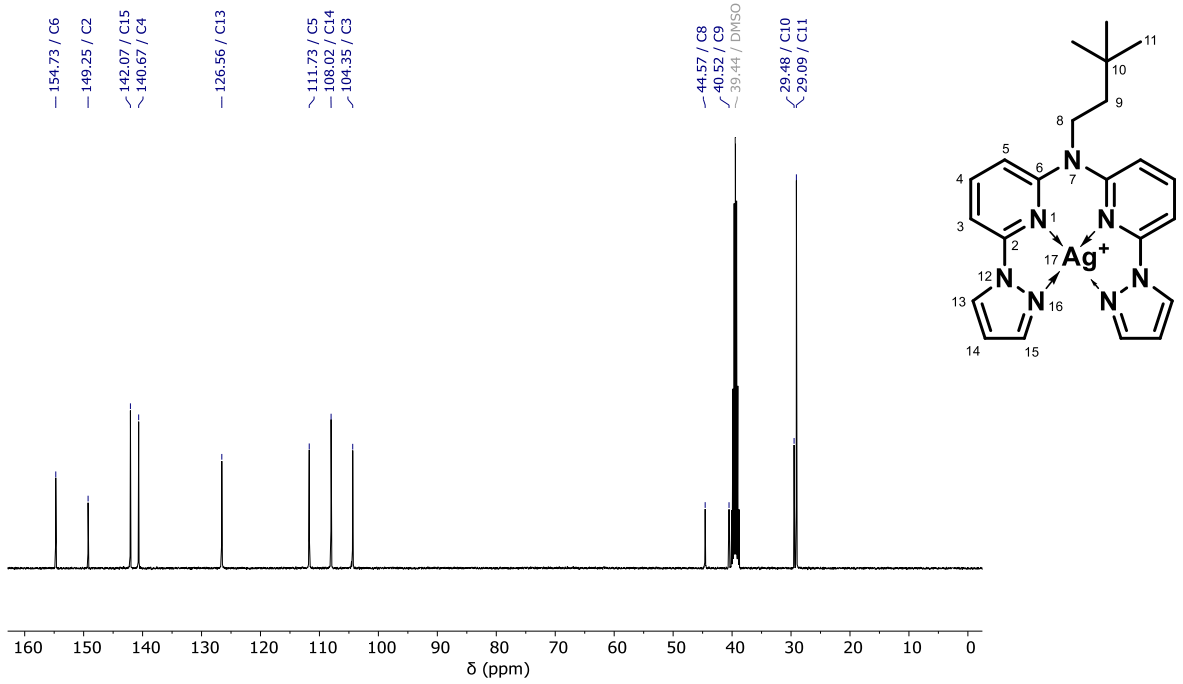

Figure S46. $^{13}C\{^{1}H\}$-NMR spectrum (101 MHz, DMSO-d_6) of **C2**.

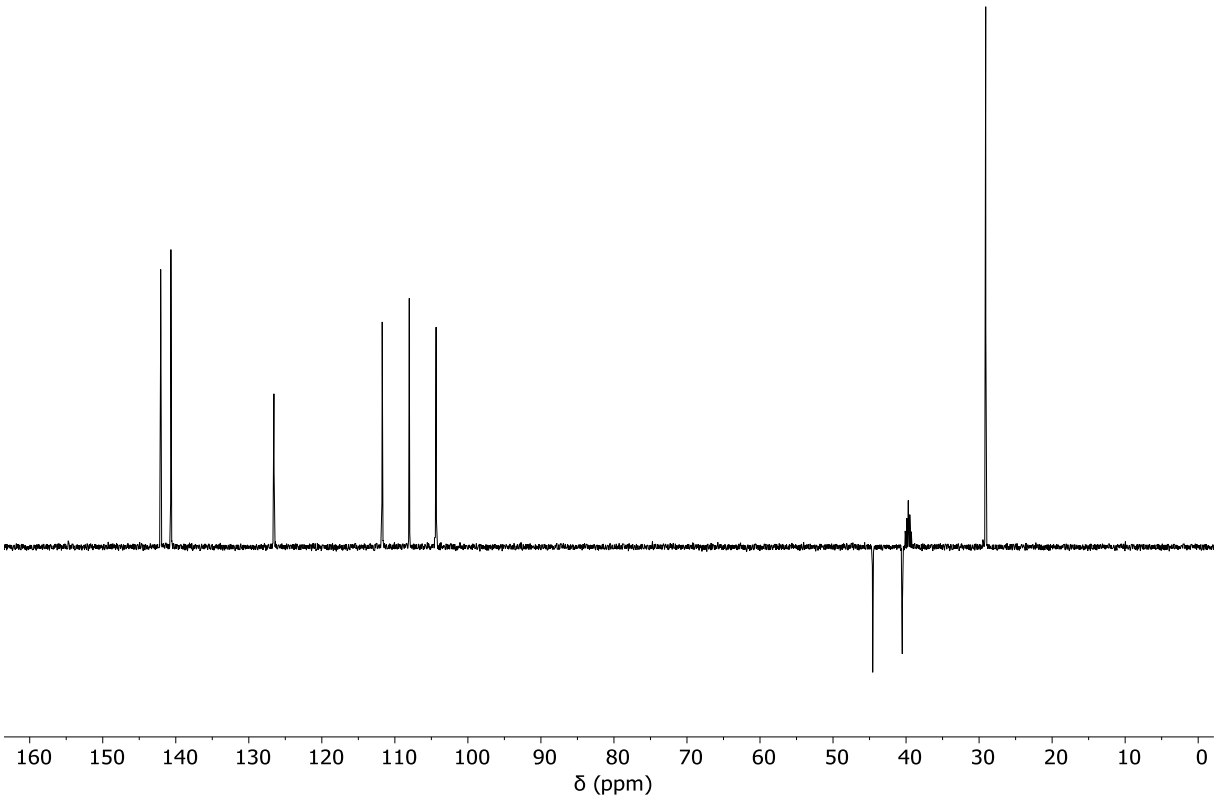

Figure S47. $^{13}C\{^{1}H\}$-NMR DEPT135 spectrum (101 MHz, DMSO-d_6) of **C2**.

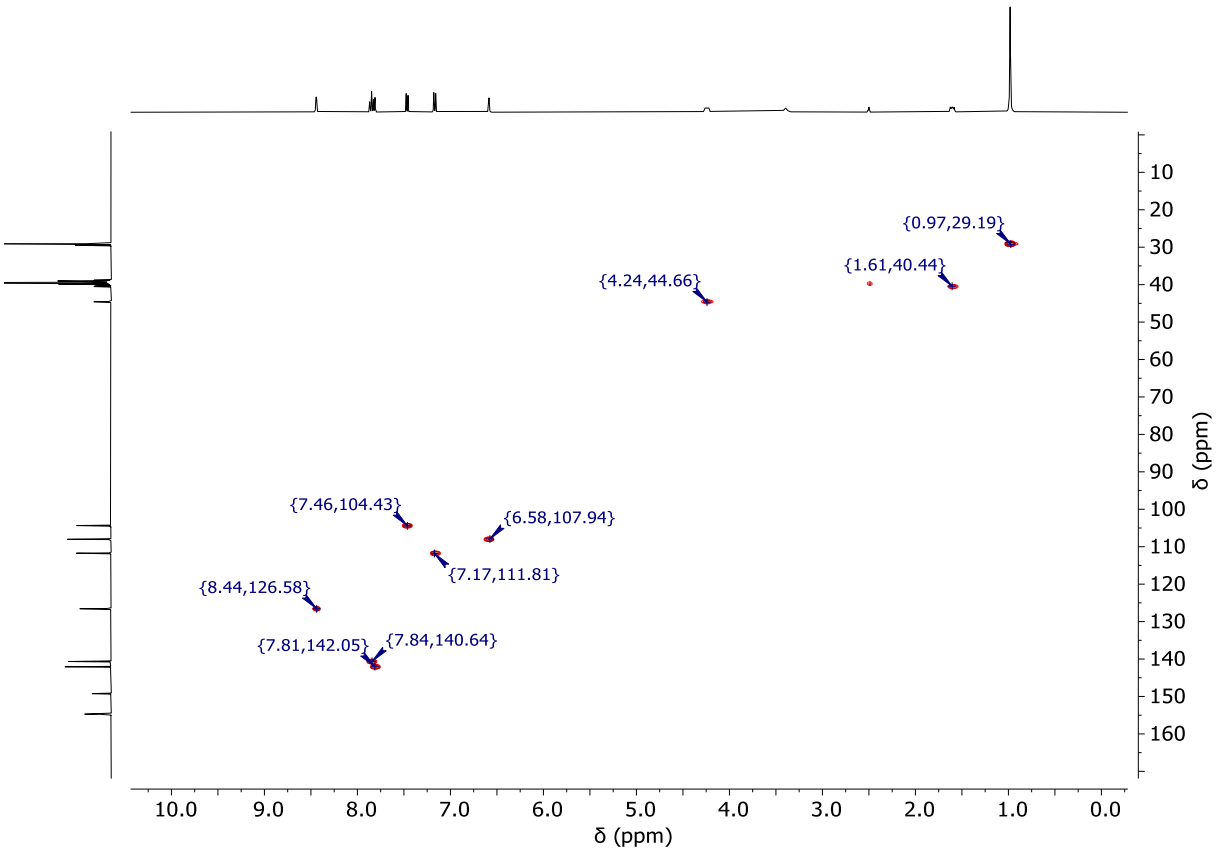

Figure S48. HC-HSQC spectrum (101 MHz (^{13}C), 400 MHz (^{1}H), DMSO-d_6) of **C2**.

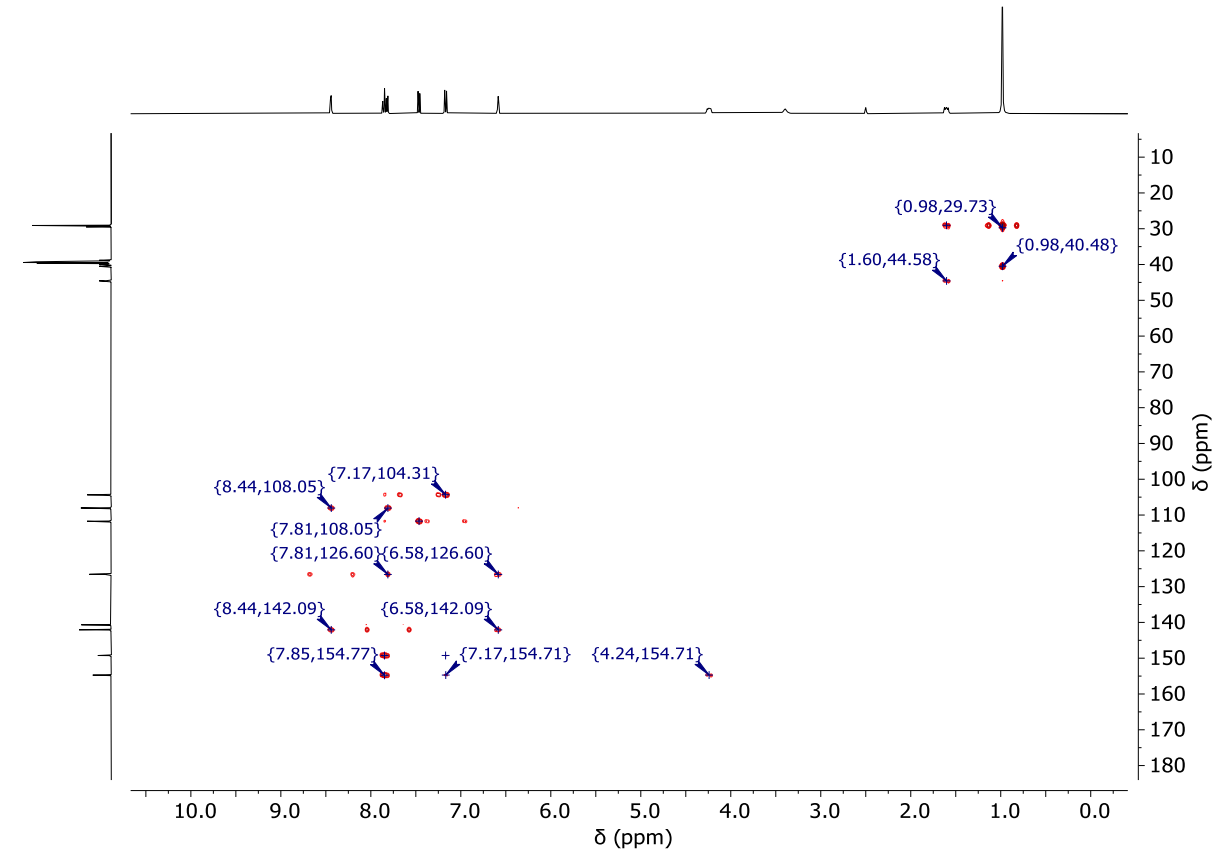

Figure S49. HC-HMBC-NMR spectrum (101 MHz (^{13}C), 400 MHz (^{1}H), DMSO-d_6) of **C2**.

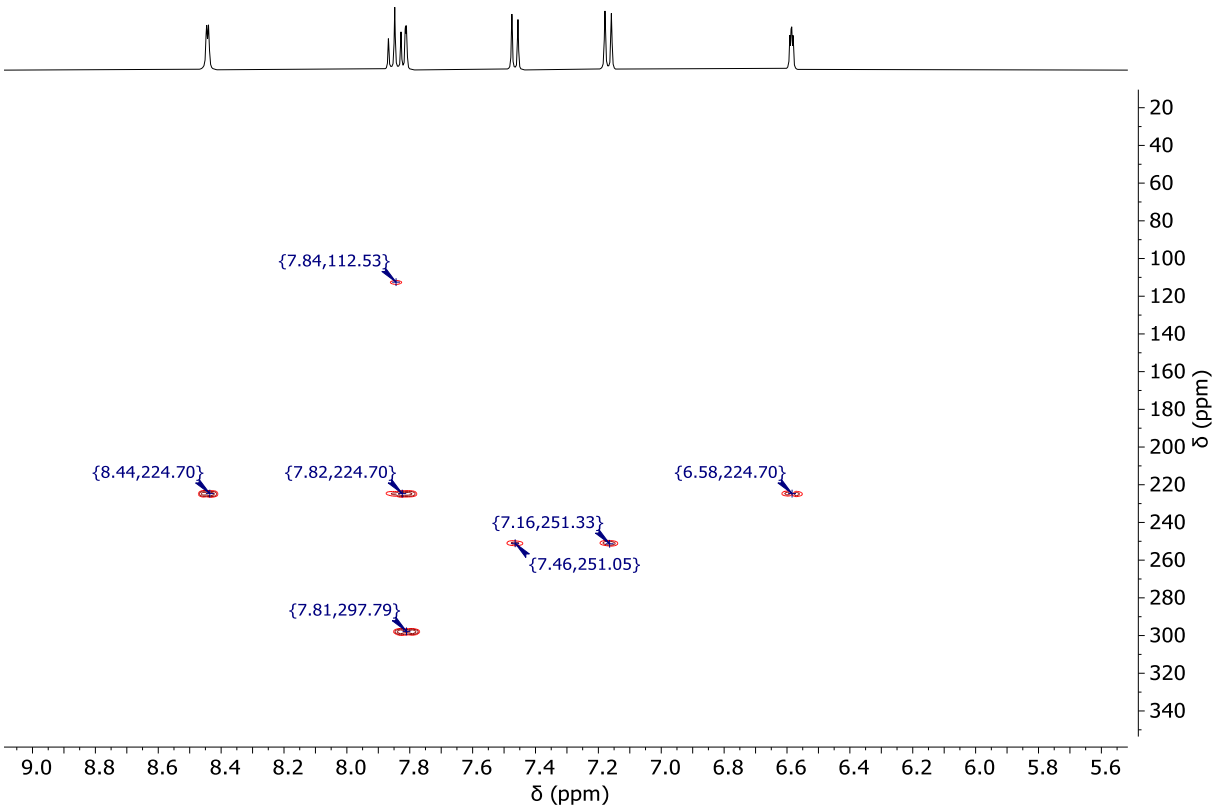

Figure S50. HN-HMBC-NMR spectrum (41 MHz (^{15}N), 400 MHz (^{1}H), DMSO-d_6) of **C2**.

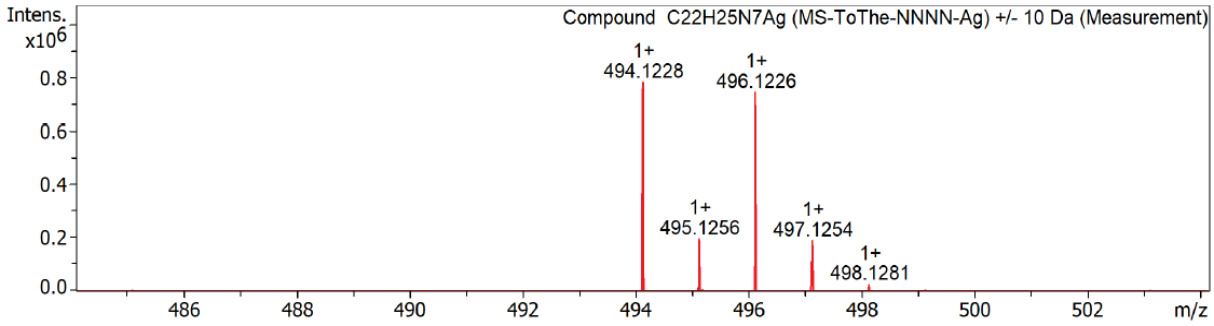

Figure S51. Mass spectrum of **C2** ($C_{22}H_{25}N_7Ag^+$).

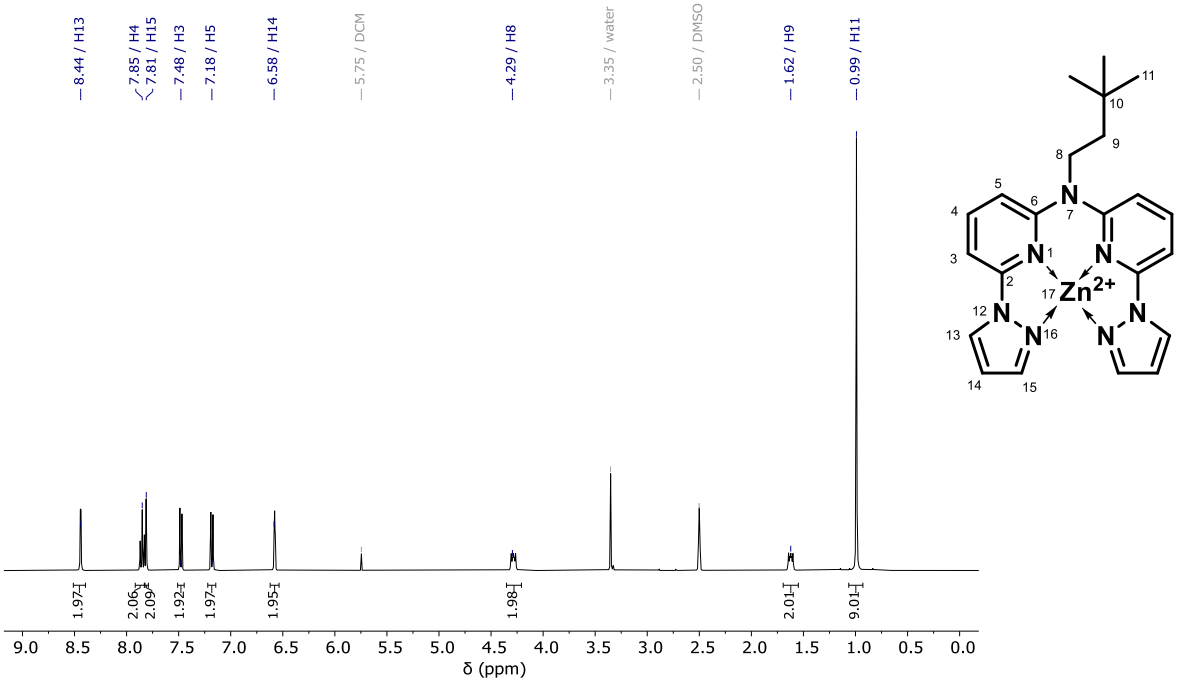

Figure S52. ^{1}H-NMR spectrum (400 MHz, DMSO-d_6) of **C3**.

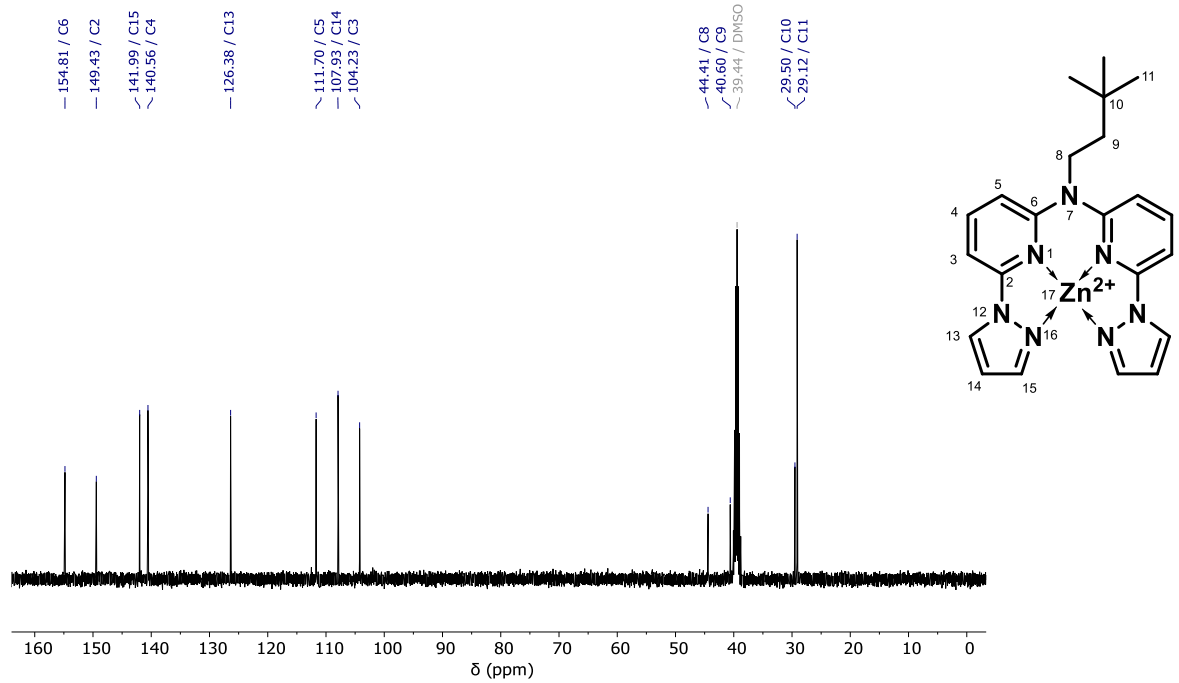

Figure S53. ^{13}C{^{1}H}-NMR spectrum (101 MHz, DMSO-d_6) of **C3**.

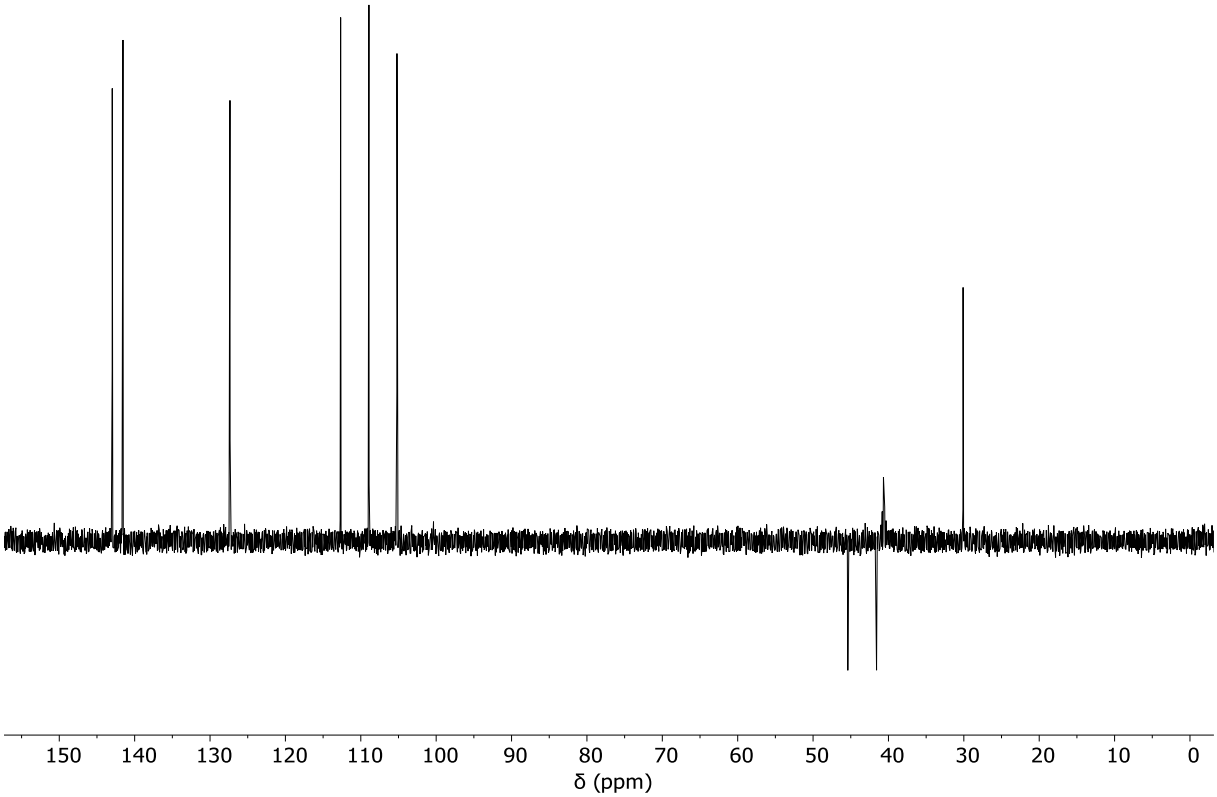

Figure S54. $^{13}C\{^{1}H\}$-NMR DEPT135 spectrum (126 MHz, DMSO-d_6) of **C3**.

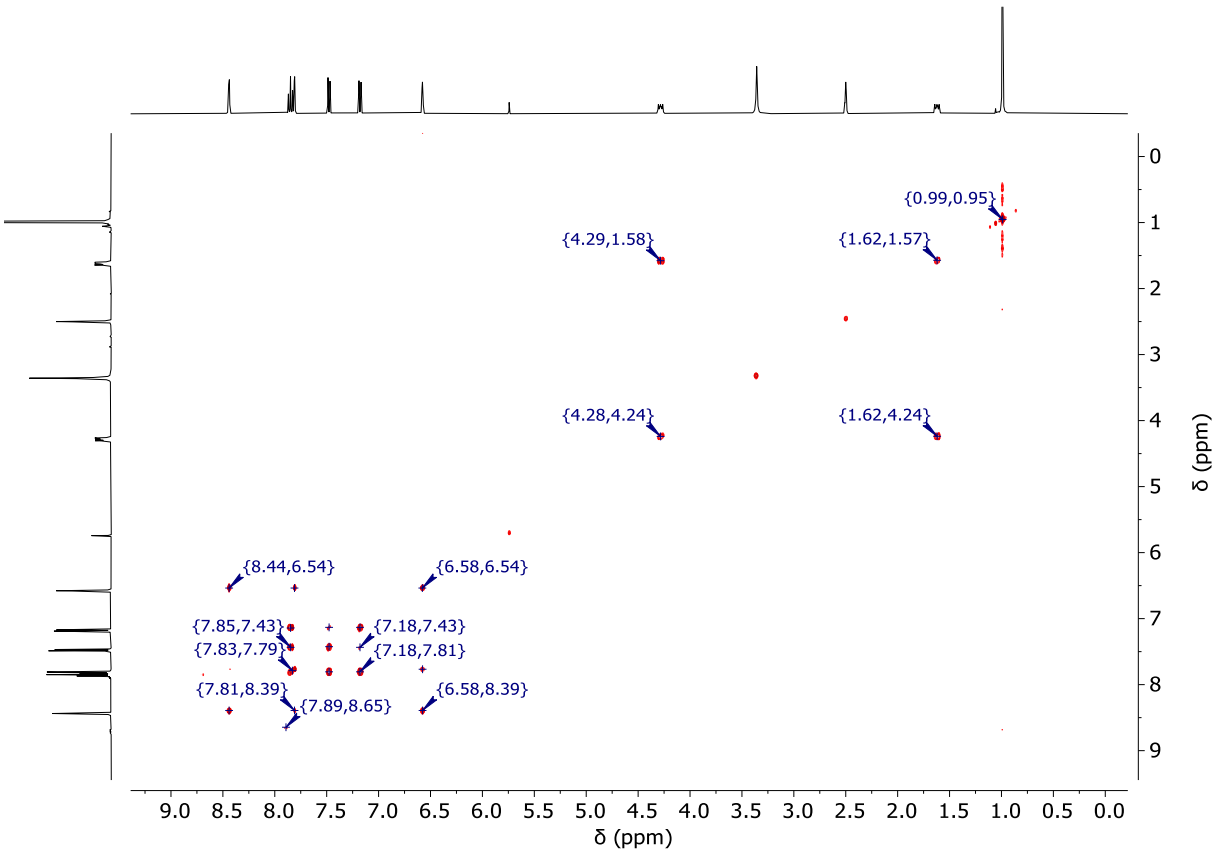

Figure S55. H,H-COSY-NMR spectrum (500 MHz, DMSO-d_6) of **C3**.

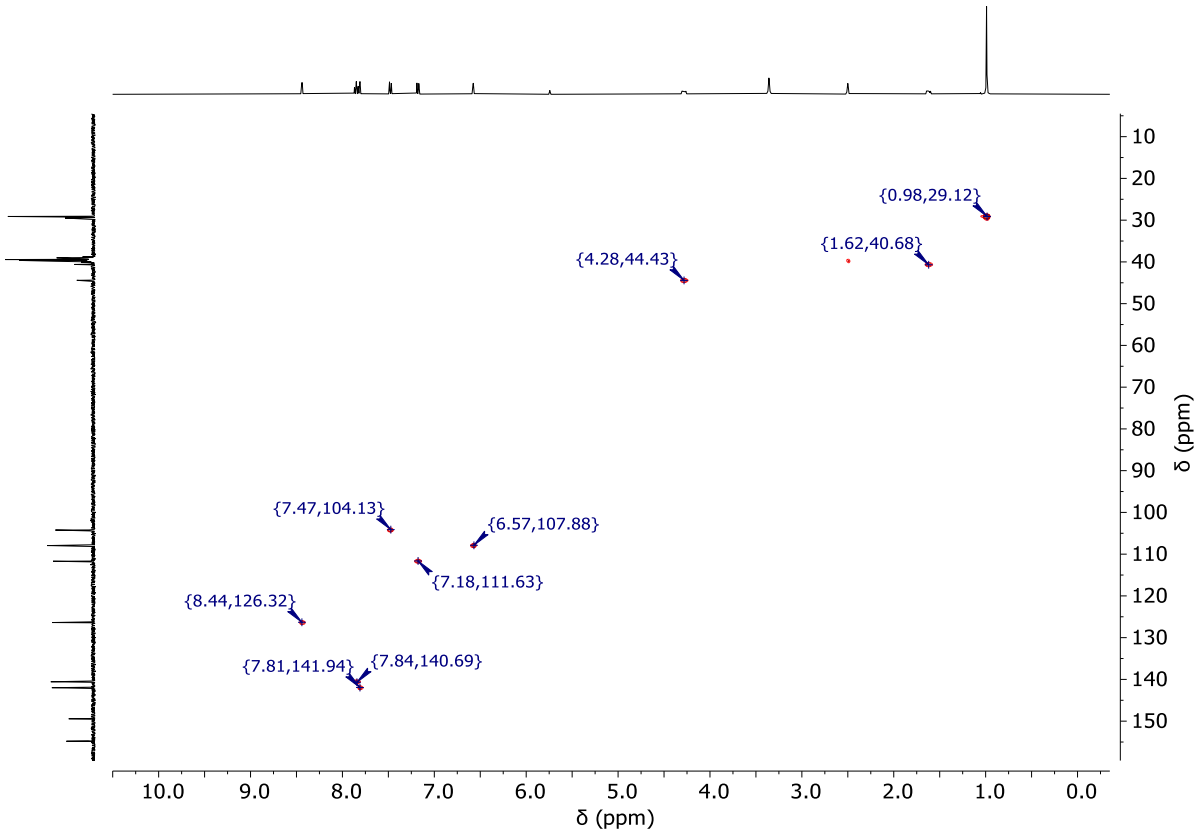

Figure S56. HC-HSQC spectrum (101 MHz (^{13}C), 400 MHz (^{1}H), DMSO-d_6) of **C3**.

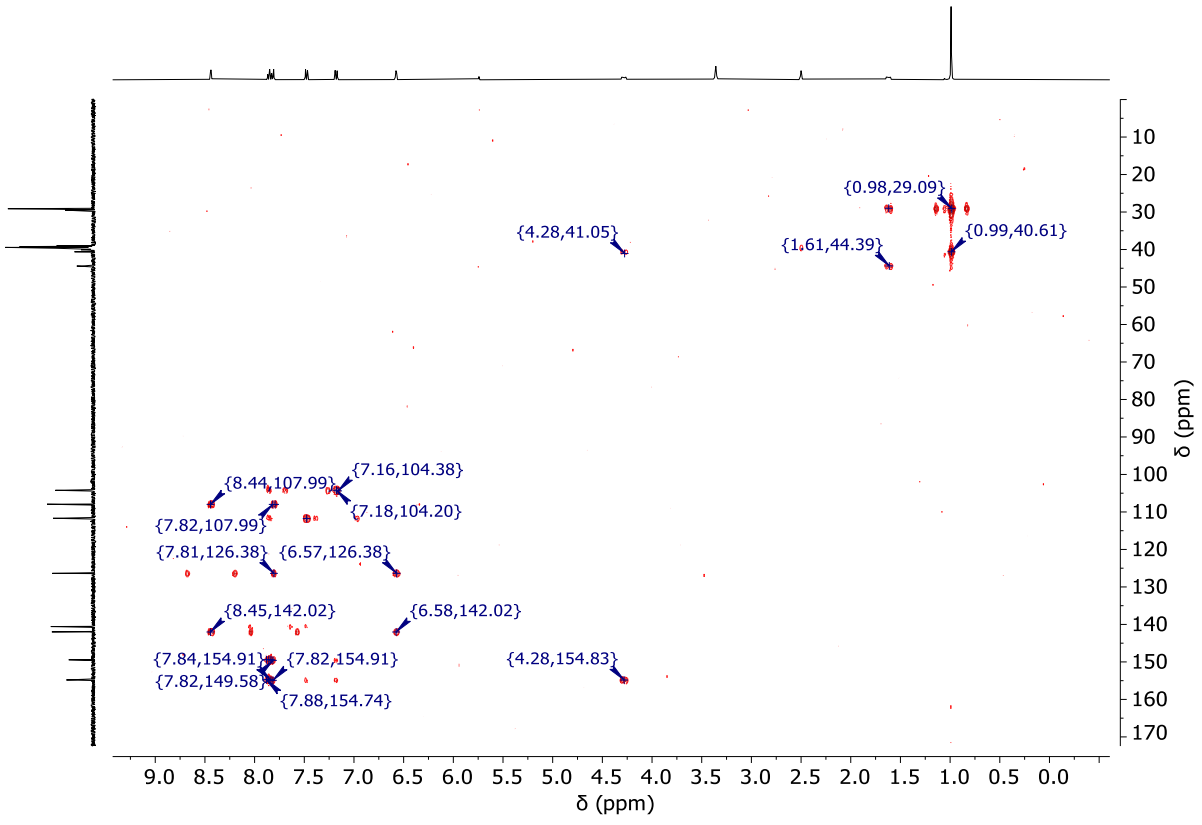

Figure S57. HC-HMBC-NMR spectrum (101 MHz (^{13}C), 400 MHz (^{1}H), DMSO-d_6) of **C3**.

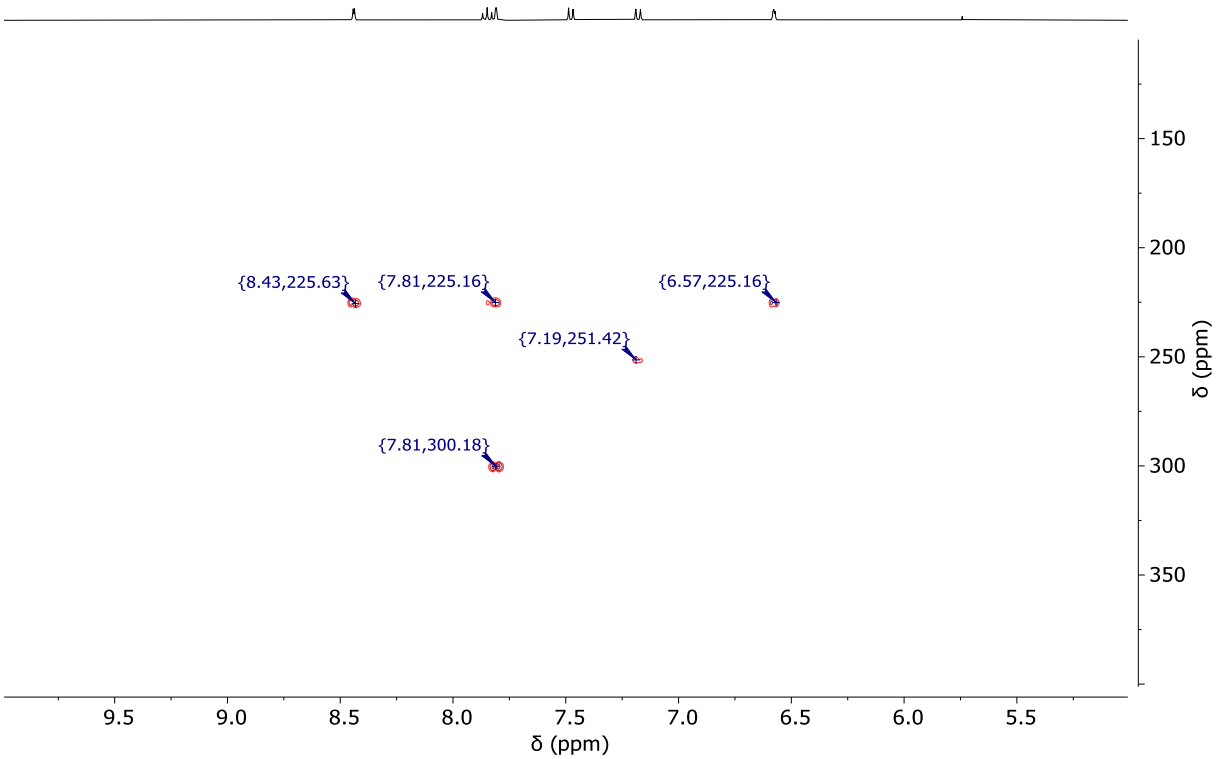

Figure S58. HN-HMBC-NMR spectrum (51 MHz (^{15}N), 500 MHz (^{1}H), DMSO-d_6) of **C3**.

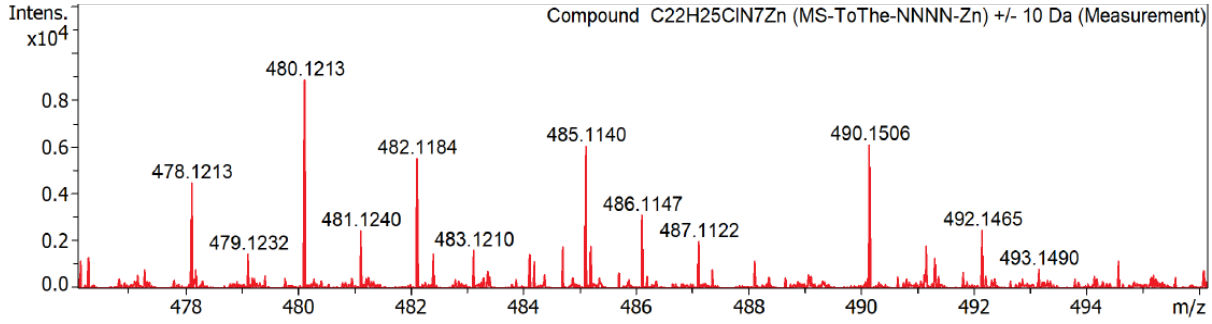

Figure S59. Mass spectrum of **C3** ($C_{22}H_{25}ClN_7Zn^+$).

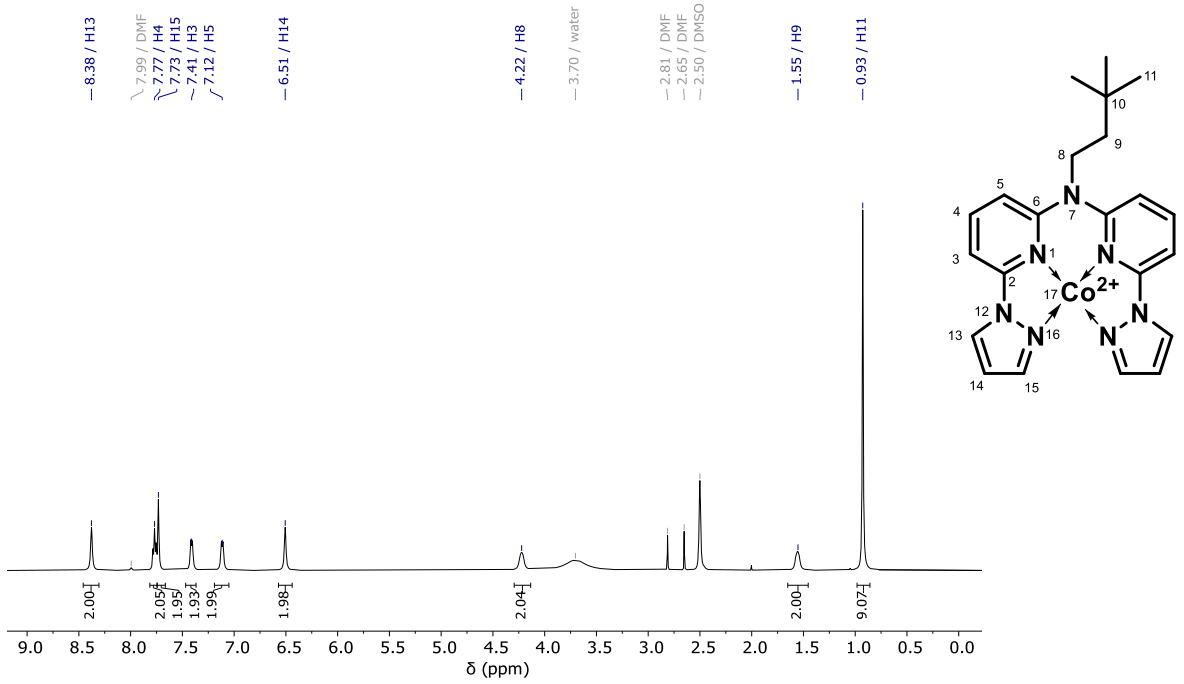

Figure S60. ^{1}H-NMR spectrum (500 MHz, DMSO-d_6) of **C4**.

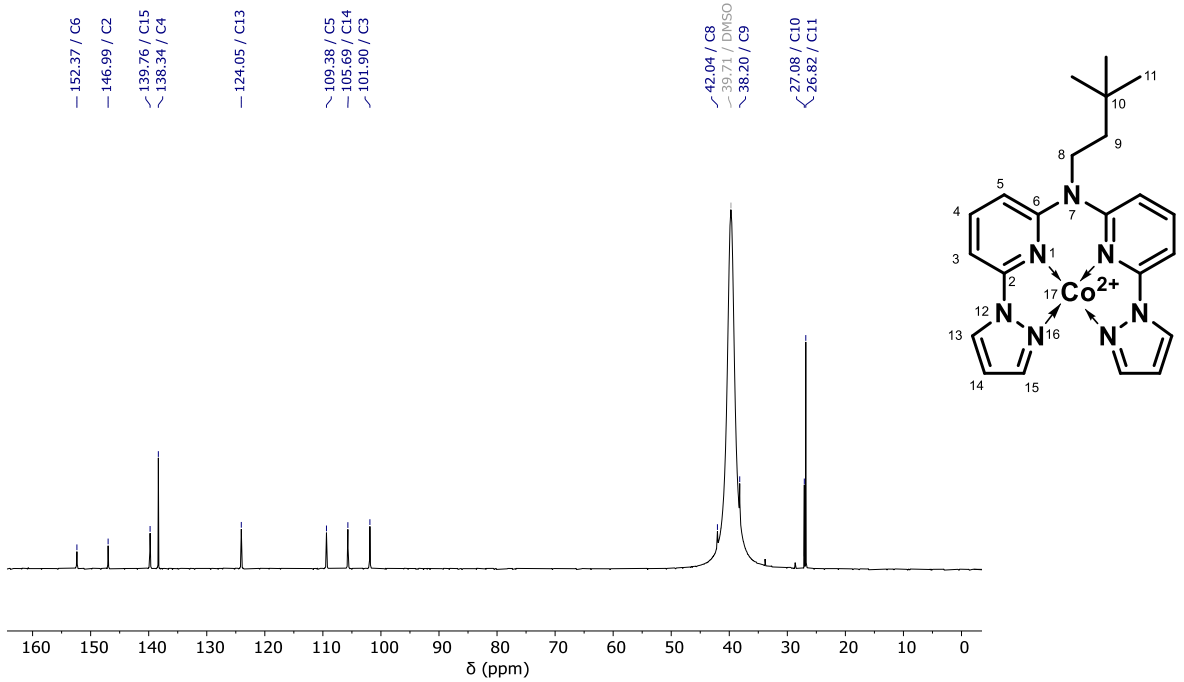

Figure S61. ^{13}C{^{1}H}-NMR spectrum (126 MHz, DMSO-d_6) of **C4**.

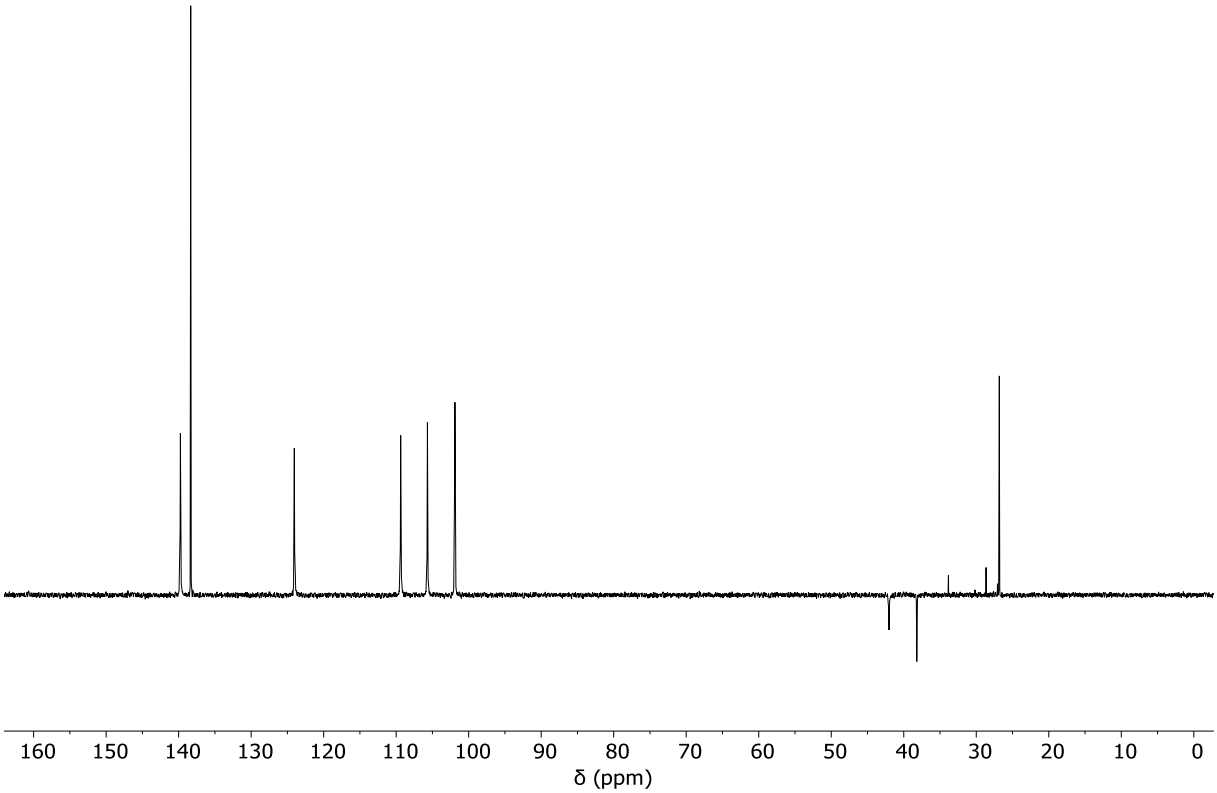

Figure S62. $^{13}C\{^{1}H\}$-NMR DEPT135 spectrum (126 MHz, DMSO-d_6) of **C4**.

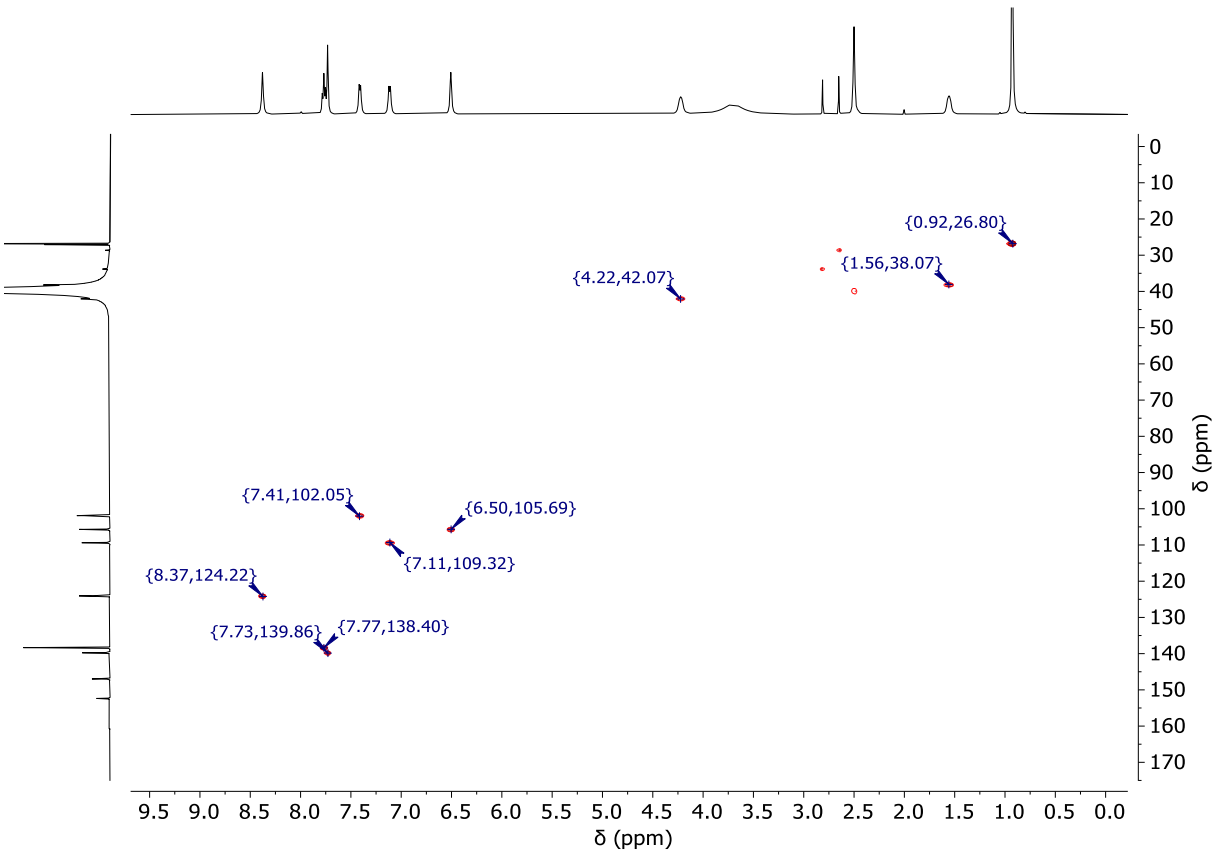

Figure S63. HC-HSQC spectrum (126 MHz (^{13}C), 500 MHz (^{1}H), DMSO-d_6) of **C4**.

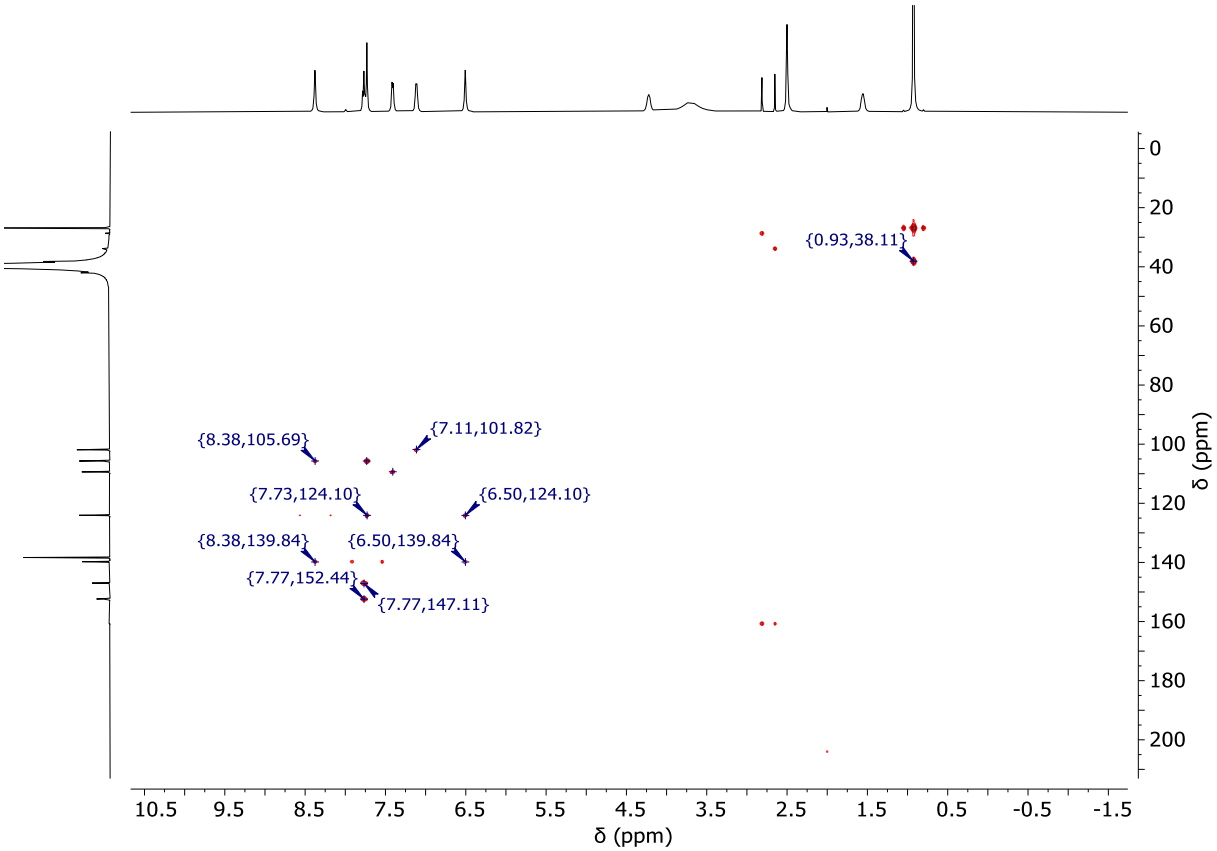

Figure S64. HC-HMBC-NMR spectrum (126 MHz (^{13}C), 500 MHz (^{1}H), DMSO-d_6) of **C4**.

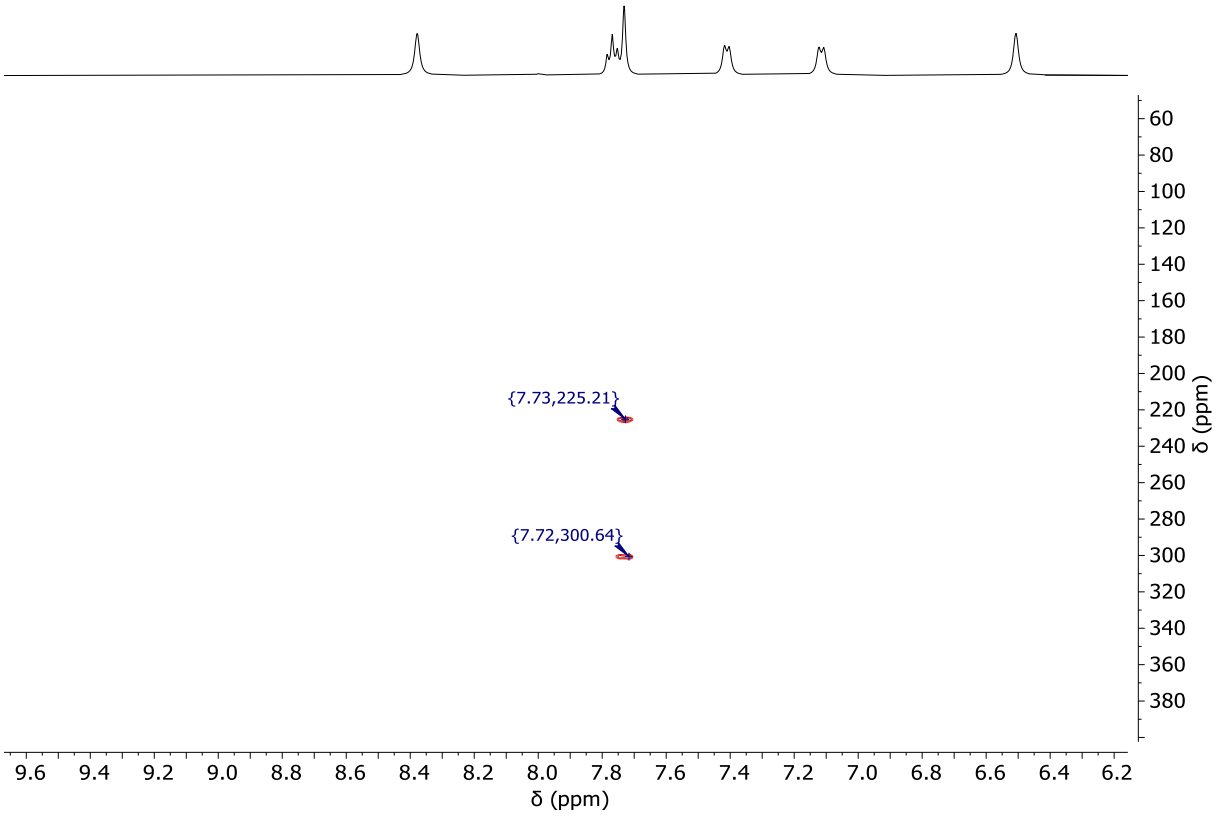

Figure S65. HN-HMBC-NMR spectrum (51 MHz (^{15}N), 500 MHz (^{1}H), DMSO-d_6) of **C4**.

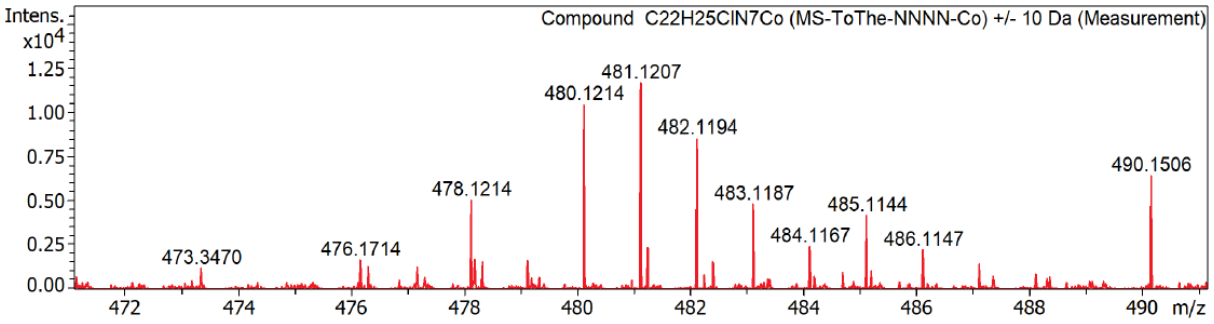

Figure S66. Mass spectrum of **C4** ($C_{22}H_{25}ClN_7Co^+$).

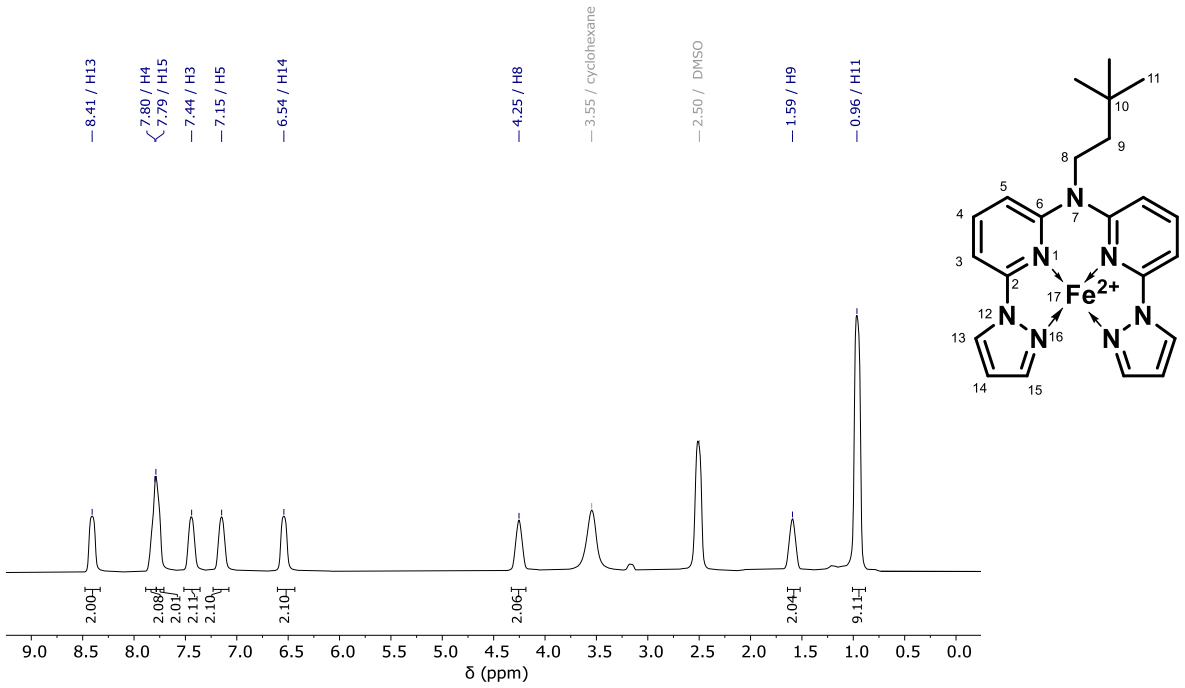

Figure S67. ^{1}H-NMR spectrum (400 MHz, DMSO-d_6) of **C5**.

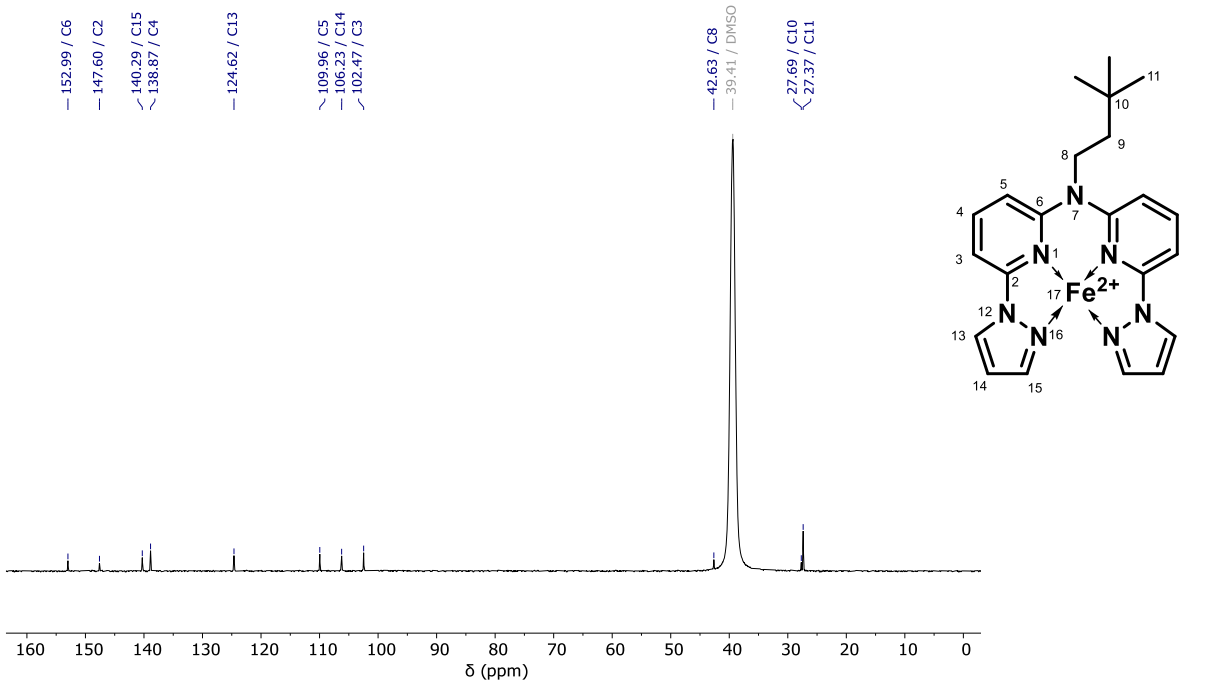

Figure S68. $^{13}C\{^{1}H\}$-NMR spectrum (101 MHz, DMSO-d_6) of **C5**.

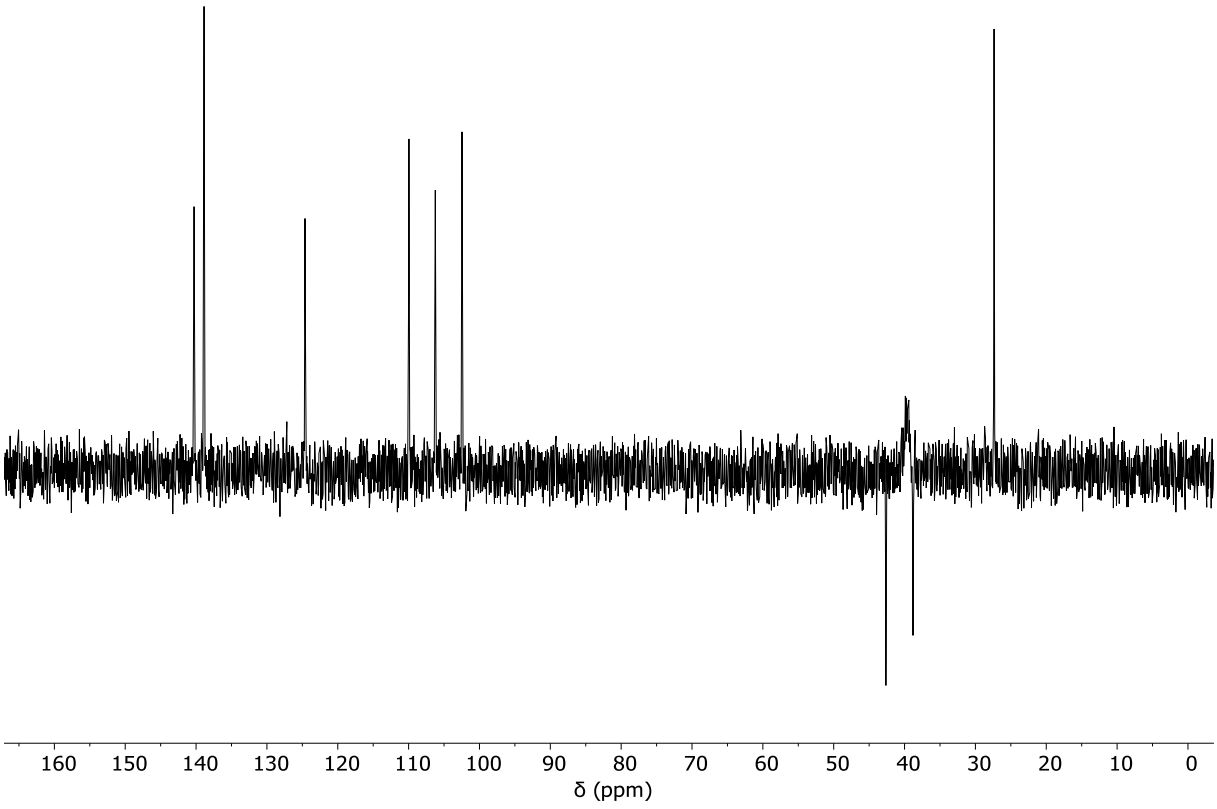

Figure S69. $^{13}C\{^{1}H\}$-NMR DEPT135 spectrum (101 MHz, DMSO-d_6) of **C5**.

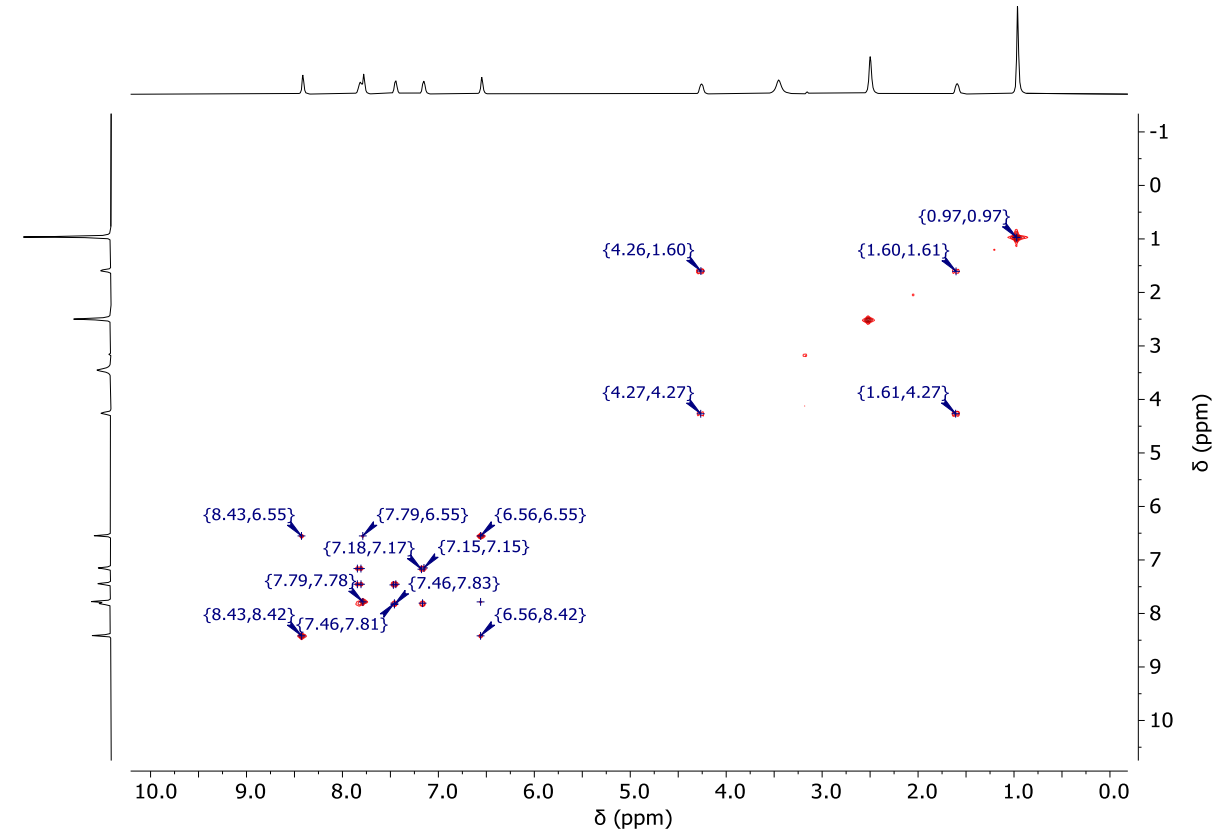

Figure S70. H,H-COSY-NMR spectrum (400 MHz, DMSO-d_6) of **C5**.

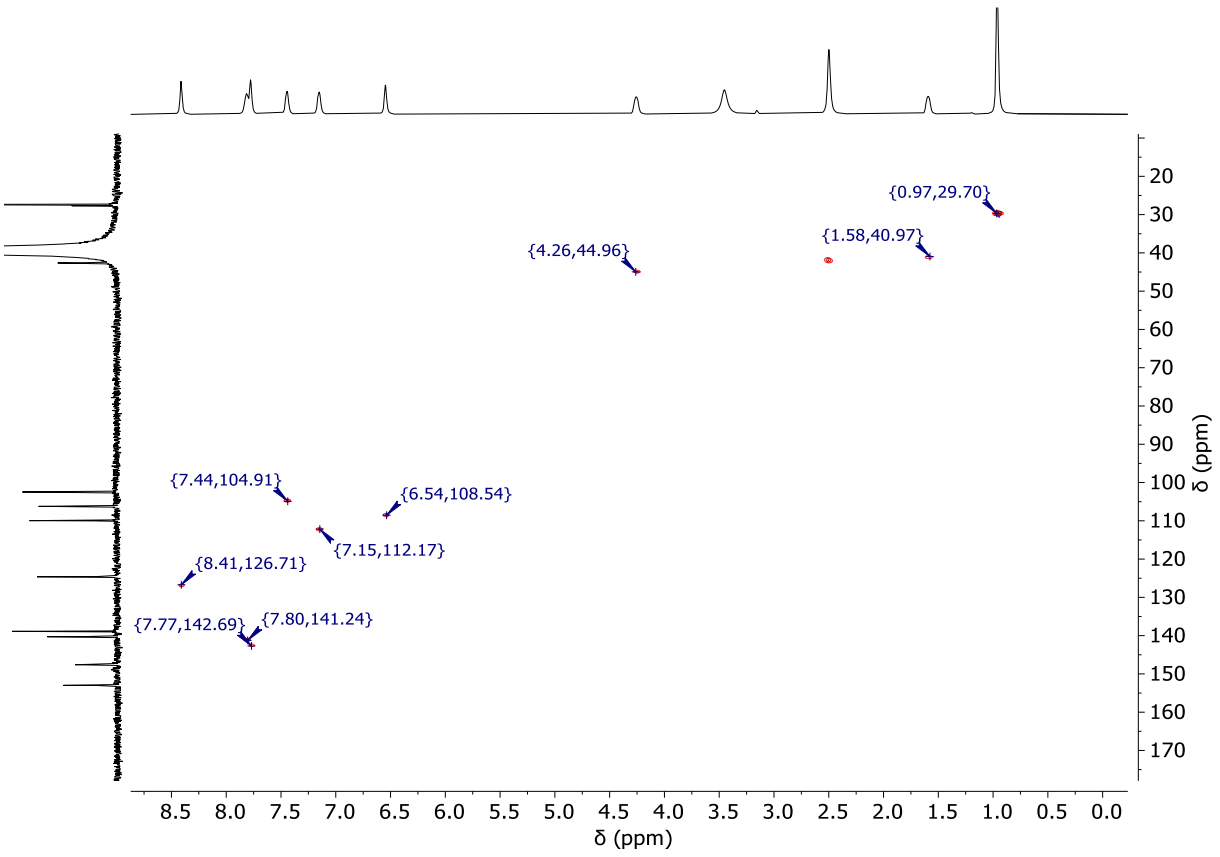

Figure S71. HC-HSQC spectrum (101 MHz (^{13}C), 400 MHz (^{1}H), DMSO-d_6) of **C5**.

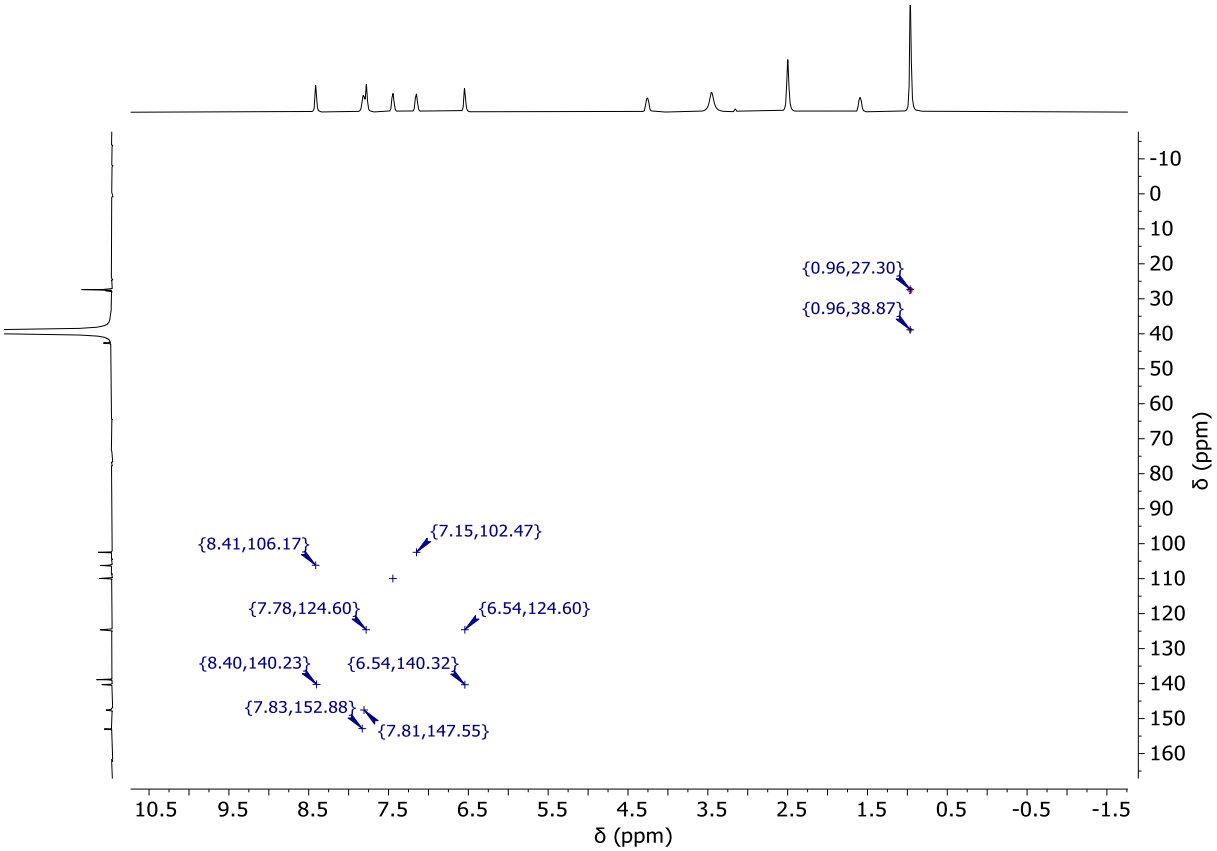

Figure S72. HC-HMBC-NMR spectrum (101 MHz (^{13}C), 400 MHz (^{1}H), DMSO-d_6) of **C5**.

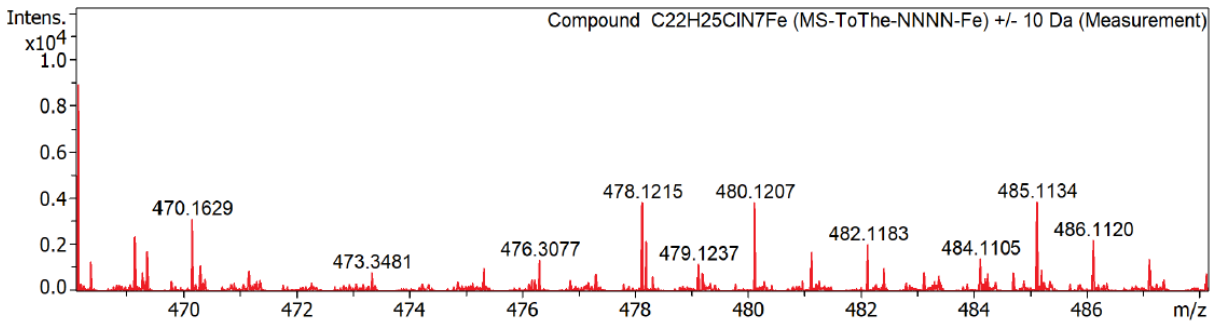

Figure S73. Mass spectrum of **C5** ($C_{22}H_{25}ClN_7Fe^+$).

Section S3: Single crystal X-ray diffraction data

Table S1. Overview of the crystallographic data of **1**, **L**, **C2**, **C3** and **C5**.

	1	**L**	**C2**	**C3**	**C5**
Formula	$C_{10}H_7Br_2N_3$	$C_{22}H_{25}N_7$	$C_{44}H_{52}Ag_2N_{16}O_7$	$C_{22.25}H_{26}C_{13}N_7O_{0.25}Zn_{1.50}$	$C_{28}H_{37}C_{15}Fe_2N_7O_2$
Mw	328.99	387.49	1132.75	599.90	792.59
CCDC No.	2286147	2292917	2286148	2286153	2286154
***a* / Å**	29.273(2)	11.9743(2)	21.8483(6)	9.3107(8)	8.725(1)
***b* / Å**	3.8382(3)	10.3581(2)	12.1445(3)	14.6832(12)	11.7665(13)
***c* / Å**	37.416(3)	32.6387(6)	9.0626(2)	20.3013(17)	18.750(2)
***V* / Å³**	4199.8(6)	4048.21(13)	2391.47(10)	2565.1(4)	1791.1(3)
α **/ °**	90	90	90	75.850(3)	107.852(4)
β **/ °**	92.533(3)	90	96.0000(8)	80.826(3)	100.659(4)
γ **/ °**	90	90	90	73.249(2)	92.254(4)
Space group	*C 2/c*	*Pbca*	*C2*	*P -1*	*P -1*
Crystal system	monoclinic	orthorhombic	monoclinic	triclinic	triclinic
***Z* value**	16	8	2	4	2
F_{000}	2528.0	1648.0	1156.0	1226.0	814.0
h, k, l_{max}	40, 5, 52	14, 12, 38	32, 17, 13	13, 20, 28	11, 15, 24
N_{ref}	6115	3607	7877	14897	8419
T_{min}, T_{max}	0.494, 0.746	0.809, 0.929	0.619, 0.746	0.527, 0.746	0.558, 0.746

Table S2. Selected bond lengths and angles in **C2**.

Bond length / angles	
Ag1 – N16 / Å	2.426(2)
Ag1 – N21 / Å	2.240(2)
Ag1 – N27 / Å	2.410(2)
Ag1 – N32 / Å	2.267(2)
N16 ··· Ag1 ··· N21 / °	70.74(8)
N16 ··· Ag1 ··· N27 / °	116.61(6)
N16 ··· Ag1 ··· N32 / °	127.76(7)
N21 ··· Ag1 ··· N27 / °	159.22(8)
N21 ··· Ag1 ··· N32 / °	121.73(8)
N27 ··· Ag1 ··· N32 / °	70.68(7)

Table S3. Selected bond lengths and angles in **C3**.

Bond length / angles	
Zn1A – N15A / Å	2.134(2)
Zn1A – N20A / Å	2.096(1)
Zn1A – N26A / Å	2.133(1)
Zn1A – N31A / Å	2.098(2)
Zn1A – Cl2A / Å	2.2154(4)
N15A ··· Zn1A ··· N20A / °	76.15(6)
N15A ··· Zn1A ··· N26A / °	79.85(6)
N15A ··· Zn1A ··· N31A / °	132.12(6)
N20A ··· Zn1A ··· N26A / °	138.45(6)
N20A ··· Zn1A ··· N31A / °	95.47(6)
N26A ··· Zn1A ··· N31A / °	76.37(6)
Zn1 – N15 / Å	2.095(2)
Zn1 – N20 / Å	2.070(2)
Zn1 – N26 / Å	2.121(1)
Zn1 – N31 / Å	2.089(2)
Zn1 – Cl2 / Å	2.2206(5)
N15 ··· Zn1 ··· N20 / °	77.98(6)
N15 ··· Zn1 ··· N26 / °	83.16(6)
N15 ··· Zn1 ··· N31 / °	130.76(6)
N20 ··· Zn1 ··· N26 / °	147.13(6)
N20 ··· Zn1 ··· N31 / °	95.65(6)
N26 ··· Zn1 ··· N31 / °	76.69(6)

Table S4. Selected bond lengths and angles in **C5**.

Bond length / angles	
Fe1 – N15 / Å	2.136(2)
Fe1 – N20 / Å	2.101(1)
Fe1 – N26 / Å	2.129(2)
Fe1 – N31 / Å	2.115(2)
Fe1 – Cl2 / Å	2.2324(6)
N15 ··· Fe1 ··· N20 / °	76.12(7)
N15 ··· Fe1 ··· N26 / °	82.59(7)
N15 ··· Fe1 ··· N31 / °	137.83(7)
N20 ··· Fe1 ··· N26 / °	139.35(7)
N20 ··· Fe1 ··· N31 / °	97.13(7)
N26 ··· Fe1 ··· N31 / °	76.18(7)

Section S4.1: Single crystal X-ray diffraction analysis of 1

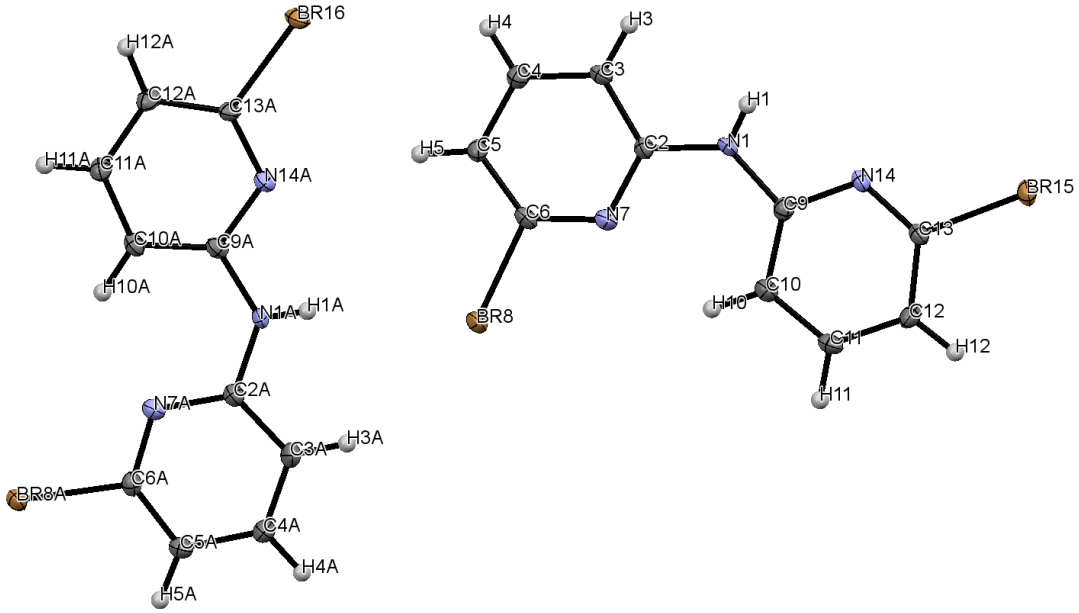

Figure S74. Molecular structure in the single crystal of **1** with labelled atoms. Displacement ellipsoids are shown at 50% probability.

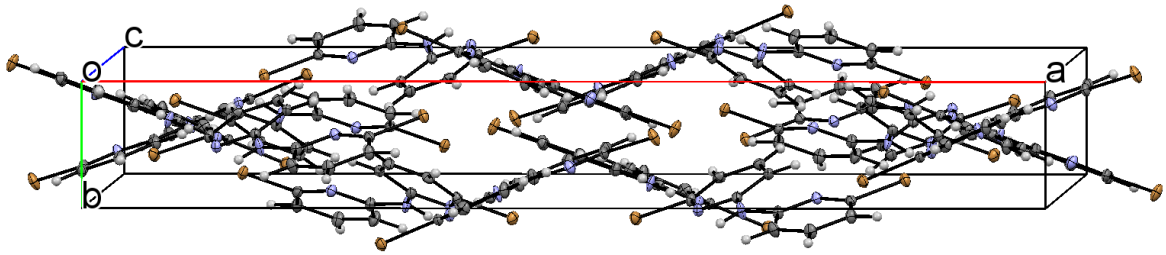

Figure S75. Unit cell of **1**. Displacement ellipsoids are shown at 50% probability.

Section S4.2: Single crystal X-ray diffraction analysis of L

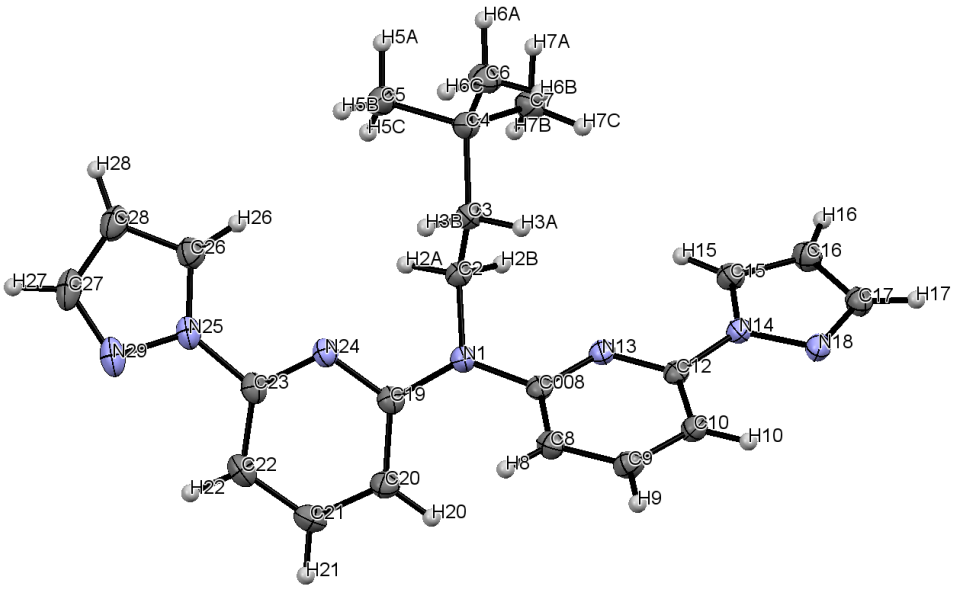

Figure S76. Molecular structure in the single crystal of **L** with labelled atoms. Displacement ellipsoids are shown at 50% probability.

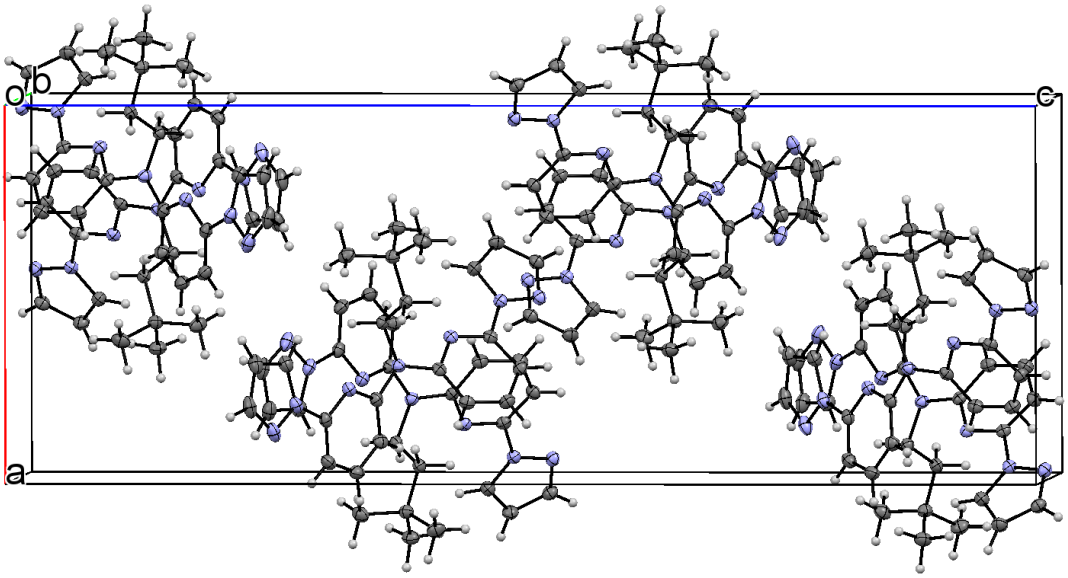

Figure S77. Unit cell of **L**. Displacement ellipsoids are shown at 50% probability.

Section S4.3: Single crystal X-ray diffraction analysis of C2

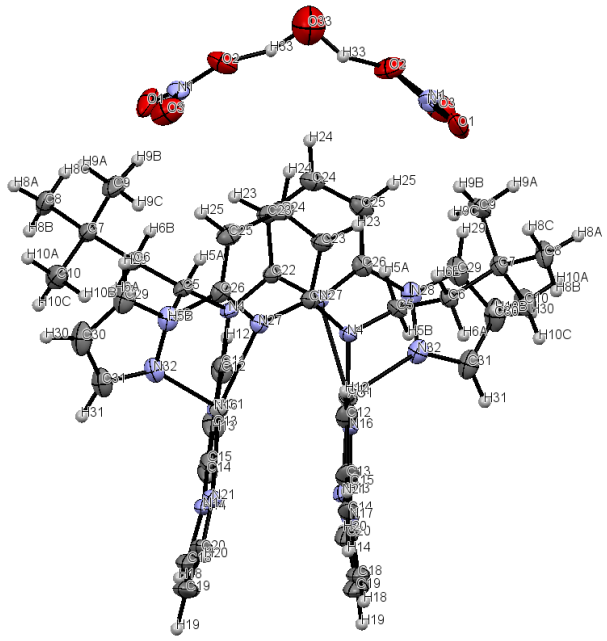

Figure S78. Molecular structure in the single crystal of **C2** with labelled atoms. Displacement ellipsoids are shown at 50% probability. The nitrate anions are disordered but have been manually optimized for clarity.

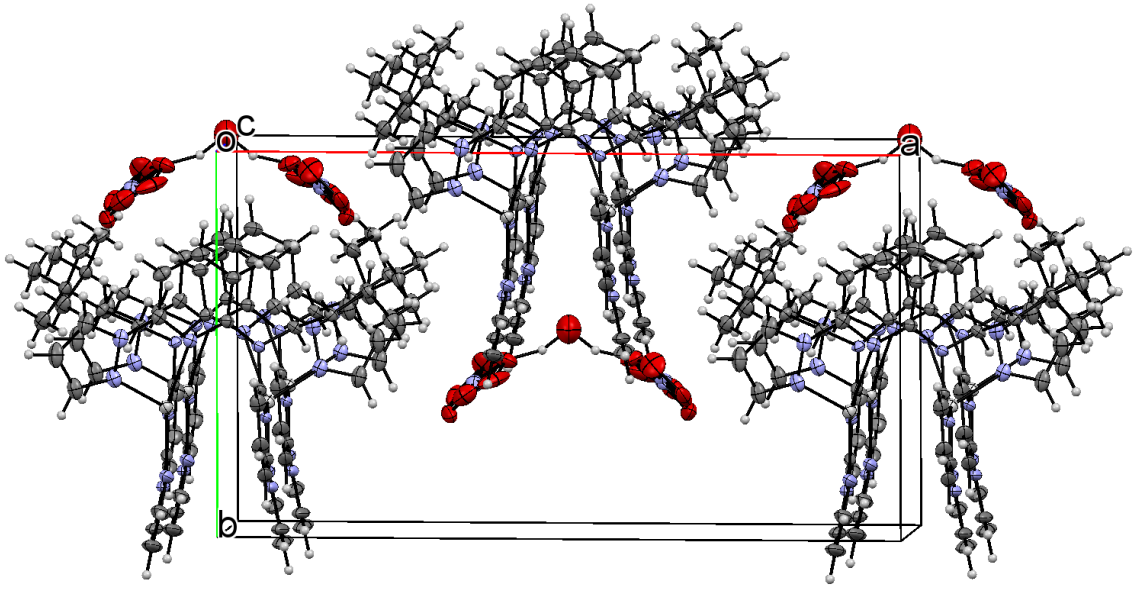

Figure S79. Unit cell of **C2**. Displacement ellipsoids are shown at 50% probability.

Section S4.4: Single crystal X-ray diffraction analysis of C3

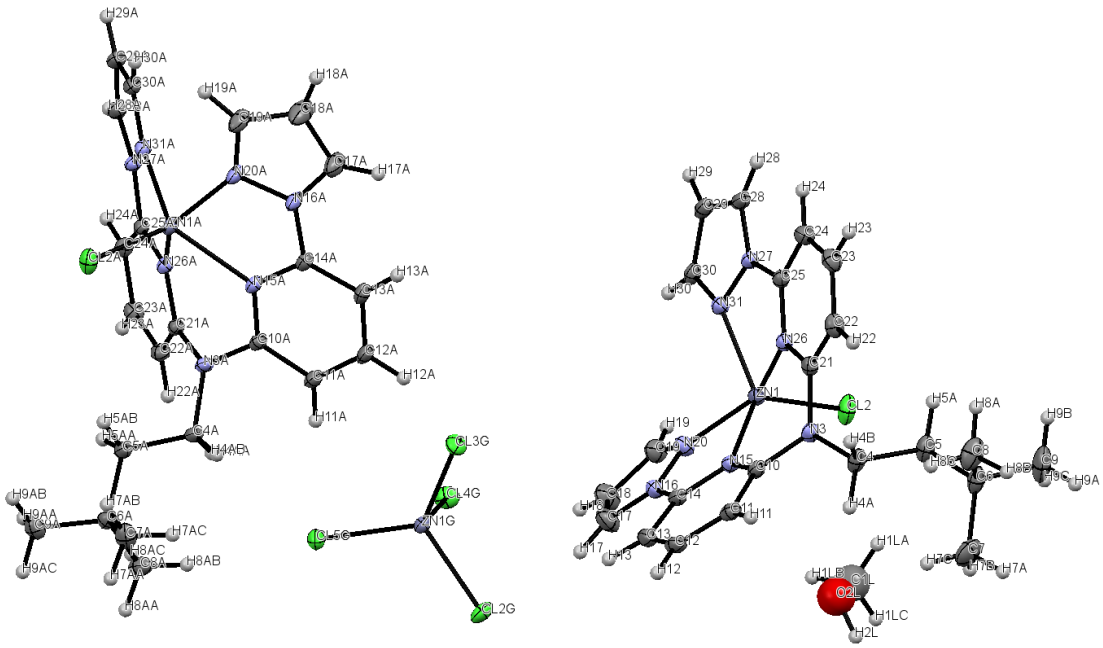

Figure S80. Asymmetric unit of **C3** with labelled atoms. Displacement ellipsoids are shown at 50% probability. The disordered methanol molecule has been manually optimized for clarity.

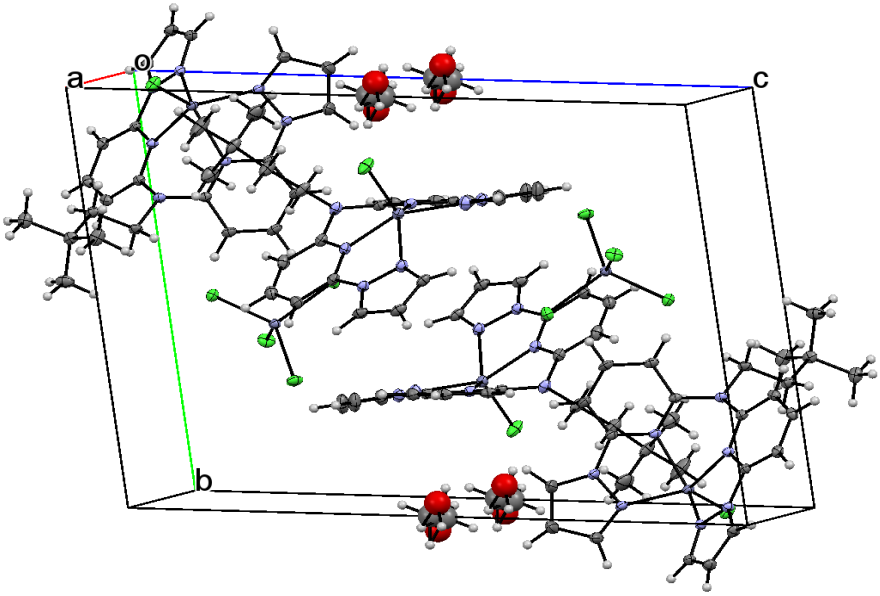

Figure S81. Unit cell of **C3**. Displacement ellipsoids are shown at 50% probability.

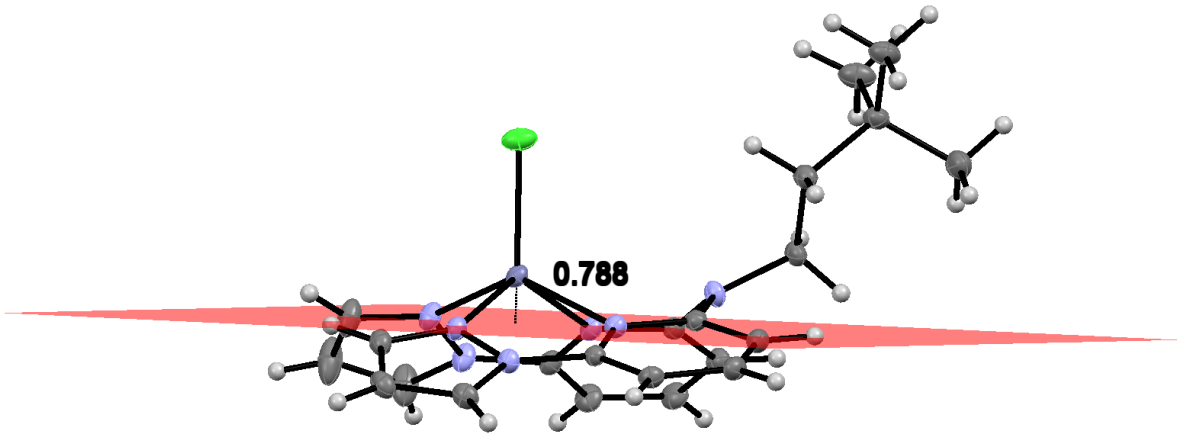

Figure S82. Molecular structure in the single crystal of **C3**. The zinc(II) ion is locates above the coordination plane (shown in red). Distance is given in Ångstrom (Å).

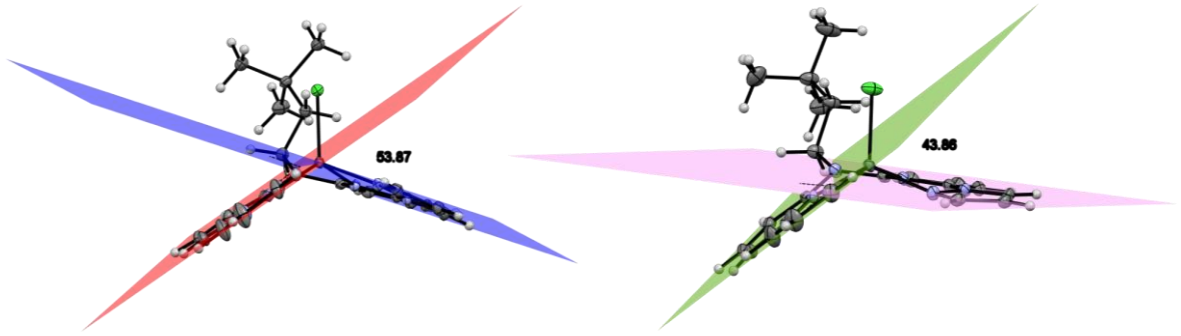

Figure S83. Depiction of the two different Zn(II) complexes of the asymmetric unit of **C3**. The two N^N moieties in both complexes are not coplanar but in an angle of 53.87° and 43.86° to each other.

Section S4.5: Single crystal X-ray diffraction analysis of C5

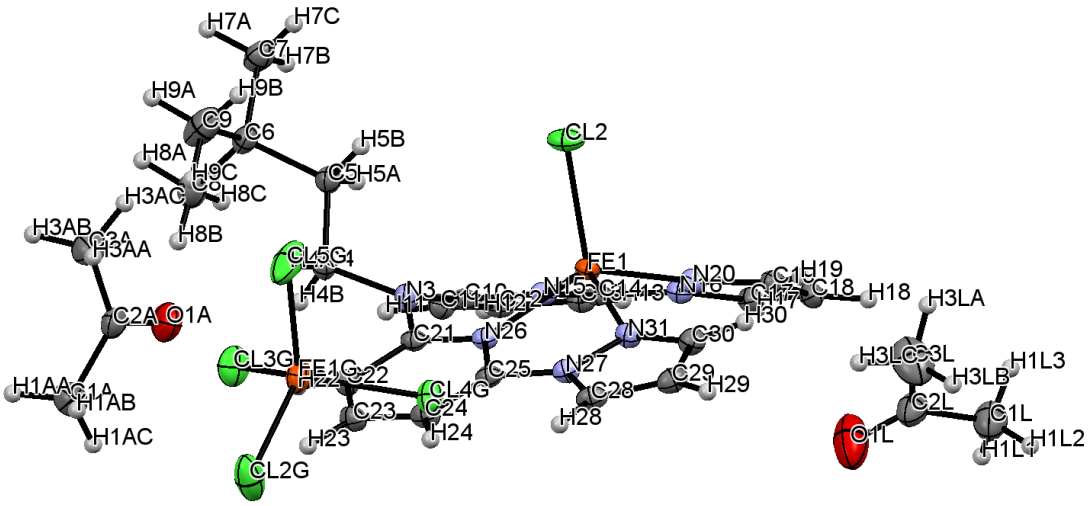

Figure S84. Molecular structure in the single crystal of **C5** with labelled atoms. Displacement ellipsoids are shown at 50% probability.

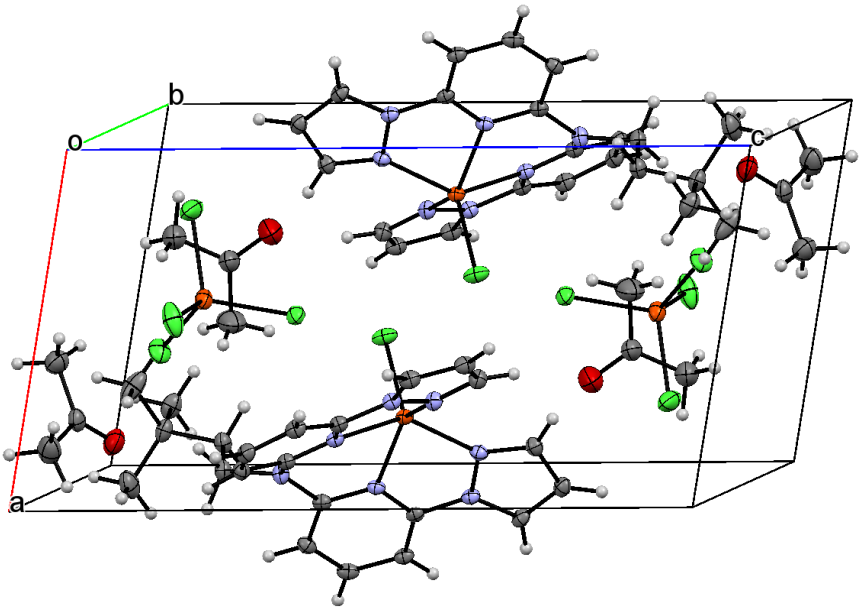

Figure S85. Unit cell of **C5**. Displacement ellipsoids are shown at 50% probability.

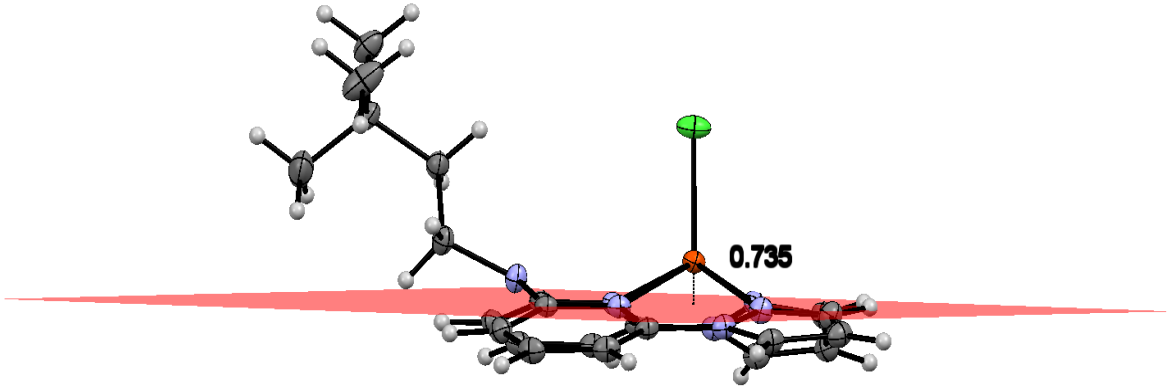

Figure S86. Molecular structure in the single crystal of **C5**. The iron(II) ion is placed above the coordination plane (shown in red). Distance is given in Ångstrom (Å).

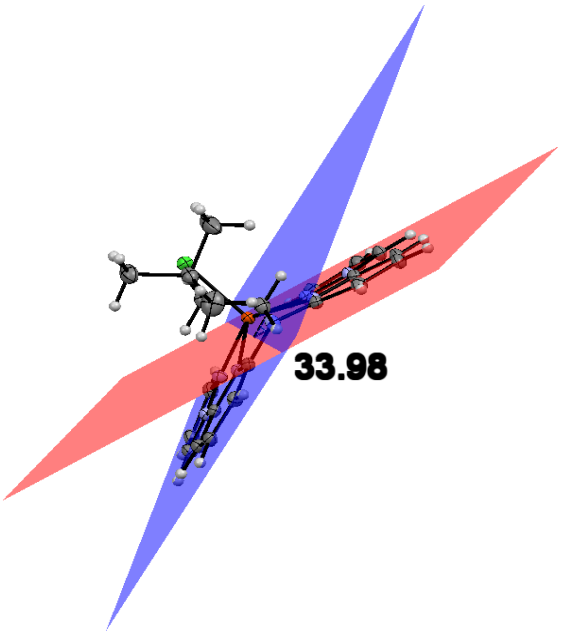

Figure S87. Molecular structure in the single crystal of **C5**. The two N^N moieties are not coplanar but in an angle of 33.98° to each other.

Section S4: Photophysical characterization

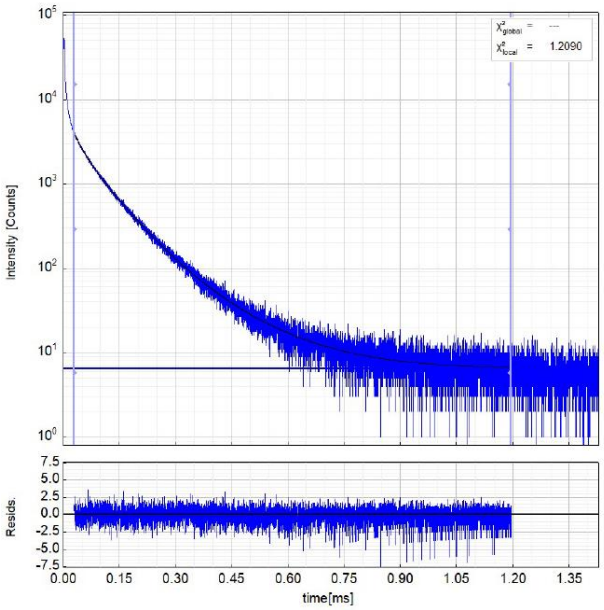

Parameter	Value	Δ	δ
A_1[kCnts/Chnl]	0.33	±0.11	32%
τ_1[ns]	163 000	±15 000	9.1%
I_1[kCnts]	410	±98	24%
A_{Rel1}[%]	8.2	±2.7	32%
I_{Rel1}[%]	20.3	±4.9	24%
A_2[kCnts/Chnl]	2.432	±0.034	1.4%
τ_2[ns]	73 800	±3 800	5.1%
I_2[kCnts]	1 402	±59	4.1%
A_{Rel2}[%]	62.0	±0.9	1.3%
I_{Rel2}[%]	69.3	±2.9	4.1%
A_3[kCnts/Chnl]	1.18	±0.12	9.5%
τ_3[ns]	23 500	±1 700	7.3%
I_3[kCnts]	215	±38	17%
A_{Rel3}[%]	29.9	±3.0	9.8%
I_{Rel3}[%]	10.6	±1.9	17%
$Bkgr_{Dec}$[kCnts]	0.0065	±0.0003	3.4%
τ_{AvInt}[ns]	86 440	±560	0.6%
τ_{AvAmp}[ns]	66 030	±330	0.5%

Figure S88. Left: Raw (experimental) time-resolved photoluminescence decay of **C1** (Pt(II) complex) in the solid state at 298 K including the residuals (λ_{exc} = 376.7 nm, λ_{em} = 588 nm). Right: Fitting parameters including pre-exponential factors and confidence limits.

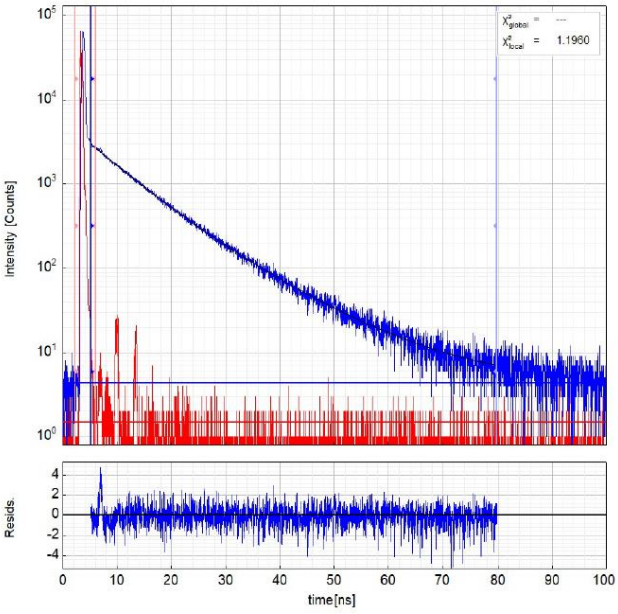

Parameter	Value	Δ	δ
A_1[kCnts/Chnl]	0.89	±0.20	22%
τ_1[ns]	13.16	±0.82	6.2%
I_1[kCnts]	364	±63	17%
A_{Rel1}[%]	23.5	±5.6	24%
I_{Rel1}[%]	36.4	±6.5	18%
A_2[kCnts/Chnl]	2.88	±0.27	9.1%
τ_2[ns]	7.09	±0.27	3.7%
I_2[kCnts]	638	±77	12%
A_{Rel2}[%]	76.6	±5.6	7.2%
I_{Rel2}[%]	63.7	±6.5	10%
$Bkgr_{Dec}$[kCnts]	0.0044	±0.0007	14%
$Bkgr_{IRF}$[Cnts/Chnl]	1.5000	---	---
$Shift_{IRF}$[ps]	- 450	±210	46%
τ_{AvInt}[ns]	9.291	±0.055	0.6%
τ_{AvAmp}[ns]	8.511	±0.037	0.4%

Figure S89. Left: Raw (experimental) time-resolved photoluminescence decay of **C2** (Ag(I) complex) in the solid state at 298 K including the residuals (λ_{exc} = 376.7 nm, λ_{em} = 388 nm; the instrument response function is shown in red). Right: Fitting parameters including pre-exponential factors and confidence limits.

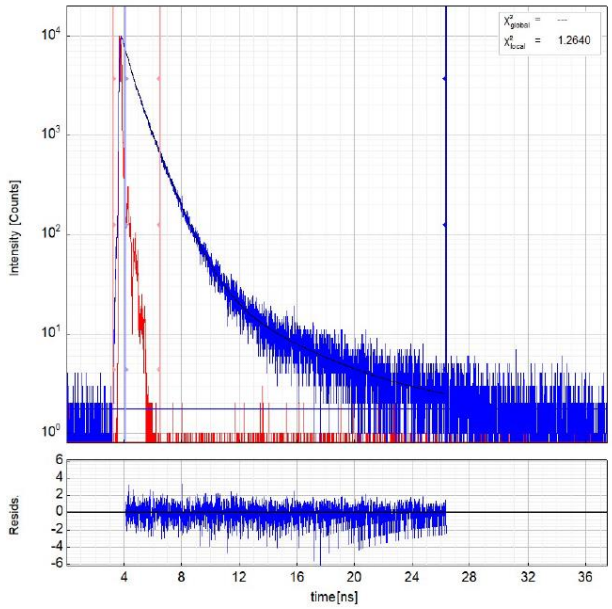

Parameter	Value	Δ	δ
A_1[kCnts/Chnl]	0.069	±0.012	17%
τ_1[ns]	5.03	±0.59	12%
I_1[kCnts]	42.9	±3.2	7.5%
A_{Rel1}[%]	0.6	±0.1	18%
I_{Rel1}[%]	3.4	±0.6	17%
A_2[kCnts/Chnl]	6.29	±0.31	4.8%
τ_2[ns]	1.144	±0.017	1.5%
I_2[kCnts]	899	±41	4.5%
A_{Rel2}[%]	48.0	±1.7	3.4%
I_{Rel2}[%]	70.5	±1.5	2.1%
A_3[kCnts/Chnl]	6.77	±0.78	11%
τ_3[ns]	0.396	±0.016	4.0%
I_3[kCnts]	335	±38	11%
A_{Rel3}[%]	51.6	±1.7	3.2%
I_{Rel3}[%]	26.3	±1.7	6.4%
$Bkgr_{Dec}$[kCnts]	0.0018	±0.0004	20%
$Bkgr_{IRF}$[Cnts/Chnl]	0.8000	---	---
$Shift_{IRF}$[ps]	64	±52	81%
τ_{AvInt}[ns]	1.078	±0.019	1.7%
τ_{AvAmp}[ns]	0.779	±0.015	1.8%

Figure S90. Left: Raw (experimental) time-resolved photoluminescence decay of **C3** (Zn(II) complex) in the solid state at 298 K including the residuals (λ_{exc} = 376.7 nm, λ_{em} = 390 nm; the instrument response function is shown in red). Right: Fitting parameters including pre-exponential factors and confidence limits.

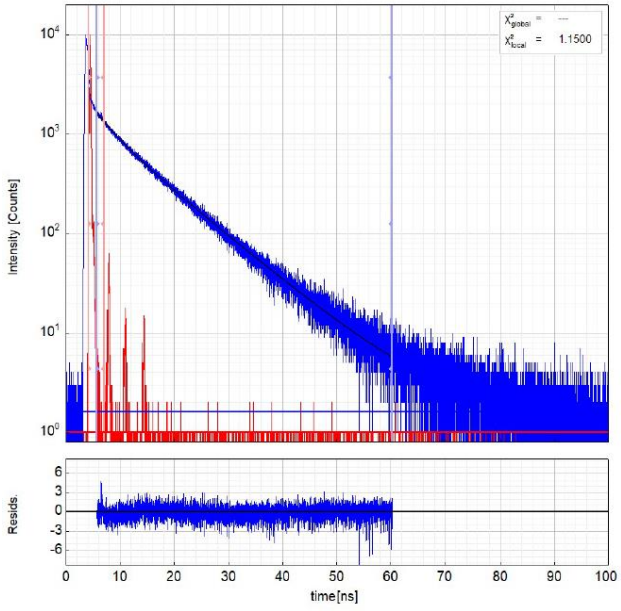

Parameter	Value	Δ	δ
A_1[kCnts/Chnl]	1.313	±0.063	4.8%
τ_1[ns]	9.69	±0.16	1.6%
I_1[kCnts]	1 589	±50	3.1%
A_{Rel1}[%]	65.0	±2.8	4.2%
I_{Rel1}[%]	83.7	±3.1	3.7%
A_2[kCnts/Chnl]	0.708	±0.053	7.4%
τ_2[ns]	3.53	±0.46	13%
I_2[kCnts]	312	±60	19%
A_{Rel2}[%]	35.1	±2.8	7.9%
I_{Rel2}[%]	16.4	±3.1	19%
$Bkgr_{Dec}$[kCnts]	0.0016	---	---
$Bkgr_{IRF}$[Cnts/Chnl]	1.0000	---	---
$Shift_{IRF}$[ps]	473	±81	17%
τ_{AvInt}[ns]	8.674	±0.019	0.2%
τ_{AvAmp}[ns]	7.527	±0.099	1.3%

Figure S91. Left: Raw (experimental) time-resolved photoluminescence decay of **C4** (Co(II) complex) in the solid state at 298 K including the residuals (λ_{exc} = 376.7 nm, λ_{em} = 388 nm; the instrument response function is shown in red). Right: Fitting parameters including pre-exponential factors and confidence limits.

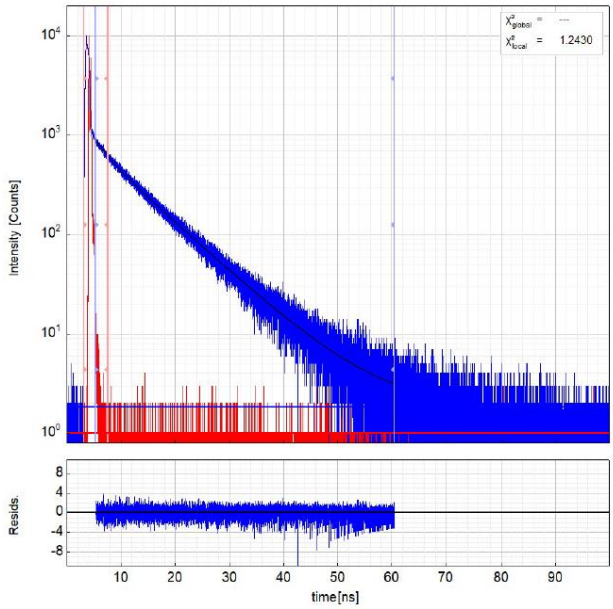

Parameter	Value	Δ	δ
A_1[kCnts/Chnl]	0.791	±0.037	4.6%
τ_1[ns]	8.779	±0.095	1.1%
I_1[kCnts]	1 735	±61	3.5%
A_{Rel1}[%]	75.0	±2.4	3.2%
I_{Rel1}[%]	90.8	±2.2	2.3%
A_2[kCnts/Chnl]	0.265	±0.034	13%
τ_2[ns]	2.66	±0.34	13%
I_2[kCnts]	177	±48	27%
A_{Rel2}[%]	25.1	±2.4	9.5%
I_{Rel2}[%]	9.3	±2.2	23%
$Bkgr_{Dec}$[kCnts]	0.0019	±0.0002	9.0%
$Bkgr_{IRF}$[Cnts/Chnl]	1.0000	---	---
$Shift_{IRF}$[ps]	380	±250	65%
τ_{AvInt}[ns]	8.215	±0.051	0.6%
τ_{AvAmp}[ns]	7.25	±0.15	2.0%

Figure S92. Left: Raw (experimental) time-resolved photoluminescence decay of **C5** (Fe(II) complex) in the solid state at 298 K including the residuals (λ_{exc} = 376.7 nm, λ_{em} = 388 nm; the instrument response function is shown in red). Right: Fitting parameters including pre-exponential factors and confidence limits.

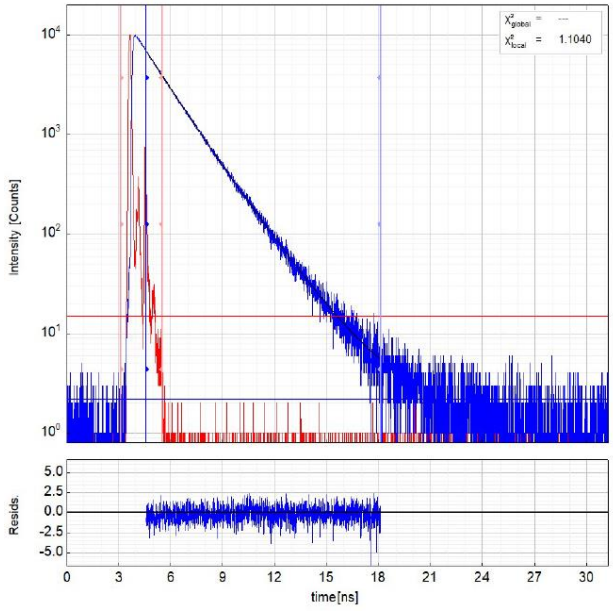

Parameter	Value	Δ	δ
A_1[kCnts/Chnl]	5.19	±0.13	2.4%
τ_1[ns]	1.958	±0.017	0.8%
I_1[kCnts]	1 269	±35	2.7%
A_{Rel1}[%]	41.8	±0.8	1.8%
I_{Rel1}[%]	50.3	±1.2	2.3%
A_2[kCnts/Chnl]	7.23	±0.23	3.1%
τ_2[ns]	1.393	±0.022	1.5%
I_2[kCnts]	1 257	±39	3.0%
A_{Rel2}[%]	58.3	±0.8	1.3%
I_{Rel2}[%]	49.8	±1.2	2.3%
$Bkgr_{Dec}$[kCnts]	0.0022	±0.0004	17%
$Bkgr_{IRF}$[Cnts/Chnl]	14.9	±4.6	31%
$Shift_{IRF}$[ps]	- 195	±15	7.3%
τ_{AvInt}[ns]	1.6762	±0.0038	0.2%
τ_{AvAmp}[ns]	1.6285	±0.0075	0.5%

Figure S93. Left: Raw (experimental) time-resolved photoluminescence decay of the ligand system **L** in the solid state at 298 K including the residuals (λ_{exc} = 376.7 nm, λ_{em} = 390 nm; the instrument response function is shown in red). Right: Fitting parameters including pre-exponential factors and confidence limits.

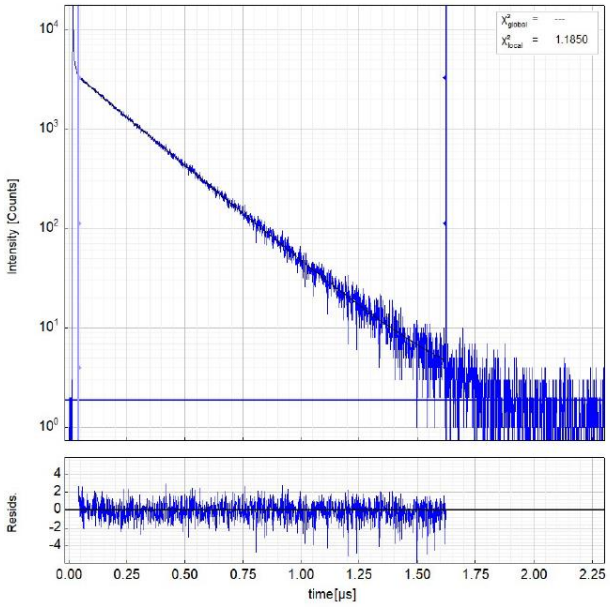

Parameter	Value	Δ	δ
A_1[kCnts/Chnl]	3.361	±0.017	0.5%
τ_1[ns]	223.99	±0.63	0.3%
I_1[kCnts]	752.8	±2.6	0.3%
A_{Rel1}[%]	100.0	---	---
I_{Rel1}[%]	100.0	---	---
$Bkgr_{Dec}$[kCnts]	0.0019	±0.0004	17%
τ_{AvInt}[ns]	223.99	±0.63	0.3%
τ_{AvAmp}[ns]	223.99	±0.63	0.3%

Figure S94. Left: Raw (experimental) time-resolved photoluminescence decay of **C1** (Pt(II) complex) in an air-equilibrated MeOH solution at 298 K including the residuals (λ_{exc} = 376.7 nm, λ_{em} = 450 nm). Right: Fitting parameters including pre-exponential factors and confidence limits.

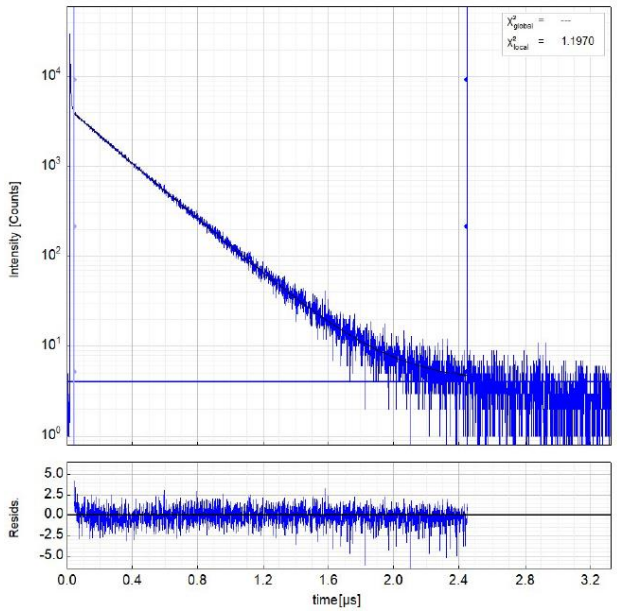

Parameter	Value	Δ	δ
A_1[kCnts/Chnl]	3.913	±0.020	0.5%
τ_1[ns]	280.24	±0.98	0.3%
I_1[kCnts]	1 096.6	±3.0	0.3%
A_{Rel1}[%]	100.0	---	---
I_{Rel1}[%]	100.0	---	---
$Bkgr_{Dec}$[kCnts]	0.0041	±0.0003	5.2%
τ_{AvInt}[ns]	280.24	±0.98	0.3%
τ_{AvAmp}[ns]	280.24	±0.98	0.3%

Figure S95. Left: Raw (experimental) time-resolved photoluminescence decay of **C1** (Pt(II) complex) an in Ar-purged MeOH solution at 298 K including the residuals (λ_{exc} = 376.7 nm, λ_{em} = 450 nm). Right: Fitting parameters including pre-exponential factors and confidence limits.

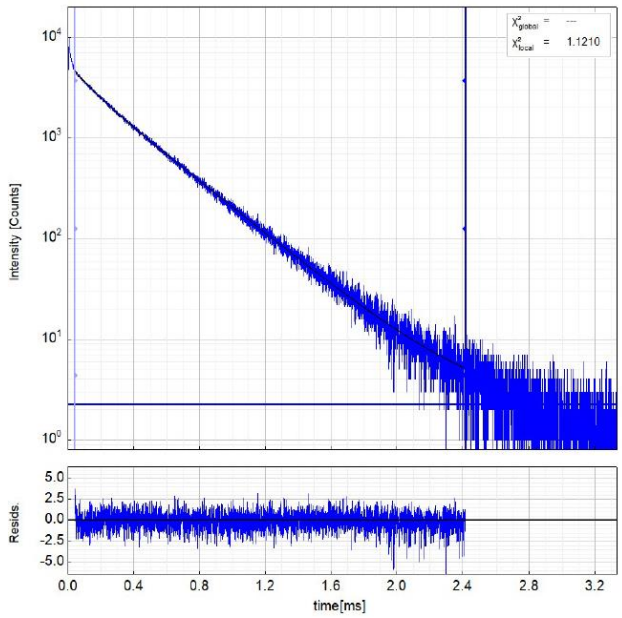

Parameter	Value	Δ	δ
A_1[kCnts/Chnl]	3.626	±0.071	2.0%
τ_1[ns]	333 200	±2 400	0.7%
I_1[kCnts]	2 360	±30	1.3%
A_{Rel1}[%]	78.0	±1.4	1.7%
I_{Rel1}[%]	91.1	±1.2	1.2%
A_2[kCnts/Chnl]	1.025	±0.060	5.8%
τ_2[ns]	116 400	±9 900	8.5%
I_2[kCnts]	233	±30	13%
A_{Rel2}[%]	22.1	±1.4	6.1%
I_{Rel2}[%]	9.0	±1.2	13%
$Bkgr_{Dec}$[kCnts]	0.0023	±0.0004	14%
τ_{AvInt}[ns]	313 710	±690	0.2%
τ_{AvAmp}[ns]	285 400	±2 400	0.8%

Figure S96. Left: Raw (experimental) time-resolved photoluminescence decay of **C1** (Pt(II) complex) in a frozen glassy matrix (DCM-MeOJ 1:1) at 77 K including the residuals (λexc = 376.7 nm, λem = 450 nm). Right: Fitting parameters including pre-exponential factors and confidence limits.

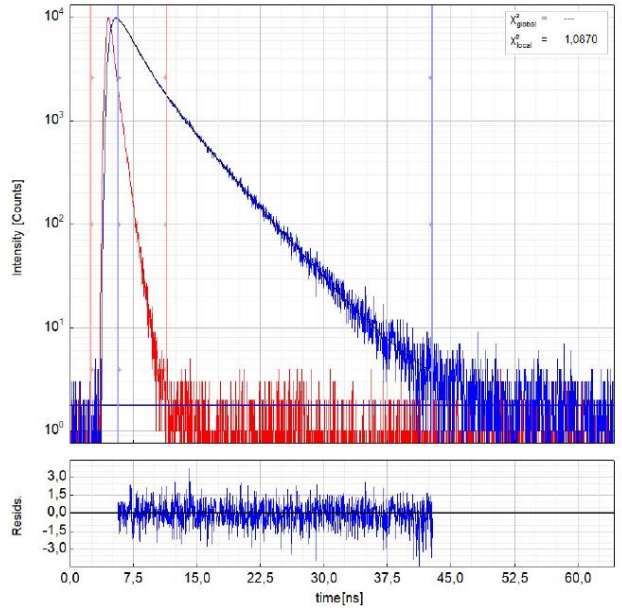

Parameter	Value	Δ	δ
A_1[kCnts/Chnl]	5,91	±0,30	4,9%
τ_1[ns]	4,722	±0,048	1,0%
I_1[kCnts]	872	±37	4,2%
A_{Rel1}[%]	35,4	±1,4	3,8%
I_{Rel1}[%]	60,8	±2,0	3,2%
A_2[kCnts/Chnl]	10,81	±0,33	3,1%
τ_2[ns]	1,670	±0,056	3,3%
I_2[kCnts]	564	±36	6,3%
A_{Rel2}[%]	64,7	±1,4	2,1%
I_{Rel2}[%]	39,3	±2,0	5,0%
$Bkgr_{Dec}$[kCnts]	0,0018	±0,0004	19%
$Bkgr_{IRF}$[Cnts/Chnl]	-1	±18	1200%
$Shift_{IRF}$[ps]	-41	±80	190%
τ_{AvInt}[ns]	3,523	±0,038	1,1%
τ_{AvAmp}[ns]	2,749	±0,064	2,3%

Figure S97. Left: Raw (experimental) time-resolved photoluminescence decay of **L** in an air-equilibrated MeOH solution at 298 K including the residuals (λ_{exc} = 376.7 nm, λ_{em} = 450 nm; the instrument response function is shown in red). Right: Fitting parameters including pre-exponential factors and confidence limits.

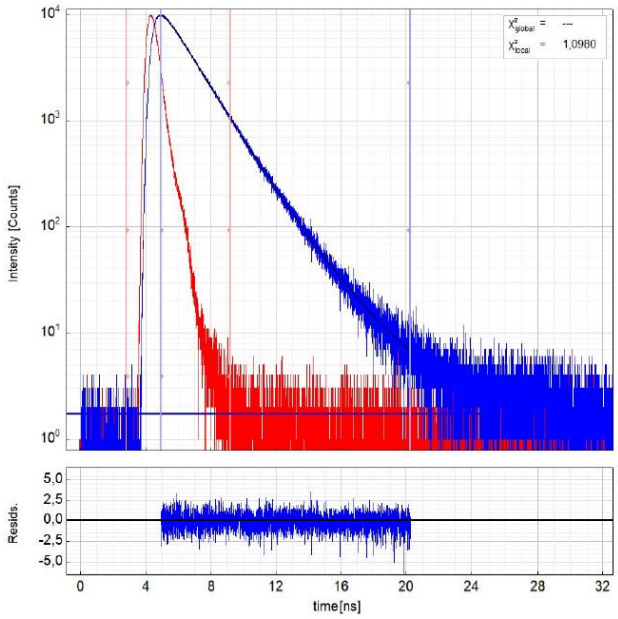

Parameter	Value	Δ	δ
A_1[kCnts/Chnl]	0,75	±0,49	65%
τ_1[ns]	3,0	±1,1	35%
I_1[kCnts]	560	±280	50%
A_{Rel1}[%]	4,8	±3,1	64%
I_{Rel1}[%]	8,4	±4,3	50%
A_2[kCnts/Chnl]	14,90	±0,51	3,4%
τ_2[ns]	1,643	±0,041	2,4%
I_2[kCnts]	6 120	±360	5,8%
A_{Rel2}[%]	95,3	±3,1	3,2%
I_{Rel2}[%]	91,7	±4,3	4,6%
$Bkgr_{Dec}$[kCnts]	0,0018	±0,0022	126%
$Bkgr_{IRF}$[Cnts/Chnl]	-0,8	±5,1	705%
$Shift_{IRF}$[ps]	-55	±22	39%
τ_{AvInt}[ns]	1,756	±0,025	1,4%
τ_{AvAmp}[ns]	1,707	±0,020	1,1%

Figure S98. Left: Raw (experimental) time-resolved photoluminescence decay of **L** in frozen glassy matrix at 77 K including the residuals (λ_{exc} = 376.7 nm, λ_{em} = 450 nm; the instrument response function is shown in red). Right: Fitting parameters including pre-exponential factors and confidence limits.